HEMODYNAMICS IN THE CEREBRAL CIRCULATION: NUMERICAL STUDIES AND EXPERIMENTAL INVESTIGATION

CHEN LIANG

SCHOOL OF MECHANICAL AND AEROSPACE ENGINEERING

NANYANG TECHNOLOGICAL UNIVERSITY

2005

Hemodynamics in the Cerebral Circulation: Numerical Studies and Experimental Investigation

Chen Liang

School of Mechanical and Aerospace Engineering

A thesis submitted to Nanyang Technological University

in fulfillment of the requirement for the degree of

Doctor of Philosophy

2005

ABSTRACT

One-dimensional numerical model has been frequently used in the study of cerebral hemodynamics due to its high possibility of patient-specific clinical application. Very recent clinical tests have proved that blood flow modeling can be used to identify patients who have an elevated risk of ischemic stroke resulting from hypotension in the circle of Willis (CoW). Previous numerical studies focused on the hemodynamics of complete CoW, although complete CoW only accounted for less than 50% of the patients. In those numerical models, seldom authors considered the function of cerebral autoregulation, which might result in underestimate of calculated blood flow. In addition, many numerical studies on blood flow in the CoW can be found in the literature, but in vitro experimental validation is hardly found.

The aim of this project is to develop a nonlinear one-dimensional numerical model to study the hemodynamics in complete and incomplete CoW with consideration of cerebral autoregulation and then use in vitro experiment to validate the numerical model. This project is closely related to solve clinical difficulties in investigating cerebral hemodynamics of the patients who have the risk of ischemic stroke. The numerical model is built up by solving a set of nonlinear partial differential equations using MATLAB. The tube law (describing the elasticity of arterial vessels) and friction term (describing the friction resulting from blood viscosity) are carefully chosen by comparing different models in the literature. By using various time steps in the numerical model, the calculation time for one case is less than six minutes, which makes it possible for clinical application of the numerical model.

ABSTRACT

In patients with stenoses or occlusions of the internal carotid arteries (ICAs), collateral pathways play important roles in ensuring enough blood flow to the brain tissue. For patients with severe stenoses or occlusions, carotid endarterectomy (CEA) can help to prevent resulting ischemic strokes. During CEA, it is necessary to clamp the arteries around the stenosis. Therefore, the clamped arteries stop supplying blood to the corresponding brain tissues. It is of clinical significance but difficult for neurosurgeon to make accurate prognosis on whether the patient can tolerate the clamping of the arteries. If the patient is at risk for intraoperative stroke after the clamping of the arteries, shunt may be necessary, but the shunt itself increases the risk of postoperative stroke.

The first numerical study is to investigate the hemodynamic change in the CoW during CEA before and after the clamping of the ICA. In this study, the diameters of communicating arteries are fixed at 1 mm. A clinical-static autoregulative model obtained from in vivo experimental measurements is applied in the numerical model. It is assumed that the patient has bilateral 75% stenosis of ICA with or without left posterior communicating artery (LPCoA) missing. The results show that bilateral 75% stenosis of ICA does not cause redistribution of cerebral blood flow compared with the normal CoW. The LPCoA missing does not influence significantly the cerebral blood supply pattern. In the complete CoW, occlusion of LICA results in significant redistribution of blood flow in the CoW. Collateral flows in ACoA and LPCoA increase from 0 to 2.35 ml/s and from 0.36 to 1.34 ml/s, respectively. A comparison between numerical results with and without autoregulation shows that the maximum underestimate of blood flow is 13.7% due to the omission of autoregulation.

The second numerical study is designed to investigate the interactive role of the diameters of ACoA and PCoA in the collateral circulation. There is a conflicting finding about the role of ACoA and PCoA in the clinical survey. Some authors found that collateral flow in ACoA played a more important role in the cerebral hemodynamics, but others found that only absence of collateral flow in PCoA was associated with clinical symptoms. This study is conducted in an incomplete CoW with combination of anatomic anomaly of the CoW and carotid artery disease. The autoregulative model used in the first numerical study is also applied in this study. The results show that the degree of stenosis of LICA and the diameters of ACoA and RPCoA strongly interactively influence the cerebral hemodynamics. The collateral capacity of ACoA increases with the increase of diameter of ACoA and decreases with the increase of both diameter of RPCoA and degree of stenosis of LICA. In cases of LICA stenosis less than 75%, the relative flows of right middle cerebral artery (RMCA) and right anterior cerebral artery (RACA) are strongly modulated by both ACoA and RPCoA when diameter of ACoA is less than 1 mm and diameter of RPCoA is less than 1.4 mm. Above this range, relative flows of RMCA and RACA are slightly influenced by the diameters of ACoA and RPCoA.

To the best of our knowledge, details of in vitro experimental study on blood flow in the CoW have not been found in the literature. Therefore, the in vitro experiment of this project is built up from the concept. The programmable motion control pump can produce physiological pressure waveform. The CoW is built up by coupled rigid and elastic tubes with the same sizes as that in the numerical model. Several carotid artery diseases are simulated in this experiment. The results show that steady and unsteady pressure inputs do not result in significant difference in the experimental

measurements. Compared with the numerical results, experimental measurements in the CoW with unilateral or bilateral 75% stenosis of ICA have no significant difference. In the CoW with unilateral or bilateral occlusion of ICA, experimental measurements show significant difference with the numerical results. The significant difference indicates that the energy loss in ACoA and PCoAs in experiment could be higher than that in numerical model when ICA is occluded.

In summary, the thesis focuses on the application of a simplified non-linear one-dimensional numerical model in the investigation of cerebral hemodynamics and in vitro experimental validation of the numerical model. The results presented in this study could help researchers to better understand the role of CoW geometry, carotid artery stenoses and autoregulation in the etiology of ischemic stroke.

ACKNOWLEDGEMENTS

First, I would like to express my sincere gratitude to my supervisors. To Assistant Professor Tsai Tse Min, thank you for your help, guidance and trust throughout this project! To Associate Professor Yeo Joon Hock, thank you for your help and guidance in finalizing the thesis!

Second, I would like to thank all the professors and friends who have contributed to the completion of my PhD project. Specially, I would like to express my sincere thanks to Mr. Yuan Kee Hock of Thermal and Fluid Research Lab for his continuous help and support, without whom my experiments would not have been completed.

In addition, I should thank my parents and the other family members for their understanding and continuous support.

Last, I would like to express my gratitude to Nanyang Technological University for providing scholarship for my PhD study and Student Development Strategy Fund (SDS 17/2001) for my experiment.

TABLE OF CONTENTS

TABLE OF CONTENTS

LIST OF FIGURES

LIST OF TABLES

NOMENCLATURE

A	Cross-sectional area	cm^2
A_0	Initial cross-sectional area	cm^2
c	Wave velocity	cm/s
D	Diameter	cm
D_0	Initial diameter	cm
E	Young's modulus	$dyne \cdot cm^{-2}$
E_L	Elasticity coefficient	$dyne \cdot cm^{-2}$
F	Friction	$dyne$
F_1	First part of friction	$dyne$
F_2	Second part of friction	$dyne$
g	Gravity acceleration	$cm \cdot s^{-2}$
h	Thickness of the vessel	cm
h_0	Initial thickness of the vessel	cm
p	Pressure	$dyne \cdot cm^{-2}$
p_{in}	Input pressure	$dyne \cdot cm^{-2}$
p_{out}	Output pressure	$dyne \cdot cm^{-2}$
P_I	Input mean pressure	$dyne \cdot cm^{-2}$
P_O	Output mean pressure	$dyne \cdot cm^{-2}$
p_d	Diastolic pressure	$dyne \cdot cm^{-2}$
p_v	Venous pressure	$dyne \cdot cm^{-2}$

q	Flow rate	$cm^3 \cdot s^{-1}$
q_t	Instantaneous total flow rate	$cm^3 \cdot s^{-1}$
Q_t	Total mean flow rate	$cm^3 \cdot s^{-1}$
R	Radius	cm
R_0	Initial Radius	cm
R_p	Peripheral resistance	$dyne \cdot s \cdot cm^{-5}$
t	Time	s
T	Total time	s
u	Average velocity	$cm \cdot s^{-1}$
W	Weight function	
x	Distance	cm

GREEK LETTERS

α	Womersley number	
β	Stiffness parameter	
Re	Reynolds number	
τ	Dimensionless time	
ρ	Density	$g \cdot cm^{-3}$
ϕ	Elasticity coefficient	$dyne \cdot cm^{-2}$
μ	Viscosity coefficient	$dyne \cdot s \cdot cm^{-2}$
υ	Kinematic viscosity coefficient	$cm^2 \cdot s^{-1}$
κ	Dimensionless coefficient for ratio of Re and α	

Chapter 1

Introduction

1.1 Clinical Background

1.1.1 Ischemic stroke

Stroke is the third leading cause of death in America, ranking behind diseases of the heart and all forms of cancer. On average, every 45 seconds someone in the United States suffers a stroke and every 3.1 minutes someone dies of a stroke (American Heart Association; Heart Disease and Stroke Statistics - 2004 Update). As a type of cardiovascular disease, stroke is also a leading cause of serious and long-term disability in the world. A stroke occurs when blood vessel that carries oxygen and nutrients to the brain is either blocked by a clot or bursts. When that happens, part of the brain cannot get the blood (and oxygen) it needs, so it starts to die.

Ischemic stroke is the most common type of stroke and accounts for more than 80% of all strokes (http://www.strokecenter.org). It results from an obstruction within a blood vessel supplying blood to the brain. The underlying condition for this type of obstruction is the development of fatty deposits lining the vessel walls. This condition is called atherosclerosis. These fatty deposits can cause two types of obstruction, cerebral thrombosis and cerebral embolism. Cerebral thrombosis refers to a thrombus (blood clot) that develops at the clogged part of the vessel. Cerebral embolism refers generally to a blood clot that forms at another location in the circulatory system,

usually the heart and large arteries of the upper chest and neck. A portion of the blood clot breaks loose, enters the bloodstream and travels through the brain's blood vessels until it reaches vessels too small to let it pass. A second important cause of embolism is an irregular heartbeat, known as atrial fibrillation. It creates conditions where clots can form in the heart, dislodge and travel to the brain. Figure 1.1 gives an illustration for the ischemic stroke due to an embolus in MCA. Red vessels are filled with oxygenated blood, see Figure 1.1a. When this vessel is blocked by a clot, oxygenated blood can not go through the vessel. The blue vessel is filled with deoxygenated blood, which is an indication of ischemic stroke, see Figure 1.1b.

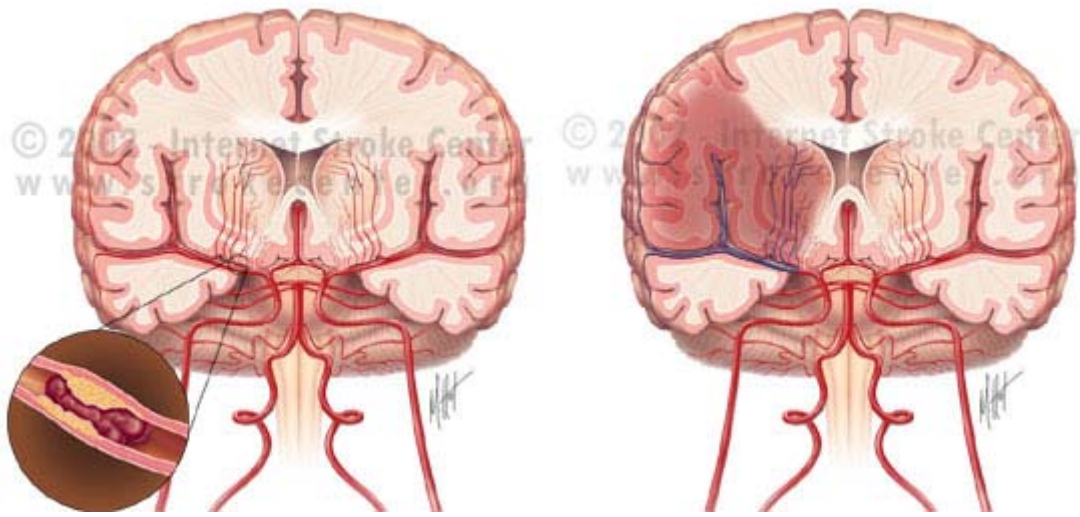

1.1a 1.1b

Figure 1.1 Ischemic stroke due to an embolus in MCA
(http://www.strokecenter.org)

Despite being only about 2 percent of total body weight, the brain continuously receives about 13 percent of the blood that flows through entire body (Nichols et al., 1990). The brain is highly vulnerable to disturbance of the blood supply; anoxia and ischemia lasting only seconds can cause neurological symptoms and within minutes

can cause irreversible neuronal damage. When part of the brain dies from lack of blood flow, the part of the body it controls is affected.

1.1.2 Circle of Willis

The circle of Willis (CoW) is a circle of arteries at the base of brain which receives blood supply from the heart by way of the aortic arch that gives rise to the brachiocephalic artery, common carotid artery (CCA) and subcalvian artery, see Figure 1.2. Then this circle supplies the blood into all parts of the brain by its many branches, see Figure 1.3. At the CoW, the internal carotid arteries (ICAs) branch into smaller arteries that supply oxygenated blood to about 80% of the cerebrum.

Although Sir Thomas Willis was not the first to describe the arterial circle at the base of the brain, he was the first to provide a complete description, an illustration of this vascular pattern, and to indicate that he understood the probable function of the arterial circle in his publication Cerebri Anatome in 1664 (Ustun, 2004). Therefore, the pattern of vessels called the cerebral arterial circle before the eponym was named after him as the circle of Willis. Following his step, lots of work has been done about the collateral function of the CoW.

1.1.2.1 Geometry of the CoW

Figure 1.2 is a schematic illustration of the brain's blood vessels. Each cerebral hemisphere is supplied by an internal carotid artery (ICA), which arises from the CCA and divides into the anterior cerebral artery (ACA) and middle cerebral artery (MCA). Each vertebral artery (VA) arises from the subclavian artery and joins at the junction of the pons and the medulla to form the basilar artery (BA). The BA then divides into

the two posterior cerebral arteries (PCAs), which supply the inferior temporal and medial occipital lobes and the posterior corpus callosum.

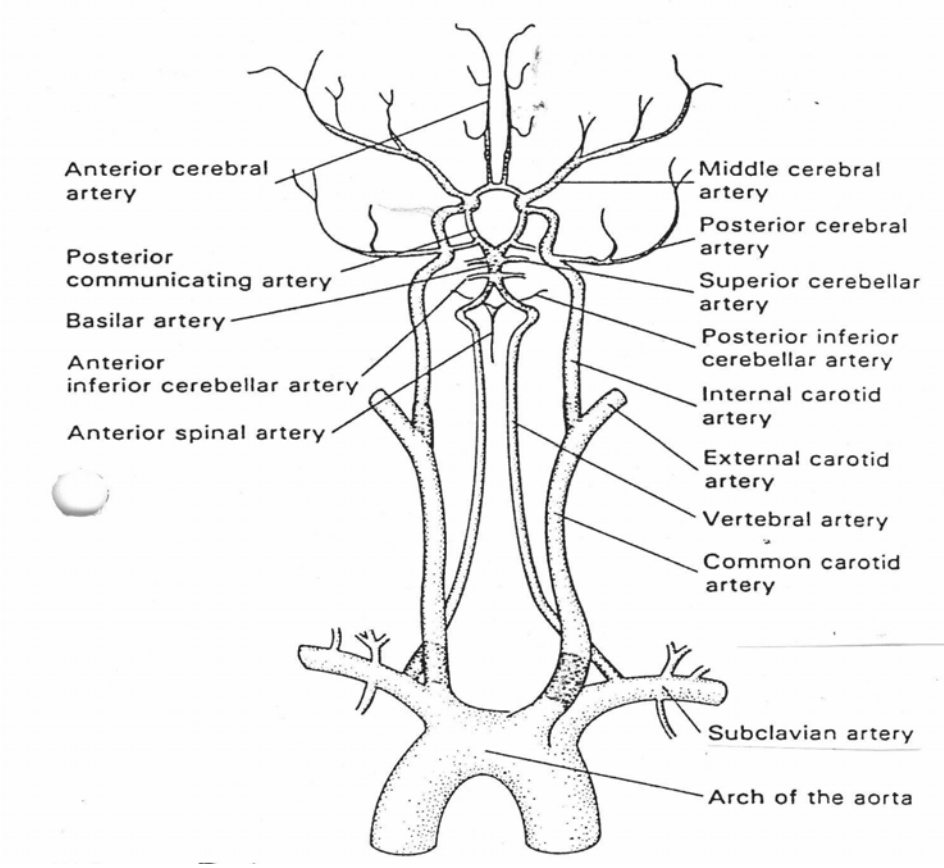

Figure 1.2 Blood vessels of the brain
(Adapted from Barnett 1988)

The CoW is composed of the proximal segments of ACAs (A1) and PCAs (P1), two posterior communicating arteries (PCoAs) and one anterior communicating artery (ACoA). Compared with the other components of the CoW, communicating arteries usually have small diameters but play important roles in the collateral function of the CoW.

Figure 1.3 shows the CoW and the supplying areas in the brain by its many branches. Blood is pumped by the heart into the CoW through the four afferent arteries, two

ICAs and two VAs, and then distributed into brain tissues by the circle's branches, mainly by its six efferent arteries which are two ACAs, two MCAs and two PCAs, see Figure 1.3. The six efferent arteries branch further into small arteries, arterioles and capillaries. Oxygenated blood supplies oxygen and nutrients to brain tissue in the capillaries and then blood becomes deoxygenated. Finally deoxygenated blood goes back to heart through venous system.

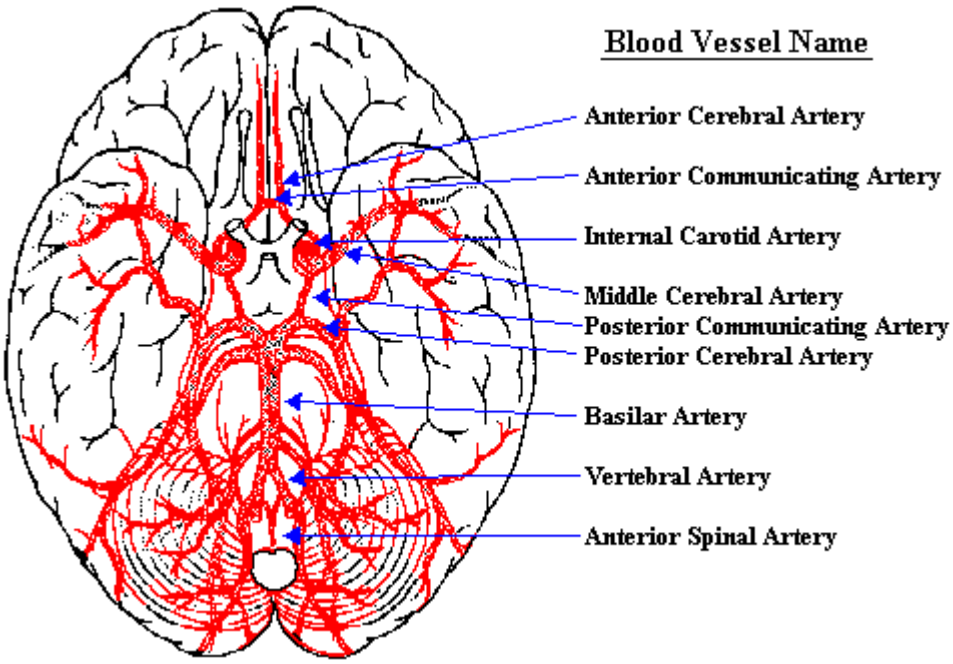

Figure 1.3 Circle of Willis and its supply areas
(http://faculty.washington.edu/chudler/vessel.html)

1.1.2.2 Collateral function of the CoW

In normal condition, the CoW is symmetrical and pressure between two hemispheres is almost balanced. Therefore, there is no blood flow cross the ACoA. Also, in normal condition, ICA and BA can supply enough blood to their corresponding territories. Hence, the blood flow cross PCoA, usually from ICA system to BA system, is very

small, see Figure 1.4. In Figure 1.4 the blood flow directions in normal CoW are given.

.

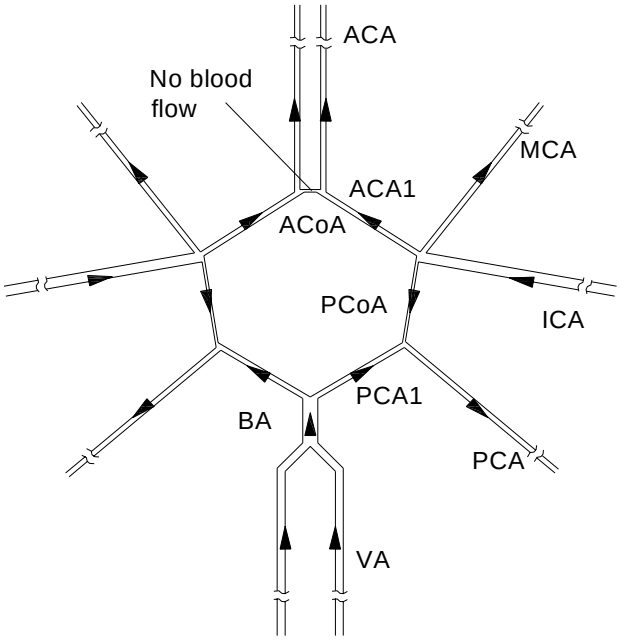

Figure 1.4 Blood flow directions in normal CoW

The special circular structure of the CoW makes it sensitive to the pressure difference and able to equalize the pressure among different parts of brain. The ACoA connects two hemispheres and allows blood flow of one side to go into the other side if there is unbalance in perfusion pressure between two sides. At each hemisphere, PCoA connects posterior part and the other two parts, anterior part and middle part. When one ICA can not provide enough blood flow to the corresponding area, the other ICA and BA compensate blood through ACoA and PCoAs to the deprived carotid side.

Due to the tortuous geometrical structure of the ICA, atheromatous plaque is often found to accumulate on the wall of ICA. The accumulated atheromatous plaque narrows the path of ICA and therefore stenosis occurs. The slow progression of the

stenosis finally occludes the ICA and occluded ICA can not supply blood any more. Figure 1.5 illustrates the changes of blood flow directions in the CoW due to right ICA (RICA) occlusion. Since occluded RICA stops supplying blood, blood from LICA and BA compensates RACA and RMCA through ACoA and PCoAs. We can see from Figure 1.5 that blood flows in ACoA, PCoAs and RACA1 change their directions compared with that in Figure 1.4. These vessels recruited for compensation of blood flow are called collateral pathways.

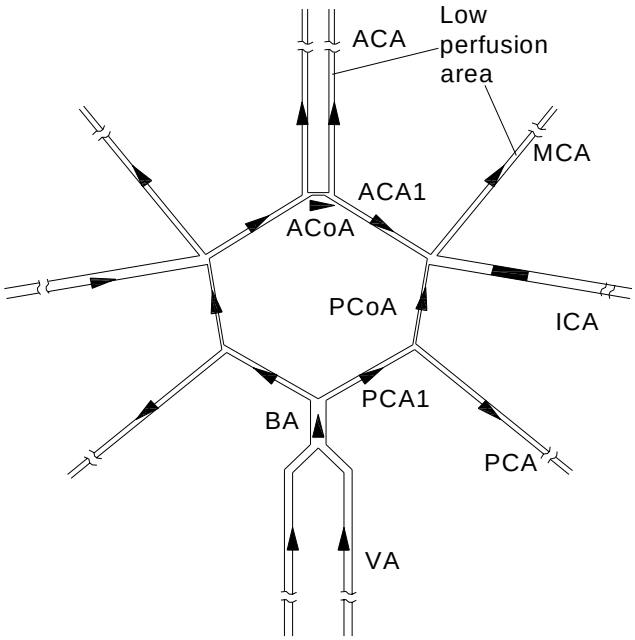

Figure 1.5 Blood flow directions in the CoW with RICA occlusion

The components of the CoW play primary roles in compensating blood flow to the deprived area. Therefore, the CoW is considered as the primary collateral pathways. Besides the primary collateral pathways, there are two kinds of secondary collateral pathways in the cerebrovasculature. External carotid artery (ECA) supplies a part of blood to the eye, and ophthalmic artery (OphA) also supplies blood from ICA to the

eye. When the pressure in ICA becomes very low due to severe stenosis or occlusion, blood flow in OphA may reverse. Therefore OphA is considered as one type of secondary collateral pathway. The other type of secondary collateral pathway is given by leptomeningeal anastomoses. In deep brain, the branches of main supply arteries, for example MCAs and ACAs, may merge at the borderline area. Through the borderline area blood may penetrate from this part to the other part. The recruitment of secondary collateral pathways is a sign of compromised cerebral hemodynamics.

1.1.3 Carotid Endarterectomy

Carotid endarterectomy (CEA) is the surgical procedure to prevent ischemic stroke by removing fatty plaque from carotid arteries. During CEA, it is necessary to clamp the arteries around the stenosis, see Figure 1.6. Therefore, the clamped arteries will stop supplying blood to their territories. In many patients sufficient blood is able to get to these territories from other arteries which come from the collateral pathways.

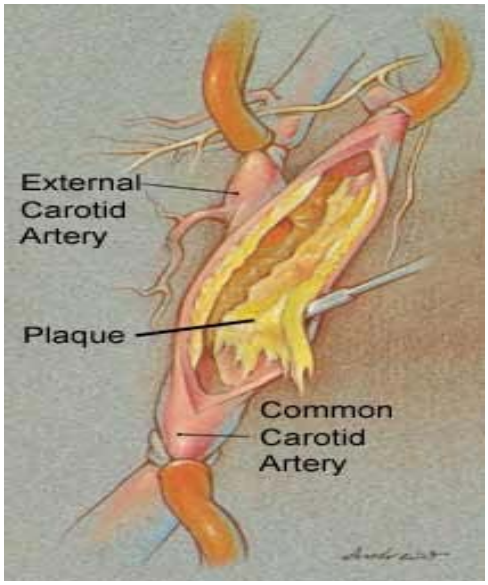

Figure 1.6 CEA without shunt
(http://www.texheartsurgeons.com/CarotidEndarter.htm)

If collateral pathways are not effective and the brain is not getting enough flow then a shunt can be placed around the blockage and blood flow can be delivered again. Figure 1.7 shows the CEA with a shunt. Studies have shown that for patients with high grade stenosis, CEA is more beneficial than other medical treatments for prevention of stroke.

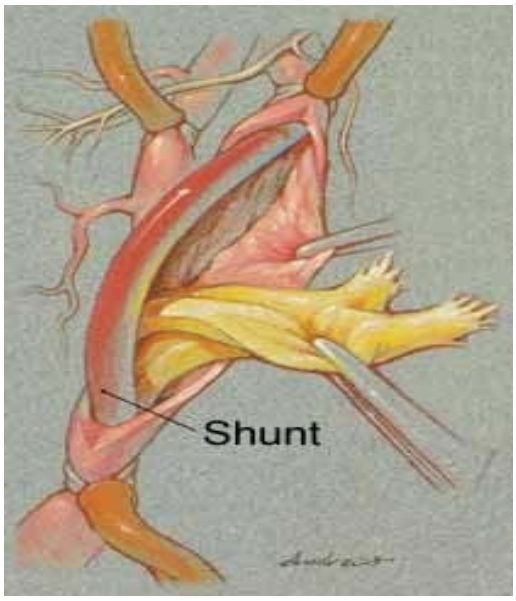

Figure 1.7 CEA with shunt
(http://www.texheartsurgeons.com/CarotidEndarter.htm)

1.2 Cerebral hemodynamics

Hemodynamics is defined as the study of the flow of the blood and the forces concerned therein. When the heart ejects a bolus of blood by left ventricle into the already pressurized aorta, the pressure rises further so the vessel, being elastic, becomes locally distended and the blood in it is set into motion. The coupling between the restoring force of arterial elasticity and the inertia of the blood results in a pressure wave propagating along the aorta.

1.2.1 Cerebral blood flow

Insufficient cerebral blood flow (CBF) causes transient ischemic attacks and ischemic stroke. CBF is influenced and regulated by a number of factors, including arterial blood pressure (ABP), intracranial pressure (ICP), venous outflow, blood viscosity, arterial perfusion of carbon dioxide (PCO_2), arterial perfusion of oxygen (PO_2), collateral flow, vasomotor reactivity (VMR) and the status of cerebral autoregulation (CA). The regulation of vascular resistance lies mainly in the arterioles and precapillary segments.

ABP is the pressure exerted by the blood on the walls of the blood vessels. CPP is defined as the difference between the mean arterial blood pressure (mABP) and the ICP which is the pressure inside the skull. CPP represents the pressure gradient driving CBF and hence oxygen and metabolite delivery. CBF is governed by CPP and cerebral vascular resistance (CVR).

Because ICP is stable and low, CPP can be represented by ABP in some studies. CVR is determined by the resistance in the CoW and the resistance of the distal areas of the CoW, such as small arteries, arterioles and capillaries. In normal condition, the communicating arteries of the CoW are not recruited and hence the resistance of CoW depends on the other components. When communicating arteries are recruited, the resistance of CoW is mainly dependent on the size of the communicating arteries. In the distal areas of CoW, the resistance of arteriole and capillary is mainly controlled by metabolic factors, such as PCO_2 and PO_2. The arterioles and precapillary segments conduct the function of autoregulation.

The resistance of blood flow through arterial walls is influenced by the blood viscosity and the friction between blood and arterial walls. The viscosity of the blood is around four times of that of water. The friction between blood and arterial wall is time-dependent and influenced by the blood viscosity and the viscoelasticity of the arterial wall.

1.2.2 Cerebral autoregulation and vasomotor reactivity

Since brain tissue is very sensitive to blood supply, too much or too little blood flow will hurt brain cells in short time. There is an intrinsic function of brain called autoregulation that prevents brain tissue from the damage due to unstable blood supply. CBF is governed by CPP and CVR as formulated by following equation:

$$CBF = \frac{ABP - ICP}{CVR} = \frac{CPP}{CVR}$$

In a certain range of pressure fluctuation, CBF can be maintained at relative constant level by adjusting the CVR. The mechanism of maintaining constant blood flow in brain is implemented mainly by arterioles and precapillaries by vasodilation when pressure decreases and vasoconstriction when pressure increases, and the subsequent change of CVR is governed by following equation:

$$CVR = \frac{128\mu L}{\pi D^4}.$$

μ represents blood viscosity, L vessel length and D vessel diameter. Since CVR is inversely proportional to the forth power of diameter, small change of diameter results

in large change of CVR. In normal condition, in the range of perfusion pressure between 60-160 mmHg, CBF has small difference. Below the low limits of autoregulation (LLA) or above the upper limits of autoregulation (ULA), blood flow is regulated passively by CPP. It is important to note that cerebral metabolism is the major determinant factor of regional blood flow.

With the slow progression of stenosis of ICA, perfusion pressure in stenosed side reduces. Responding to the reduced CPP, in order to maintain constant CBF, distal cerebral vessels enlarge their diameters to reduce peripheral resistance. Enlarged vessels do not return to their original sizes unless local perfusion pressure improves. Such vasodilating behavior of the vessels is called vasomotor reactivity (VMR). Once the distal vessels extend to the maximum, their diameters do not change any more despite lower local perfusion pressure. This means that the VMR is totally damaged. Impairment of VMR is associated with impairment of autoregulation and also associated with high risk for ischemic stroke.

Stenosis or occlusion of the afferent arteries of the CoW will influence cerebral hemodynamics. Whether the influence is significant depends on the degree of stenosis, the collateral capacity of CoW and the VMR (or CA). Well-developed CoW provides good collateral blood flow which compensates the deprived side and can afford severe stenosis or occlusion of afferent arteries. Well-preserved VMR reduces the distal resistance and mitigates the impairments of cerebral hemodynamics caused by carotid artery disease.

1.2.3 Clinical significance of cerebral hemodynamics

Over the last decade evidence has accumulated that compromised cerebral hemodynamics plays an important role for the ischemic stroke in patients with severe carotid artery disease. Due to the lethality caused by ischemic stroke and its unable rehabilitation, accurate prognosis and optimal treatment for patients are expected by clinicians. Currently, because of the non-invasive properties of human skull and the limitations of monitoring equipments, thorough information about cerebral hemodynamics in the patients is not available. Clinical studies on cerebral hemodynamics present a lot of conflicting findings due to the extensive anatomical variances of the CoW, the difference of study purpose and various measuring equipments.

The significance of thorough evaluation of cerebral hemodynamics for the patients with occlusive diseases is clarified as follow. The stenosis of ICA is slowly progressive and finally occluded. Occluded ICA is not able to supply blood to brain tissue any more. Can the patients tolerate the chronic carotid occlusive disease? Do the patients need surgical treatment? Can the patients be selected for surgical treatment? It is difficult for neurosurgeon to make accurate prognosis. Thorough evaluation of cerebral hemodynamics is able to provide useful information to increase the accuracy of the prediction.

When the patient is selected for surgical treatment by which neurosurgeon removes the atheromatous plaque in the ICA, preoperative, intraoperative and postoperative investigation on the cerebral hemodynamics of the patients can reduce the risk for intraoperative and postoperative stroke due to the surgery itself. During the process of

operation, the diseased ICA is clamped to stop the local blood supply. The intraoperative cerebral hemodynamics of the patients is the important factor for neurosurgeon's prediction and decision on whether the patient can afford the temporary clamping and whether a shunt is needed. After the vascular surgery, the clamped ICA is released. Some patients suffer postoperative stroke due to local hypertension after CEA. What would be the cerebral hemodynamic status postoperatively for the patients? Can the patient tolerate such hemodynamic change due to local hyperperfusion after CEA? The acute postoperative strokes in the patients due to the surgery itself require careful investigation or prediction for postoperative cerebral hemodynamics of the patients.

1.3 Thesis objectives, scope and organization

1.3.1 Thesis objectives

The objective of this project is to study cerebral hemodynamics in the CoW using one-dimensional numerical models and in vitro experiment by considering the anatomic variances of the CoW, degree of stenoses of ICAs and autoregulation. The main objectives are:

1. To develop a nonlinear one-dimensional numerical model of the CoW using MATLAB and find out the accurate friction term and tube law for the numerical model by comparing different friction terms and tube laws in a single vessel.

2. To apply an autoregulative model into the numerical model and simulate the cerebral hemodynamic changes between before and after clamping carotid arteries during CEA using the numerical model.

3. To study the interactive role of ACoA and PCoA in the collateral function of the CoW with combination of carotid artery disease and anomaly of the CoW in numerical models.

4. To set up an in vitro experiment to study blood flow in the CoW and validate the numerical model.

1.3.2 Thesis scope

This project is designed to study cerebral hemodynamics of the CoW from point of view of fluid mechanics using numerical model and in vitro experiment. The aim of this study is to use simple numerical model to help clinician to understand the hemodynamics in cerebral circulation. Although many factors influence the cerebral circulation, except for the factor of hemodynamics, other factors such as metabolic, myogenic and nervous mechanism are not included in this study. Component vessels formed the CoW are not only the communicating arteries, but also the proximal segments of ACAs and PCAs. Only are the variances of diameters of the communicating arteries studied. Stenosis and occlusion can be found in many locations of the afferent arteries, but we only consider the stenosis and occlusion of the ICAs.

1.3.3 Thesis organization

The first chapter of this thesis introduced the background, objectives and scope of this study. Specifically, physiological background such as the ischemic stroke, the CoW and the CEA are introduced. Then the definition, parameters and clinical significance of cerebral hemodynamics are given.

In Chapter 2 extensive clinical survey about the study of cerebral hemodynamics in the literature is conducted. Several important factors influencing cerebral hemodynamics such as anatomic variances of the CoW, degree of stenosis of ICA and hemodynamic adaptive ability of the cerebrovasculature are reviewed separately. The surgical method in reducing the risk of ischemic stroke is also reviewed. In the second part of Chapter 2, thorough numerical studies of cerebral circulation are reviewed. The last part of Chapter 2 is a brief review of in vitro experimental studies on blood flow in the CoW.

Chapter 3 introduces the numerical model used in this study which is based on the literature. Some assumptions used to develop the numerical model are given at the beginning of this chapter. Then a brief introduction of numerical model in a single vessel is given. Main attention of this chapter is paid on the comparison of three friction terms and two tube laws in a single vessel. Subsequently, procedures of building up numerical model of network of the CoW are given. Finally, numerical results of an idealized model of CoW are shown.

In Chapter 4 we conduct a numerical study which simulates the hemodynamic change between before clamping of ICA and after clamping of ICA during CEA. An autoregulative model is applied in this study. The comparison of numerical models with and without autoregulative model is also shown in this chapter. The purpose of this specific simulation is to provide information in the prediction on whether a shunt is needed during CEA.

In Chapter 5 a conflicting clinical finding about the role of ACoA and PCoA in the collateral circulation is explained by the results of numerical model. Chapter 6 introduces the procedures of setting up experiment which is used to in vitro study the hemodynamics of the CoW. Preliminary results from the experiments are obtained and compared with that of numerical model. In chapter 7 conclusions for this study are given and some future works are also suggested.

Chapter 2

Literature Review

2.1 Clinical survey

Extensive clinical studies indicate that cerebral hemodynamics plays an important role in the risk of ischemic stroke (Klijn et al., 1997). Clinical findings show that the status of cerebral hemodynamics is influenced by various factors such as carotid artery disease (Zachrisson et al., 2001), collateral circulation (Liebeskind, 2003; Yamauchi et al., 2004) and hemodynamic adaptation (Hartkamp et al., 1999). Vernieri et al. (2001) evaluated the relationships among carotid occlusive disease, type and number of collateral pathways, VMR, and the risk of ischemic stroke in 104 patients. They suggested that cerebral hemodynamic status in patients with carotid occlusive disease was influenced by both individual anatomic and functional characteristics of the CoW. The planning of strategies to define the risk profile and any attempt to influence patient's outcome should be based on the evaluation of the intracranial hemodynamic adaptive status, with particular attention to the number of collateral vessels and the related VMR. Based on the study of Vernieri et al. (2001), an extensive clinical survey about the influence of anatomical variances of the CoW, carotid artery disease and hemodynamic adaptation on the cerebral hemodynamics is conducted.

2.1.1 Anatomical variances of the CoW

Anatomic configuration of the CoW is an important factor for the cerebral hemodynamics (Hartkamp et al., 1999). Anatomic anomaly of the CoW impairs its ability of adaptation to change of cerebral hemodynamics and therefore increases the risk of ischemic stroke. Imaging monitoring and anatomical investigation find that the CoW presents various anomalies. The association of CoW dysfunction with the risk of ischemic stroke originates from autopsy studies performed in the 1960s. Alpers and Berry (1963), who compared the configuration of the CoW of 350 normal brains with that of 194 brains with signs of infarction, were among the first to report that infracted brains showed a high proportion of hypoplastic CoW collaterals.

2.1.1.1 Complete and incomplete CoW

There is evidence that patients with progressive carotid artery disease and incomplete CoW have increased stroke risk. Various authors have shown through anatomical studies of normal brains that a complete CoW occurs in only about 20% to 50% of individuals (Hoksbergen et al., 1999; Hartkamp et al., 1999). If any component of the CoW is missing or non-functional, the circle is considered as incomplete. The missing of a vessel is due to inborn absence and there exists no path for blood flow. The absence of components significantly impairs the collateral capacity of the CoW.

A hypoplastic or thread-like vessel is still able to supply blood, but the blood flow is too small to be measured by all kinds of imaging systems. It is quite possible that in the future, particularly in patients with an asymptomatic severe carotid stenosis, the decision whether to operate or not will be influenced in part by the collateral ability of the CoW (Nicolaides et al., 1995; Kim et al., 2002). Therefore, uniformity in the

definition of a complete CoW is a first requirement. However, till now there is no uniformity in the definition of a complete CoW. The ultrasound criteria used in the literature to discern functional from non-functional collateral arteries presents significant differences in arterial size (Hoksbergen et al., 2000a; Chaudhuri et al., 1992; Keunen et al., 1990; Baumgartner et al., 1996). The varying definitions of hypoplasia of CoW collaterals and the different measuring equipments used in clinical studies have resulted in a large variability of anomalous or "incomplete" CoW throughout the literature.

There exists debate on the threshold of the diameter of a non-functional vessel in the literature. Because conventional angiography such as MRA only can measure blood flow in the vessel with diameter of >1mm, a threshold of 1mm to define hypoplasia or inadequacy of collateral vessels has been widely used in anatomic studies (Saeki et al., 1977; Gomes et al., 1986; Battacharji et al., 1967; Fisher et al., 1965; Yasargil et al., 1984; Hegedus et al., 1987; Tulleken et al., 1987;). Transcranial Color-Coded Duplex Ultrasonography (TCCD) can measure blood flow in vessels with 0.5mm diameter, but the flow is small and how significant a role it plays for the collateral flow is not clear (Hoksbergen et al., 2003b).

Hoksbergen et al. (2000a) conducted a study in 12 acute stroke patients to determine the collateral artery threshold diameters for supplying collateral flow. They compared the collateral integrity of the CoW of the patients assessed by TCCD and carotid compression tests with their postmortem anatomy. The lengths and diameters of the collateral arteries were measured before and after the patients' death. Finally they concluded that the threshold diameter allowing for cross-flow through the primary

collateral arteries of the CoW is between 0.4 and 0.6mm. Because of the longer length of PCoA, its threshold diameter is larger than that of ACoA. This threshold diameter might be used in prospective studies on evaluating the influence of the collateral ability of the CoW on the development of ischemic strokes in patients with carotid artery occlusive disease.

2.1.1.2 Types of anomalies of the CoW

Various types of anomalies of the CoW have been found in the literature. In the study of Hartkamp et al. (1999) individual configurations of the CoW of seventy five patients with minor disabling neurological deficits and with ICA stenoses or occlusions were presented. For the anterior part of the CoW, 88% of patients and 68% of control subjects were found with complete morphology shown as type a-f in Figure 2.1. For the posterior part of the CoW, MRA demonstrated a complete posterior configuration in 63% of patients and 47% of control subjects shown in Figure 2.2 (type a, b and c). The entirely complete CoW was found in 55% of patients and 36% control subjects.

The proportion of different types of anomalies in Figure 2.1 is shown in table 2.1. From table 2.1, we can find that 7% of patients and 22% of control subjects have hypoplasia or absence of an ACoA and 5% of patients and 10% of control subjects present one hypoplastic or absent A1 segment. A “normal” complete anterior CoW is found 56% in patients and 57% in control subjects. “Normal” complete means complete without redundant branches like type a in Figure 2.1.

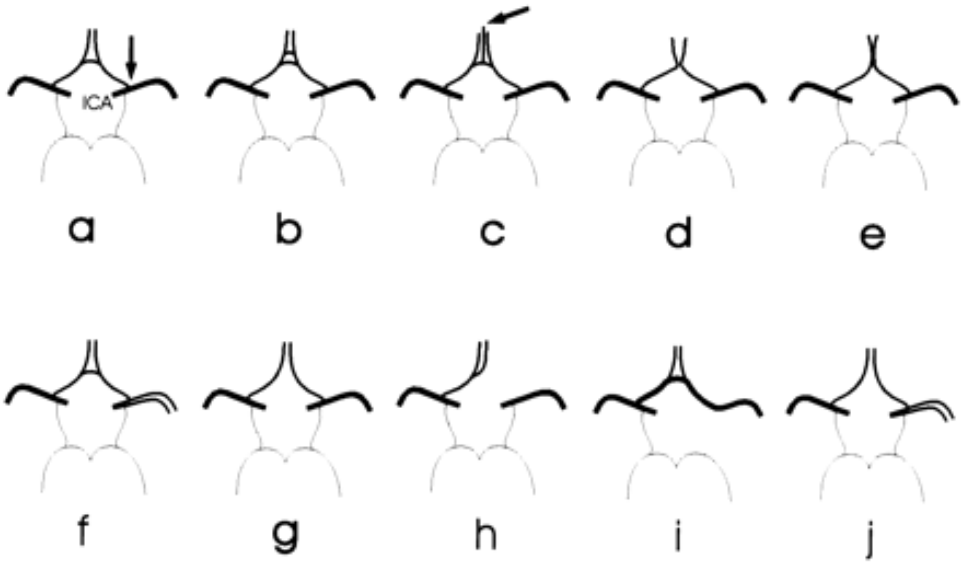

Figure 2.1 Scheme of anatomic variations of the anterior part of the CoW: types a through f are complete, whereas types g through j are incomplete. a, A single ACoA. The ICA bifurcates (arrow) into the A1 segment of the ACA and the MCA. b, Two (or more) ACoAs. c, A medial artery of the corpus callosum (arrow) arising from the ACoA. d, Fusion of the ACAs over a short distance. e, ACAs forming a common trunk and splitting distally into two A2 segments. f, MCA taking origin from the ICA as 2 separate trunks. g, Hypoplasia or absence of an anterior communication. h, One A1 segment shown as hypoplastic or absent, with the other A1 segment giving rise to both A2 segments. j, Hypoplasia or absence of an anterior communication, with the MCA arising as 2 separate trunks. (From Hartkamp et al., 1999)

Table 2.1 Morphology of anterior part of the CoW (Types a through j correspond to the schematic representations of anterior variants as shown in Figure 2.1)

Group	n	Prevalence, %									
		Complete						Incomplete			Total Complete
		a	b	c	d	e	f	g	h	j	
Patients	75	56	21	3	4	0	4	7	5	0	88
Controls	100	57	5	0	2	2	2	20	10	2	68

Figure 2.2 shows the posterior configurations of the CoW. Type a through c are complete. In type b and c, the diameter of PCoA is larger than that of PCA which is called fetal-type PCA.

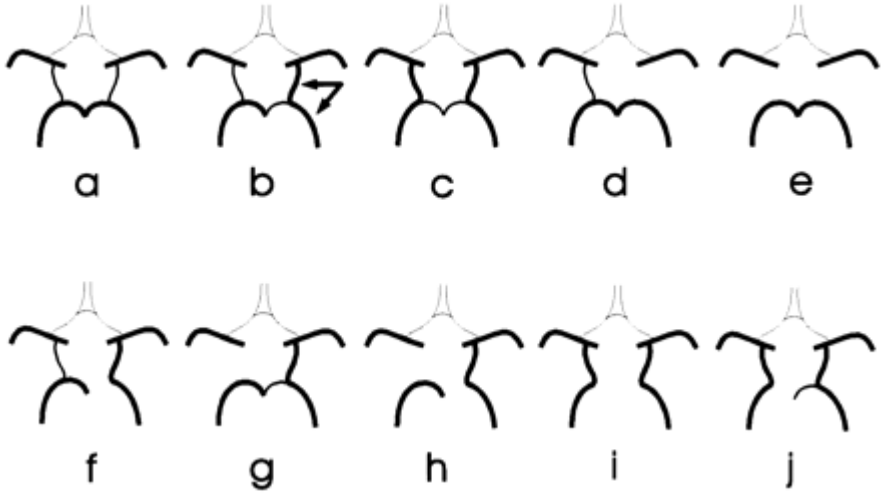

Figure 2.2 Scheme of anatomic variations of the posterior part of the CoW: variant types a through c are complete, whereas the remainder are incomplete. a, Bilateral PCoA present. b, PCA originating predominantly from the ICA. This type is known as a unilateral fetal-type PCA (FTP), indicated by the arrows; the PCoA on the other side is present. c, Bilateral FTP, with both P1 segments patent. d, Unilateral PCoA present. e, Hypoplasia or absence of both PCoAs, with isolation of the anterior and posterior circle parts at this level. f, Unilateral FTP, with hypoplasia or absence of the P1 segment. g, Unilateral FTP, with hypoplasia or absence of the contralateral PCoA. h, Unilateral FTP, with hypoplasia or absence of the P1 and PCoA. i, Bilateral FTP, with hypoplasia or absence of both P1 segments. j, Bilateral FTP, with hypoplasia or absence of one P1 segment. (From Hartkamp et al., 1999)

Table 2.2 shows the proportion of different types of posterior part of the CoW shown in Figure 2.2. From table 2.2 we can see that 63% of patients and 47% of control subjects present complete posterior configuration. A “normal” complete posterior CoW is found in 54% of patients and 25% of control subjects. Unilateral PCoA absence is found in 27% of patients and 30% of control subjects. Bilateral PCoA absence is found in 7% of patients and 12% of control subjects.

Table 2.2 Morphology of posterior part of the CoW (Types a through j correspond to the schematic representations of posterior variants as shown in Figure 2.2.)

Group	n	Prevalence, %										
		Complete						Incomplete				Total Complete
		a	b	c	d	e	f	g	h	i	j	
Patients	75	54	8	1	27	7	1	0	1	0	1	63
Controls	100	25	14	8	30	12	2	5	1	1	2	47

In the same year, Hoksbergen et al. (1999) studied the anatomical variances in 76 patients using TCCD. They found that in 22 (29%) of the patients, the ACoA and both PCoAs were functionally patent, resulting in a hemodynamically complete CoW. Figure 2.3 shows the different anomalies of the CoW and the number and ratio to the total number of the patients. Various anatomic anomalies of the CoW increase the uncertainty of the results of the carotid artery disease and require clinicians to consider the anatomic configuration of the CoW when they predict the cerebral hemodynamics of the patients.

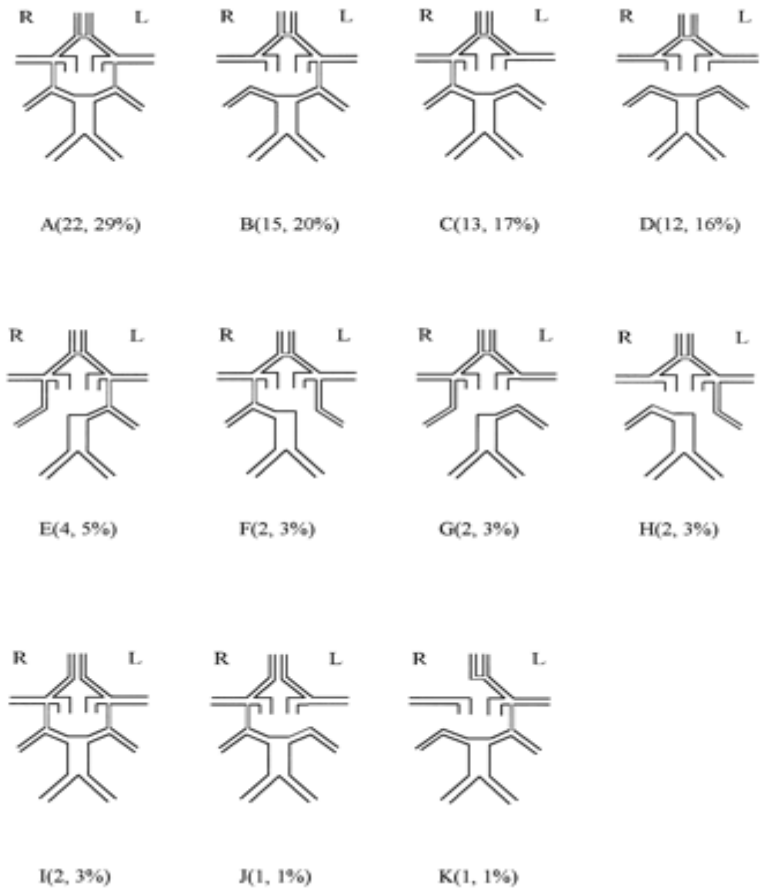

Figure 2.3 Schematic drawings of the collateral variations found in the CoW in the study of Hoksbergen et al. (1999). Numbers and percentages of patients are shown in parentheses for the following conditions: A, complete circle; B, hypofunctional right PCoA; C, hypofunctional left PCoA; D, bilateral hypofunctional PCoAs; E, fetal right posterior cerebral artery; F, fetal left posterior cerebral artery; G, hypofunctional left PCoA and fetal right posterior cerebral artery; H, hypofunctional right PCoA and fetal left posterior cerebral artery; I, hypofunctional ACoA; J, hypofunctional ACoA and hypofunctional left PCoA; and K, hypoplasia right A1 and hypofunctional right PCoA.

In Figure 2.3 R indicates right and L left. The first number in the parentheses is the number of patients with the corresponding configuration of the CoW, and the second number is the ratio to the total number of patients. In this study unilateral missing or non-functional PCoA were found in 37% of the patients and bilateral missing or non-functional PCoAs were in 16% of the patients. Non-functional ACoAs were found in 4% of the patients.

2.1.1.3 Importance of individual pathway of the CoW

Although the role of the CoW in protecting patients with carotid occlusive disease against ischemic stroke is recognized, there is still much confusion about the importance of the individual pathway in the circle itself. ACoA and PCoAs of the CoW provide main routes for collateral blood flow in cases with severe ICA stenosis or occlusion. Absence of collateral function due to hypoplasia of ACoA or PCoA may lead to a higher risk of stroke. For this reason, insight into the individual collateral pathway of the CoW is of clinical importance. The association of individual ACoA and PCoA with the risk of ischemic stroke in patients with occlusive ICA diseases has been widely studied. In the clinical studies, although collateral flows can be detected by TCCD, it is impossible to evaluate the collateral volume flow capacity (Zachrisson et al., 2001). Therefore, the quality of collateral flow of ACoA or PCoAs cannot be differentiated in clinical studies.

2.1.1.3.1 Collateral function of PCoA

Felice et al. (2000) found that 20 of 22 (91%) sudden hearing loss patients with cerebrovascular disease-free had at least ipsilateral non-functional PCoA. These findings suggest a strong association between a non-functional PCoA of the CoW and sudden hearing loss. Schomer et al. (1994) studied 29 patients with ICA occlusion and evaluated four collateral pathways to the occluded vessel: A1, PCoA, OphA and leptomeningeal collateral vessels from the PCA. They found that only a small (<1mm) or absent ipsilateral PCoA was a risk factor for ischemic cerebral infarction in patients with ICA occlusion. The other collateral pathways were not found to be associated with the risk of ischemic cerebral infarction.

Hendrikse et al. (2001) found that the presence of collateral flow via the PCoA in the CoW was associated with a low prevalence of border zone infarcts. For the PCoA there was a strong association between the presence of collateral flow and PCoA vessel diameter, whereas no such relation in the anterior part of the CoW was found, indicating that the presence of retrograde PCoA flow may protect against low-flow infarctions. But very low (retrograde) flow in the PCoA is not expected to contribute substantially to cerebral perfusion and has limited value in protecting against low-flow infarcts.

However, other authors found collateral flow via only PCoA was a sign of deteriorated cerebral perfusion (Kluytmans et al, 1999). Hendrikse et al. (2002) also found that collateral flow via the PCoA was not a major collateral pathway in asymptomatic and symptomatic ICA stenosis and consequently did not play an important role in the occurrence of symptoms.

2.1.1.3.2 Collateral function of ACoA

While some authors focused on the importance of collateral flow of PCoA, various authors studied the collateral function of ACoA and found that ACoA was the preferential route of collateral flow in some patients. In the study of Kluytmans et al (1999), the authors concluded that in patients with unilateral ICA occlusion, the pattern of collateral supply had significant influence on hemodynamic status and collateral flow via ACoA was a sign of well-preserved hemodynamic status. Hartkamp et al. (1999) also found that patients with unilateral ICA occlusion had a high prevalence of collateral flow through anterior CoW and significantly increased diameters of communicating channels which showed the importance of ACoA.

Hendrikse et al. (2002) studied 40 patients with severe unilateral ICA stenosis (>70%) and found that patients with an asymptomatic ICA stenosis had a higher prevalence of collateral flow via the ACoA compared with patients with a symptomatic ICA stenosis and control subjects.

2.1.1.4 Collateral capacity of the complete CoW

It is showed that a complete collateral circulation provides better perfusion during carotid occlusion as compared with collateral supply through only ACoA or PCoA in an incomplete CoW (Hoksbergen et al., 1999). Even for the complete circle, the collateral capacity is not the same and dependent on geometrical structure of communicating arteries, such as their lengths and diameters. Those CoW with larger diameters of communicating arteries have better collateral ability than those with smaller ones. Complete CoW affords the patient to tolerate severe stenosis or occlusion of ICA. Therefore, in the patients with severe stenosis or occlusion of ICA complete CoW is often found (Hartkamp et al., 1999). On the other side, incomplete CoW has lower collateral capacity than complete one and therefore, patients with incomplete CoW have less ability to afford severe stenosis or occlusion of ICA.

In conclusion, morphological factors of the CoW, such as the diameter and length of the circle's components, are determinant factors for the collateral capacity of the CoW (Hartkamp et al., 1999). Therefore, the type and number of collateral pathways, or the patency and geometry of communicating arteries play important roles in the status of cerebral hemodynamics of the patients.

2.1.2 Carotid artery stenosis and occlusion

In the individual patient, cerebral hemodynamics is dependent not only on the patency and number of collateral pathways but also on the degree of stenoses of carotid arteries. Battacharji et al. (1967) reported that a significant association between cerebral infarction and hypoplastic collaterals was demonstrated only in a group with stenoses of the carotid and/or vertebral arteries. As the main supply route, the two ICAs supply around 80% of total CBF to brain tissue. Although a well-developed and complete CoW can afford even severe stenosis or occlusion of ICA and prevent patients from ischemic stroke by providing collateral blood supply, the severity of stenosis or occlusion of ICA is the main factor of impairing the cerebral hemodynamics.

The stenosis starts to form first at unilateral ICA (S) or bilateral ICA (SS). With the chronic progress, stenosis of ICA grows and finally becomes occlusion. In unilateral occlusion of ICA (O), the contralateral ICA is stenosis-free. Often is the contralateral ICA not stenosis-free but has different degree of stenosis (OS). When the contralateral ICA stenosis finally becomes occlusion, the patient is in severe condition of bilateral occlusion of ICA (OO). Responding to the development of stenosis of ICA, intracranial hemodynamics is chronically impaired due to the hypoperfusion caused therein. Whether the patients can tolerate severe carotid artery diseases is dependent on the anatomic configuration of CoW and the hemodynamic adaptation of cerebral vasculature. Metabolic factor such as oxygen extraction fraction (OEF) is also a predictive one for the severity of hemodynamic impairment (Derdeyn et al., 1998, 1999b).

Although in patients with stenosis of the ICA, the cause of stroke is primarily thromboembolic, the presence of resulting low regional CBF is also recognized as an additional risk factor (Caplan et al., 1998). The presence of low flow areas in the brain may lead to regionally impaired washout of emboli and, therefore, increased risk of infarction, predominantly in the borderzone areas of the brain. In addition, clinical symptoms due to global hypoperfusion are also found in the literature. AhChong et al. (1999) reported on an 80-year-old patient who has severe carotid artery disease (Occlusion of two main divisions of the left CCA and the right VA; 82% stenosis of right ICA; 60% stenosis of left VA). After excluding other causes of symptoms such as postural hypoperfusion, hypoglycaemia, cardiac arrhythymia, and epileptic seizure, a diagnosis of global ischemia was made. The symptoms of the patient were relieved after CEA.

2.1.2.1 Unilateral and bilateral ICA stenosis (S and SS)

The grade of stenosis of ICA has different influence on the cerebral hemodynamics. In the literature researchers have different classifications about the degree of ICA stenosis. In the study of Zbornikova et al. (1985) 125 patients were classified in groups representing slight (<50% diameter reduction), moderate (50% to 75%), or severe (>75%) ICA stenosis. In the comprehensive survey about the benefit of CEA, Barnett et al. (1998) stratified symptomatic patients into two groups according to the degree of stenosis: severe carotid stenosis (defined as stenosis of 70-99% of the luminal diameter) and moderate carotid stenosis (defined as stenosis of less than 70%). Furthermore, the patients with moderate carotid stenosis were separated into two subgroups: stenosis of 50-69% and less than 50%.

Kluytmans et al (1999) found that patients with severe ICA stenosis (>70%, S and SS) had well-preserved cerebral perfusion and were in general not dependent on collateral supply. Hartkamp et al (1999) also found that from the statistical data even in the patients with severe ICA stenosis (70-99%, S and SS), only very few developed collateral flow through the anterior or posterior circle, indicating that stenosed ICAs are able to provide an adequate contribution. The investigators of the NASCET group have shown that the presence of functional CoW collaterals in patients with ≤70% ICA stenosis is associated with a lower risk of hemispheric stroke and transient ischemic attack, both in the long term and perioperatively (Henderson et al, 2000). For the patients with high-grade ICA stenosis, the flow through stenosed ICA still play an important role in supplying blood. The flow velocities within high-grade ICA stenosis vary depending on the collateral perfusion pressure gradient (Zachrisson et al. 2001) and may be the predictive factor for cerebral hemodynamics (Kamouchi et al., 2005).

2.1.2.2 Unilateral ICA occlusion w/wo contralateral ICA stenosis (O and OS)

In patients with unilateral ICA occlusion and with or without (w/wo) contralateral ICA stenosis (O and OS), the cerebral hemodynamics is significantly impaired. Therefore, the risk of ischemic stroke is high and dependent on the degree of contralateral ICA stenosis and the collateral function of CoW. Many researchers studied clinically the cerebral hemodynamics of this group and lots of conflicting findings were presented. In patients with a unilateral ICA occlusion (O), an evident asymmetry of perfusion pressure between the two ICAs, in combination with increased demand on the occluded side, results in collateral flow in the majority of anterior circles (70%). As the severity of contralateral ICA stenosis (OS) increases, asymmetry in arterial pressure across the anterior circle becomes less evident than in group O, but in

combination with increased demand on the occluded side of the brain, it still brings about flow reversal through the A1 on the occluded side. When only one ICA is occluded (O and OS), the results show that flow in both P1 segments increases, which means both of PCoAs are recruited as collateral pathways and collateral flow is provided from basilar system to carotid systems.

Hartkamp et al. (1999) observed that the prevalence of collateral ACoA flow was higher in group O than it was in group OS, but the prevalence of collateral PCoA flow was similar in groups O and OS. This implies that the anterior circle is the preferential mode of collateral supply for patients with unilateral ICA occlusion (O and OS). They provided a possible explanation that resistance to flow across PCoA was greater than that across the ACoA, because the PCoA was usually a longer vessel. Longer vessels result in an increased resistance to flow that is due to the larger area of endoluminal vessel wall available for friction. But this explanation is dependent on that stenosed ICA still supplies significant blood to the brain.

van Everdingen et al. (1998) studied 57 patients with unilateral symptomatic occlusion of the ICA (O and OS) to evaluate the role of collateral blood flow via the ACoA, PCoA and OphA on cerebral hemodynamics, metabolism, and border zone infarcts. They found that patients with symptomatic ICA occlusion had deteriorated cerebral hemodynamics and metabolism, but different collateral flow patterns via the ACoA, PCoA, or OphA had no effect on the hemodynamic and metabolic parameters, as long as one of these pathways was present.

Kluytmans et al. (1999) had the same finding as that of van Everdingen et al. (1998) that patients with unilateral ICA occlusion (O and OS) had impaired cerebral perfusion, but they found that the pattern of collateral supply had significant influence on hemodynamic status. Hendrikse et al. (2001) selected 51 patients with unilateral occlusion of the ICA and contralateral ICA stenosis between 0% and 69% (OS) for the purpose of assessing whether the presence of border zone infarcts was related to the collateral ability of the CoW. Border zone areas are located in the most distal part of the perfusion territory of the main cerebral arteries or between the deep and superficial supply area of the MCA. They found that the presence of collateral flow via the PCoA in the CoW was associated with a low prevalence of border zone infarcts. No significant relation was found between the pattern of collateral flow via the CoW and the presence of clinical symptoms.

Significant conflicting findings in the literature about the importance of individual collateral flow to patients with unilateral occlusion (O and OS) require further study for the cerebral hemodynamics of this subgroup. The reason of such conflicting findings has been not found in the literature.

2.1.2.3 Bilateral ICA occlusion (OO)

In the bilateral ICA occlusion, CBF is mainly from basilar system. P1 and PCoA of both sides are the main routes of CBF. In the study of Hartkamp et al. (1999) it was found that patients with bilateral ICA occlusion relied on collateral flow via the posterior CoW. They observed a bilateral increase in PCoA diameters, which demonstrated that the PCoA was more important in cases of bilateral ICA occlusions than it was in cases of unilateral ICA occlusion. In patients with bilateral occlusion,

asymmetry in arterial pressure between the symptomatic and asymptomatic ICA does not apply or is negligible. Kluytmans et al (1999) found that in their study patients with bilateral ICA occlusion had severely compromised hemodynamic status despite recruitment of collateral supply.

When the ICA is occluded on both sides, the pressure difference between two hemispheres is likely to be canceled out. This explains why many patients with bilateral ICA occlusion do not have collateral flow via the A1 segment. Rutgers et al. (2000a) found that in patients with bilateral ICA occlusion collateral flow via the A1 segment was demonstrated in 0% to 11% of patients, and collateral flow via the PCoA was demonstrated in 67% to 78% of patients. Probably, other collateral pathways were important, such as OphAs and leptomeningeal anastomoses or connections between the internal and external carotid arteries. In the study of Rutgers et al. (2000a) nearly all the patients with bilateral ICA occlusion were found collateral OphA flow. Also, in the study of Hartkamp et al (1999), 7 of 9 patients with bilateral ICA occlusion showed retrograde flow through the ipsilateral OphA. Therefore, it is likely that in patients with bilateral ICA occlusion, collateral flow via both the PCoA and OphA is important. But collateral flow via OphA is often regarded as a marker of insufficient cerebral perfusion. Available data shows that leptomeningeal anastomoses may be important in understanding stroke mechanism and plays an important role in penumbra outcome. However, the literature shows no consensus between statements on the existence of leptomeningeal anastomoses and compensatory capacity (Brozici et al., 2003).

2.1.3 Hemodynamic adaptation

In patients with carotid artery disease and anatomic anomaly of the CoW, cerebral hemodynamics is significantly impaired. Although well-developed CoW protects the patients from ischemic stroke, there are a lot of patients without well-developed CoW. Anomaly of CoW only provides limited collateral capacity and increases the risk of ischemic stroke for patients with severe carotid artery disease. Cerebrovascular system has the ability of self-protection to adapt the impaired cerebral hemodynamics, mainly low CPP, by reducing the total cerebral vascular resistance. In the downstream of CoW, CA enlarges the diameters of arterioles to reduce the distal cerebral resistance. In the CoW itself, the ability of remodeling is able to improve the collateral ability by increasing the diameters of critical components of the CoW.

2.1.3.1 Cerebral autoregulation and vasomotor reactivity

CA has been studied widely in the literature (Newell et al, 1994; Kirkham et al, 2001; Simpson et al, 2001; Liu et al., 2003). Well preserved CA provides protection from acute change of CPP resulting from, for example, sudden standing up or sitting down. For the chronic hypoperfusion due to ICA stenosis or occlusion and anomaly of CoW, CA continuously enlarges the diameters of arterioles and impairs the ability of VMR.

Among the first to study the relationship between dynamic CA and impaired cerebral hemodynamics, Reinhard et al (2003a) found that dynamic CA was substantially impaired if secondary collateral pathways were activated. Then Reinhard et al. (2003b) studied 30 patients with severe bilateral carotid stenosis ($\geq 75\%$) or occlusion and found that the dynamic CA was severely impaired in the patients with bilateral critical carotid stenosis (90-100%) or occlusion. The patients were separated from two groups

according to the degree of stenosis, 75-89% and 90-100%. They found that the degree of stenosis played an important role for the status of dynamic CA.

The absence of functional collateral pathways has been associated with a reduction in ipsilateral CA (White et al., 1997; Hartl et al., 1995). Exhausted CA was significantly associated with either low CPP or vasospasm. But it is not clear about whether exhausted CA is an independent predictor of a bad outcome. Impairment of VMR results from loss of the ability of vasodilation of arteriole and precapillary. There is good evidence that exhausted VMR is an independent risk factor for stroke even in patients with asymptomatic carotid artery stenosis.

It has been shown that in patients with symptomatic ICA stenosis, absence of collateral flow via the CoW and impaired VMR are both associated with increased stroke risk (Markus et al., 2001; Silvestrini et al., 2000; Henderson et al., 2000). Using multivariate statistics, Silvestrini et al. (2000), Vernieri et al. (2001) and Markus et al. (2001) demonstrated that reduced VMR was an independent predictor of stroke and that only a few other factors like female gender and the number of collateral pathways (inverse correlation) could also be established as independent risk factors. Diehl (2002) also concluded that reduced VMR (and probably also CA) was obviously an important risk factor for ischemic stroke. But they suggested that VMR or CA investigations should guide therapeutic decisions only in clinically uncertain cases, e.g. in patients with borderline evidence for symptoms caused by an ICA stenosis. Since it has to be shown whether the stroke risk in these patients can be lowered by CEA, testing of VMR or CA before CEA could become an obligatory diagnostic tool in patients with asymptomatic carotid artery disease.

The shape of the autoregulative curve for CBF vs. CPP is of value for researchers who are interested in averaged hemodynamic parameters. Gao et al. (1998) built up a four-compartment autoregulation device model which simulated small arteries and arterioles. The model predicted an autoregulation function similar to experimental data with respect to the LLA, ULA and average slopes of the autoregulation curve below LLA and above ULA. The autoregulative model described the relationship between CBF and CPP under the conditions of perfusion pressure change of 40mmHg to 200mmHg. They found that during the range of 69-153mmHg of CPP, CBF was regulated by autoregulation.

2.1.3.2 Remodeling of CoW morphology

Besides the hemodynamic adaptation of distal parts of the CoW, the components of CoW are also able to remodel to adapt local change of hemodynamic status (Quick et al., 2000). The type of remodeling (enlargement/shrinkage) influences the lumen in all artery types that are prone to develop atherosclerotic lesions. The impact of remodeling on percent luminal stenosis differs among artery types and may therefore be considered as a regionally determined process (Pasterkamp et al., 1997).

The increase of CoW vessel diameters is frequently found in the clinical studies. Hartkamp et al. (1999) found the general trend toward increasing diameters of the communicating channels. The results from their studies indicate that remodeling of CoW morphology does occur. Furthermore, an increased diameter of the ACoA was found in asymptomatic patients with ICA occlusion (Hendrikse et al., 2001) and with ICA stenosis (Hendrikse et al., 2002). There was an association of the ACoA vessel

diameter and the presence of collateral flow via the ACoA. The potential of the collateral arteries in CoW to increase in size is regarded as a mechanism to adapt to hemodynamic changes (Coyle et al., 1990; Symon et al., 1971; Derdeyn et al., 1999a). An extrapolation to the remodeling of CoW vessels is that morphological factors play determinant roles in the collateral function of the CoW.

2.1.4 Surgical treatment in improving cerebral hemodynamics

Anomaly of the CoW impairs the collateral capacity, which may make the patients with severe ICA stenosis or occlusion incapable to tolerate compromised cerebral hemodynamics indicated by severely impaired CA or VMR. For the patients with significantly impaired CA or VMR, medical treatments may fail to provide better protection than vascular surgery. CEA is a conventional surgical method to remove the atherosclerotic plaque which narrows or occludes the ICA. Before the CEA, assessment of the cerebral hemodynamics is recommended after diagnosis of severe carotid stenosis to further investigate and evaluate whether these patients may benefit from CEA (Blaser et al., 2002).

Two possible favorable effects of CEA have been recognized. First, CEA removes the atheromatous plaque, which is a possible source of cerebral emboli (Caplan et al., 1998). Another more hypothetical explanation of the beneficial effect of CEA is the restoration of the cerebral perfusion pressure. Although the importance of the latter is questionable, many studies have shown improved hemodynamics after CEA (Vriens et al., 2001). Reduction of the CA, VMR, cerebral perfusion, and decreased CBF do suggest that at least in some patients CEA may improve the hemodynamic status of the brain.

There are many factors which play roles in determining whether the patients need the operation. Some authors only consider the degree of ICA stenosis. The initial results from the North American Symptomatic Carotid Endarterectomy Trial (NASCET) reported in August 1991 demonstrated a highly beneficial effect of CEA in patients with angiographically confirmed high-grade carotid stenosis (70 to 99%). The final results for patients with high-moderate degrees of stenosis (50 to 69%) revealed modest benefit from CEA. Kluytmans et al. (1998) reported that although CEA did improve the cerebral circulation in patients with a severe ICA stenosis and a contralateral ICA occlusion, the hemodynamic effects of CEA in patients with severe ICA stenosis but without a contralateral ICA occlusion were negligible.

Although CEA has proven to be the most effective means for stroke reduction because of significant atherosclerotic disease of the carotid artery, continued enthusiasm for performance of CEA is dependent upon maintaining a low morbidity and mortality. For patients undergoing CEA, there is a risk that the operation itself may cause neurological complications resulting from embolization, cerebral hypoperfusion during carotid clamping, or hyperperfusion after the release of the clamp (Spencer et al., 1997).

One potential source of procedure-related stroke is cerebral ischemia once the CCA is clamped to perform the CEA. Methods to determine significant intraoperative cerebral ischemia during CEA include neurological exam under regional or local anesthesia, internal carotid artery back pressure measurement, continuous electroencephalographic (EEG) monitoring and continuous transcranial Doppler

monitoring. If these techniques determine that the collateral blood flow to the ipsilateral hemisphere is insufficient, then the majority of vascular surgeons will place a temporary intraluminal shunt during the procedure. It has been observed that approximately 10-20% of patients undergoing CEA will not tolerate cross-clamping of the ICA and will require placement of an intraluminal shunt to prevent intraoperative cerebral ischemia. (Hobson et al, 1974; Evans et al, 1985).

Flow differences between patients who need intraluminal shunt and patients who do not during cross-clamping of the carotid artery were studied by some authors. Rutgers et al. (2000b) found that preoperative volume flow in the clamped ICA was significantly higher in CEA patients with ischemic EEG changes (need intraluminal shunt) during clamping than in CEA patients without such changes. The latter patients probably have better developed collateral pathways preoperatively. Vriens et al. (2001) studied 148 patients with ICA stenosis $\geq$70% and undergoing CEA and found that after CEA, flow redistribution expressed by changes in blood flow velocity values occurred in the CoW. The redistribution of flow was most pronounced in patients who needed intraoperative shunting and in patients with a contralateral ICA occlusion. In addition, the contribution of collateral sources was diminished, and the CO_2 reactivity increased, both of which reflected improvement of the hemodynamic condition.

Hyperperfusion syndrome is an uncommon but serious complication that is seen primarily in patients with preoperative long-standing cerebral hypoperfusion secondary to high-grade ICA stenosis and poor collateral capacity of the CoW (Nielsen et al., 1995). In these patients, CA might be exhausted, which lead to a state of hyperperfusion after removal of the carotid stenosis. Zachrisson et al. (2002) found

that soon after CEA a flow velocity increase was often seen bilaterally in the anterior part of the CoW. The clinical significance of bilateral flow velocity increases is uncertain, but in some situations it might be a clinically useful signal to increase surveillance for hyperperfusion syndrome.

Despite the vast body of literature on the value of selective shunting, little is known about the anatomical defects in collateral circulation that contributes to the need to shunt in selecting patients during CEA. Some authors concluded that angiographic determination of inadequate collateral cerebral circulation correlated strongly with cerebral ischemia during CEA. Depippo et al (1999) studied the association between the integrity of the CoW and ICA back pressure and targeted to determine whether the CoW with different configuration was able to provide adequate collateral cerebral circulation during CEA. Patients with an ICA back pressure < 50mmHg had an intraluminal shunt placed. They found that only one of 35 patients had a completely intact CoW and flow was absent in one or both PCoAs in 88% of patients while one or both A1 segments were occluded in 45% of patients. In conclusion, the CoW is rarely intact in patients undergoing CEA. Deficiencies in the CoW could be associated with intraoperative cerebral ischemia during CEA when evaluating collateral blood flow to the brain using MRA. If either the anterior or posterior segments of the circle are intact, then it is likely that the patient will not develop cerebral ischemia after cross-clamping the CCA. However, if both the anterior and posterior segments are not intact, then it is likely that the patient will suffer cerebral ischemia in the ipsilateral cerebral hemisphere during CEA and require placement of an intraluminal shunt. Kim et al. (2002) found that in patients with either an ACoA or a PCoA, 7.3% of them required shunting and in patients with neither ACoA nor PCoA, 83.3% required shunting.

When a stenosis or occlusion of the ICA progresses slowly, secondary collateral pathways other than the CoW may be recruited and preserve cerebral perfusion. However, OphA collateral was found a marginal effect on the compensation of cerebral perfusion (Tatemichi et al., 1990). Leptomeningeal collateral is recruited only in the chronic ICA artery disease (Brozici et al., 2003). Therefore, these connections do not contribute significant cerebral collateral blood flow under circumstances of acute occlusion of the CCA, as occurs during CEA when CCA is clamped. Thus, the CoW is the principal collateral pathway, which maintains cerebral perfusion in the event of ICA occlusion. Therefore, the number and patency of the vessels of the CoW may be risk factors for cerebral ischemia or infarction in patients undergoing CEA.

Operating CEA needs very skilled hands and the success of operation is in part dependent on the patient selection. One part of the difficulties for clinicians in determining whether to choose surgical treatments for patients with severe impaired cerebral hemodynamics is the insufficient information about the cerebral hemodynamics of the patients. Since clinical studies have found that a surgical treatment to remove the atherosclerotic plaque will benefit the patients with severe carotid artery disease (Visser GH et al., 1997), thorough evaluation of preoperative, intraoperative and postoperative cerebral hemodynamics increases the possibility of success of CEA.

2.2 Review about cerebrovascular modeling

Over the past several decades, cerebrovascular modeling has been frequently used to study the hemodynamics in CoW. Previous cerebrovascular modeling aimed at providing analyses and descriptions of the main mechanisms involved in intracranial

dynamics and clarifying their mutual inter-relationships (Ursino, 2003). Recently, researchers start to explore the clinical application of computer model. Regarding the value and future direction of cerebrovascular modeling, Ursino (2003) summarized his 15 years of working on cerebrovascular modeling and concluded that cerebrovascular models should try to enter into real clinical settings, providing a support for neurosurgeons and anesthesiologists in the management of cerebrovascular disease. He also pointed out the necessity to overcome the gap between accuracy and simplicity in modeling studies, which is possibly the main challenge that future research should be able to deal with and overcome. It was also suggested by Ursino (2003) that the presentation and functioning of cerebrovascular models should be simple enough to engender their interest and acceptance by a larger number of medical users.

Mathematical models of blood flow in the CoW have usually taken into account nonlinear and unsteady aspects of blood flow in a network of elastic vessels. The results from these models showed consistency with the available clinical data and thus appeared as a possible clinical tool for improving the understanding of the various data given by clinical tests in an individual patient.

Dickey et al. (1996) built up a computer model of cerebral circulation to address the difficulty in predicting the adequacy of the collateral blood flow in patients who underwent ICA occlusion. This model can predict changes in flow that will occur during ICA occlusion and may help clinicians predict the adequacy of collateral blood supply in patients who undergo ICA occlusion. Kailasnath et al (1998) evaluated this model with data from angiograms of 14 patients who underwent CEA. The authors

concluded that mathematical models of the cerebrovascular circulation could provide good predictions of intravascular pressure in the collateral circulation, and might provide accurate predictions of the flow as well. Dr. Charbel gave his comments on this paper that "Computerized modeling of the cerebral circulation is conceptually a worthwhile endeavor. Choosing the optimal surgical technique and/or avoiding unnecessary surgery are two advantages that such modeling may provide in reducing complications". To explore the clinical application of computer model, Charbel et al. (2004) built up a patient-specific blood flow modeling to identify patients in whom balloon occlusion test (BOT) would not be tolerated. The results showed that the patient-specific computer model could be used to identify patients who have an elevated risk of ischemic stroke during the BOT.

Since Euler introduced the one-dimensional modeling of the human arterial system in 1775, the one-dimensional computations have been used by many researchers and attention has turned to improving the basic model. Topics regarding improvement on the one-dimensional modeling include improvement of friction term and tube law, linearity and nonlinearity, description of stenosis, simulation of bifurcation, etc. Pedley (2003) reviewed the mathematical modeling of arterial fluid dynamics and concluded that, in understanding the pulse propagation of blood flow in vasculature, benefits still can be expected from one-dimensional model, especially for those who only care about averaged parameters. Chao and Hwang (1971) built up a one-dimensional model of the CoW of the dog and tested its performance by intravascular pulse pressure directly measured from the dog's right carotid artery. They were encouraged by the results because the relative pressure drop and flow distribution at

each of the junctions were comparable with clinical data both in magnitude and waveforms.

To understand the function of the CoW in healthy humans, Hillen et al (1982) built up a nonlinear one-dimensional mathematical model in which they only studied the function of one PCoA in part of CoW with stenosis of VA. Then Hillen et al (1986) extended the model to the complete CoW and studied the hemodynamic changes of the CoW due to asymmetry of PCoA. Last, Hillen et al (1988) showed how a steady model can lead to similar results as the non-steady one. In their studies, they concluded that the flux in the efferent arteries was governed by the ratio of the peripheral resistances and the flux in the afferent arteries and in the segments of the circle itself were strongly influenced by their own morphological factors.

Zagzoule and Marc-Verges (1986) built up a nonlinear one-dimensional model which included not only the CoW, but the pial network, intracerebral arteries, microcirculation and venous network. In the model they explored the function of autoregulation during hypotension. Cassot et al. (1995) used two different mathematical models to study the hemodynamic effects of the diameter of ACoA in the CoW with obstructive lesions of the ICAs. They found that ACoA diameter strongly modulated the effects of ICA lesions on cerebral hemodynamics and concluded that some proposals for CEA indications could be derived from their study.

By studying simultaneously the importance of ACoA and PCoAs in the collateral ability of CoW, Viedma et al (1997) demonstrated the need for a simultaneous consideration of both alternative flow paths (ACoA and PCoA) to the affected

hemisphere. More recently, Cassot et al (2000) developed a linear mathematical model to simulate blood flow through the CoW. In this model the influence of the ICA lesions and the role of communicating arteries on the blood pressure at the entry of the cerebral territories were quantified and analyzed. They concluded that such a model might be an essential tool for an accurate assessment of the cerebral hemodynamics in carotid diseases. But Piechnik et al (2002) pointed out some problems in application of purely linear models in cerebral circulation.

Since one-dimensional model has been extensively applied in the blood pulse propagation in compliant arteries, some authors has turned to improve the basic model. Much more recently, Sherwin et al (2003) investigated a one-dimensional model of a vascular network based on space-time variables and derived the appropriate nonlinear matching conditions at a bifurcation, assuming that there is no energy loss therein. Formaggia et al. (2003) also studied a family of one-dimensional models for blood flow in arteries.

While one-dimensional vascular system offers important insight into the physiological behavior of the hemodynamics in the human vascular system, multi-dimensional simulation of hemodynamics in the CoW has gained a great deal of attention over the last decade (Formaggia et al., 1999). Ferrandez et al (2000) developed a two-dimensional and steady model of the CoW with solid arteries. The model was used to simulate different common abnormalities of the CoW while a range of varying boundary conditions was imposed to the right ICA. The authors concluded that by this model it was possible to provide clinicians for a priority list of the severity of the flux reduction for the considered abnormalities for different degrees of the stenosis of the

right ICA. The authors found that the redistribution of blood via the CoW was mainly driven by changes in the vascular resistance of the brain rather than in the local arterial geometry. The use of valid peripheral resistances allowed for a more realistic model of the CoW but also highlighted the need for more accurate means to estimate the vascular resistance of a patient. Based on this model Ferrandez et al (2002) developed a two-dimensional time-dependent computational model of the CoW. They added a new "active" boundary condition in the model to simulate not only the peripheral resistance of the cerebrovascular tree but also its autoregulation function. David et al. (2003) applied their numerical model in the clinical studies and showed how a numerical simulation could be used to explain why the PCoAs had poor visibility in certain patients and how it could also provide guidelines in devising a different MR protocol to improve the results of the imaging process.

Cebral et al. (2003) presented a new image-based methodology for patient-specific models of the cerebral circulation and concluded that realistic patient-specific models could provide new insights into the cerebral hemodynamics. The methodology was illustrated with a finite element model constructed from magnetic resonance image data of a normal volunteer. They considered their work as a starting point in the development of realistic models that could be applied to the study of cerebrovascular diseases and their treatments. However, several challenging limitations still remained to be resolved in the future for this methodology.

To simulate the cerebrovascular system, the mathematical model has to be simple enough to allow for a numerical treatment at reasonable computational costs. For this reason, only major arteries are considered in numerical models and small arteries and

microcirculation are substituted by lumped resistance model. There is no doubt about the property of non-linearity of cerebral hemodynamics, but some authors think the effect of non-linearity is insignificant and therefore, they choose linear mathematical model to study the cerebral hemodynamics. Nevertheless, other authors think the non-linearity effect is significant and can not be neglected. Otherwise, significant error could be deduced from the linear model. Giller et al. (2003) studied the linearity and non-linearity in cerebral hemodynamics and found that there is strong evidence that the blood pressure and velocity system is non-linear.

2.3 Review about In vitro experimental investigation

To the best of our knowledge, only has one publication been found in the literature about the in vitro experimental study of the role of collateral pathways in the cerebral hemodynamics, but the details of the experiment was not given (Bossuet et al., 1997). Clinical studies and numerical simulations have shown that the CoW is an important determinant of cerebral hemodynamics distal to severe lesions of the ICA. Nowadays, we are still unable to in vivo validate these kind results, due to the lack of resolution of cerebral imaging systems. The only alternative would be an in vitro experimental validation.

Due to the protective encasement of the skull, invasive measurements on the flow rate and pressure distribution in the brain are impossible. Thanks to recent development in image monitoring systems, such as Digital Subtraction Angiography (DSA), TCD and Magnetic Resonance Angiography (MRA), it has made it available in vivo noninvasive measuring blood velocity and flow rate. Usually investigators use hydrodynamic models to simulate the blood flow in the arteries. The factors involved

in experiments include vessels, blood, impulse generator like heart, terminal resistance in the end of vessel and transducers.

Since in vitro experimental studies about the hemodynamics of CoW are seldom found in the literature, we review some previous in vitro experimental studies about flow phenomenon in elastic tubes which are used to simulate the vessels. Traditionally investigators would use some substitutions for vessels, blood and heart. Hayashi et al. (1980) used the real vessels from autopsy subjects to investigate the relationship between pressure and cross-sectional area of the vessel. And a non-linear expression, which describes the relationship between pressure and area in logarithm, has been formulated.

Few people have the opportunity of doing investigation on real vessels, because there is a complicated procedure in getting and storing the real vessels. Liepsch (1985) and Reuderink et al. (1989) took a cylindrical latex rubber tube as the substitution for the vessel to study the pressure wave propagation in arteries. In their experiment, they used an impulsator at the entrance of the tube and a resistor at the exit of the tube. Flow rate and pressure in different locations of the tube were also measured by invasive methods. Invasive methods in measuring flow rate and pressure always introduce errors into the results. Therefore, investigators began to apply non-invasive technologies to measure velocity in tubes. Siouffi et al. (1998) and Deplano et al. (1999) used the pulsed Doppler ultrasonic velocimetry to study the post-stenotic velocity flow field corresponding to oscillatory, pulsatile and physiological flow waveforms. Botnar et al. (2000) investigated the blood flow velocity in the carotid artery bifurcation by magnetic resonance imaging (MRI) and compared the results

with that of a numerical model. In the experiment, they used an anatomically realistic replica of a human carotid artery bifurcation (true-to-scale elastic model) made from silicon rubber. It was cast in a box filled with 1.5% agarose gel and then a model with nearly rigid walls arose. In order to mimic the rheologic properties of blood, they used a water-glycerin mixture with a kinematic viscosity of $\nu = 0.037\ cm^2/s$. A programmable step motor driven pump was also used as impulsator. Recently some researchers investigated the viscoelasticity of the vessel using flexible tube (Bassez et al. 2001). Khir and Parker (2002) set up an experiment to investigate the wave speed and reflected waves in elastic tubes and bifurcations, and this experiment was also used to verify their numerical model (Khir et al., 2001).

Bossuet et al. (1997) conducted an in vitro experimental study about cerebral hemodynamics in the CoW. In the experimental investigation they physically built up the CoW using a plane network of 20 tubes bored through two Perspex half plates. The sizes of tubes were equal to those of normal human vessels. Peripheral resistances at output of efferent vessels, ICAs stenosis or occlusions and the diameter of the ACoA were variable parameters in the physical model. The network model was enclosed in a circulatory loop, enabling to simulate physiological unsteady flows, pressure waveforms and viscosity. Instantaneous pressure signals, velocity profiles and volume flow were measured at a number of locations in the network. In this publication, the procedures and details of results were not given. But they presented the results of comparison between experimental measurements and numerical results and found the experimental measurements supported that ACoA was the preferential route of collateral pathway.

Chapter 3

Numerical model

As aforementioned in section 2.2, one-dimensional numerical model has been widely used to study cerebral circulation in clinical application and physiological research. Based on the literature, this chapter introduces the procedures of building up the numerical model using MATLAB. After comparing three friction terms and two tube laws obtained from the literature in a single vessel, Poiseuille's friction term and linear tube law are used in the numerical model of vascular network. Numerical results of normal CoW are given at the end of this chapter.

3.1 Assumptions in the numerical model

3.1.1 One-dimensional assumption

Blood flow in arteries is expressed as wave propagation in elastic tubes. Since the wavelength of blood flow is very long (5-10m, Nichols et al., 1997) compared to the small diameter of the vessels (Max. 4mm in this study), the slope of the deformed tube wall remains to be very small at all times. For the shape of vessels, it is assumed that the local curvature is everywhere small enough so that the propagation in a single vessel could be assumed to be one-dimensional. In addition, at the bifurcations of the CoW, there exists energy loss resulting from the change of flow direction and the tapering of vessels. It is assumed that this kind of energy loss compared to the energy transferred by the wave propagation is small so that we can assume that there is no energy loss at the bifurcation and neglect the influence caused by the effect of

bifurcation and tapering. Therefore, the whole vascular network can be assumed as one-dimensional.

3.1.2 Simplification of the geometry of the CoW

MRA shows that there are four main afferent arteries and six main efferent arteries in the CoW. For the CoW itself, there are seldom branches, see Figure 3.1. Since the cerebrovascular resistance is determined mainly by distal areas of the CoW, the small branches of the CoW are neglected. Hence, the CoW can be simplified as that shown in Figure 1.4.

Figure 3.1 Magnetic resonance angiography of the CoW

3.1.3 Newtonian fluid assumption for blood

A Newtonian liquid is, by definition, one in which the coefficient of viscosity is constant at all rates of shear (Nichols et al., 1990). Most homogenous liquids have such property such as air, other gases, alcohol, water in normal temperature and pressure, but suspensions of particles show deviations from it, especially when the particle size becomes appreciably large compared with the diameter of the tube in

which it is flowing. Blood, as a suspension of cells in plasma, is essentially non-Newtonian fluid. It shows two kinds of anomalous viscous properties (Nichols et al., 1990):

(1) At low shear rates, the apparent viscosity increases markedly.

(2) In small tubes the apparent viscosity at higher rates of shear is smaller than it is in larger tubes. This progressive diminution with tube size begins to be detectable with tubes of less than 1mm internal diameter and becomes marked in tubes of the order of 100-200 um in diameter.

These two types of anomalies may be referred to as the ‘low shear’ and ‘high shear’ effects. They are usually responsible for the errors introduced into the hydrodynamic analysis that assumes Newtonian viscosity of blood. For the first anomaly, investigators come to the conclusion that normal values of shear rate in circulation are too high for it to have significance. For second one, the anomaly occurs only in microcirculation—“small vessels”. In our study, we are focusing on the cerebral arteries whose diameters are much larger than the dimensions of cells in plasma which has been considered as a Newtonian viscous fluid, and the shear rate is more than 400/s which is high enough, therefore these two anomalies of blood viscosity can be neglected. So far most researchers consider blood as Newtonian fluid except when they study microcirculation in capillary (Rohlf et al., 2001).

3.2 Numerical model of single vessel

3.2.1 Governing equations of single vessel

The derivation of governing equations in a single elastic tube is taken from the literature (Fung, 1997) and given as follows. Considering an infinitely long, straight,

isolated, cylindrical, elastic tube containing a homogenous, incompressible, and viscous liquid, and assuming a disturbance as waves is propagating along the tube at a finite speed, we study a small segment from the tube at any site.

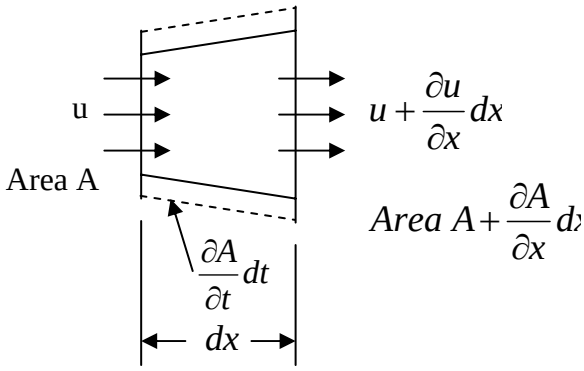

Figure 3.2 (a)

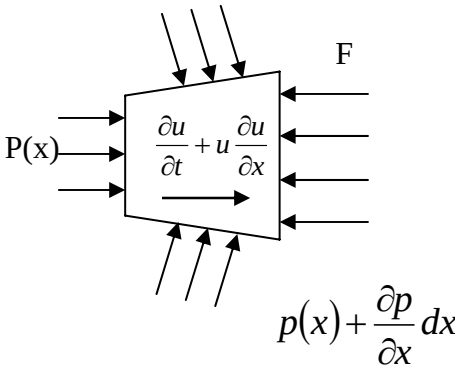

Figure 3.2 (b)

Figure 3.2 Diagram of a segment of elastic tube

We first consider the conservation of mass in a segment of the tube of length Δx , as illustrated in Figure 3.2(a). In a unit time,

$$\underbrace{\rho\{uA+[\partial(uA)/\partial x]dx\}}_{Efflux\ at\ the\ right}-\underbrace{\rho uA}_{Influx\ at\ the\ left}=\underbrace{\rho(\partial A/\partial t)dx}_{Change\ of\ volume\ in\ this\ segment} \tag{3.1}$$

Next, consider the balance of forces acting in the axial direction on a fluid element of length Δx and cross-sectional area A. A free-body diagram is shown in Figure 3.2(b). According to Newton's law,

$$\underbrace{pA}_{\substack{\text{Force acting}\\ \text{on the}\\ \text{left end}}} \underbrace{-\left[p+(\partial p/\partial x)dx\right]\times\left[A+(\partial A/\partial x)dx\right]}_{\substack{\text{Force acting on}\\ \text{the right end}}} + \underbrace{p(\partial A/\partial x)dx}_{\substack{\text{Axial force caused by}\\ \text{the pressure acting}\\ \text{on the lateral sides}}} - \underbrace{F}_{\substack{\text{Viscous}\\ \text{force}}} = \underbrace{\rho A dx}_{\text{Mass}} \times \underbrace{(\partial u/\partial t + u\partial u/\partial x)}_{\substack{\text{Acceletation caused}\\ \text{by the net force}}} \quad (3.2)$$

Rearranging (3.1) and (3.2) and neglecting the second order term, we obtain the governing equations as follows:

Conservation of mass
$$\frac{\partial A}{\partial t}+\frac{\partial (Au)}{\partial x}=0 \quad (3.3)$$

Conservation of Momentum
$$\frac{\partial u}{\partial t}+u\frac{\partial u}{\partial x}+\frac{1}{\rho}\frac{\partial p}{\partial x}=-F \quad (3.4)$$

The elastic property of the vessel wall is modeled by a functional relationship between P and A in the normal manner:

$$A=A(p). \quad (3.5)$$

Substitution of equation (3.5) in equation (3.3) and (3.4) yields a set of two nonlinear partial differential equations for p and u:

$$\frac{\partial p}{\partial t}+u\frac{\partial p}{\partial x}+\rho c^2\frac{\partial u}{\partial x}=0 \quad (3.6)$$

$$\frac{\partial u}{\partial t}+u\frac{\partial u}{\partial x}+\frac{1}{\rho}\frac{\partial p}{\partial x}=-F \quad (3.7)$$

where
$$c^2=c^2(p)=\frac{A(p)}{\rho * A'(p)} \quad (3.8)$$

These sets of equations are often applied to describe the cerebral blood flow in arteries. In the equations, u denotes average fluid velocity over the cross-section area A, p transmural pressure, c wave velocity, and ρ blood density. These equations constitute a hyperbolic set, that is, they can be written in the two characteristic forms

$$\frac{dp}{dt} \pm \rho c * \frac{du}{dt} = \mp \frac{8\pi\mu uc}{A(p)} \qquad (3.9)$$

along characteristics satisfying $dx/dt = u + c$. These characteristic forms involve only ordinary differentiation and they are the basis for the Method of Characteristics (MOC). Many authors used MOC to solve this set of Equations (Skarbek-Wazynski, 1981; Hillen et al., 1982), but they usually neglect the convection terms in the equations. And the wave velocity c and cross-sectional area A are usually considered as constant. Here we are not of interest in repeating the process of MOC.

3.2.2 Discretization of the equations and stability of the numerical method

The governing equations are solved using two-step Lax-Wendroff scheme. Here we show the discretization forms of the governing equations (3.3) and (3.4). We also apply the governing equation (3.6) and (3.7) in the program, and there is no difference between their outputs. The figures from the two sets of equations at any time and any point are completely overlapped. When we use equations (3.3) and (3.4), because the input and output signals are from pressure, we need to transform the pressure signals into cross-sectional area signals at the beginning. Although this increases the procedure in program, we choose equations (3.3) and (3.4) for the convenience of

writing the sub-program of tube law. The sub-program is very convenient for us to discuss different tube laws in a single vessel. Following are the discretization forms of the equations (3.3) and (3.4):

Step I

$$A_{i+\frac{1}{2}}^{n+\frac{1}{2}} = \frac{A_i^n + A_{i+1}^n}{2} - \frac{\Delta t}{2\Delta x}\left(A_{i+1}^n u_{i+1}^n - A_i^n u_i^n\right) \tag{3.10}$$

$$u_{i+\frac{1}{2}}^{n+\frac{1}{2}} = \frac{u_i^n + u_{i+1}^n}{2} - \frac{\Delta t}{2\Delta x}\left[\left(\frac{u^2}{2} + \frac{p}{\rho}\right)_{i+1}^n - \left(\frac{u^2}{2} + \frac{p}{\rho}\right)_i^n\right] - \frac{\Delta t}{2} F_{i+\frac{1}{2}}^n \tag{3.11}$$

where

$$F_{i+\frac{1}{2}}^n = \frac{8\pi\mu}{\rho}\frac{\left(\frac{u_{i+1}^n}{A_{i+1}^n} + \frac{u_i^n}{A_i^n}\right)}{2} \tag{3.12}$$

$$p_{i+\frac{1}{2}}^{n+\frac{1}{2}} = E_l\left(\frac{A_{i+\frac{1}{2}}^{n+\frac{1}{2}} - A_0}{A_0}\right) \tag{3.13}$$

Step II

$$A_i^{n+1} = A_i^n - \frac{\Delta t}{\Delta x}\left[(Au)_{i+\frac{1}{2}}^{n+\frac{1}{2}} - (Au)_{i-\frac{1}{2}}^{n+\frac{1}{2}}\right] \tag{3.14}$$

$$u_i^{n+1} = u_i^n - \frac{\Delta t}{\Delta x}\left[\left(\frac{u^2}{2} + \frac{p}{\rho}\right)_{i+\frac{1}{2}}^{n+\frac{1}{2}} - \left(\frac{u^2}{2} + \frac{p}{\rho}\right)_{i-\frac{1}{2}}^{n+\frac{1}{2}}\right] - \Delta t F_i^{n+\frac{1}{2}} \tag{3.15}$$

where

$$F_i^{n+\frac{1}{2}} = \frac{8\pi\mu}{\rho}\frac{\left[\left(\frac{u}{A}\right)_{i+\frac{1}{2}}^{n+\frac{1}{2}} + \left(\frac{u}{A}\right)_{i-\frac{1}{2}}^{n+\frac{1}{2}}\right]}{2} \tag{3.16}$$

$$p_i^{n+1} = E_l\left(\frac{A_i^{n+1} - A_0}{A_0}\right) \tag{3.17}$$

The i subscript indicates internals in distance x along the vessel and n superscript denotes the time step. Since the transmural pressure depends solely upon the local cross-section and not upon its derivatives, according to the property of Two-step Lax-Wendroof scheme and the characteristics of the governing equation, the hyperbolic stability criterion is $\left|(|u|+c)\frac{\Delta t}{\Delta x}\right| \le 1$.

3.2.3 Initial conditions and boundary conditions

Since the governing equations are a set of hyperbolic equations, we need two boundary conditions and one initial condition with respect to each dependent variable. We consider the fluid in a finite, straight and viscoelastic tube, and the fluid is of unsteady, viscous, laminar and nonlinear. At the beginning, there is no blood flow in the vessel and the pressure along the whole vessel equals to diastolic pressure p_d. A periodic pressure signal p_{in} begins to propagate into the vessel from the proximal end at the beginning. Therefore, the boundary conditions and the initial condition of the pressure and velocity are shown in table 3.1.

Table 3.1 Boundary and initial conditions of the numerical model

	Boundary condition at the proximal end	Boundary condition at the distal end	Initial condition
Pressure	p_{in}	Output pressure p_{out} calculated by a lumped resistance	p_d
Velocity	Uncentered approximation	Uncentered approximation	Zero

Figure 3.3 shows the figure of the input pressure p_{in}. This figure was obtained from the literature where it was given as the pressure signals in the brachiocephalic artery and was smoothed to eliminate the original spurious oscillations (Hillen et al. 1982). According to the physiological properties of the pressure in human brain, the maximum, the minimum and the period of the input pressure are defined in 120 mmHg, 80 mmHg and 1 second, respectively.

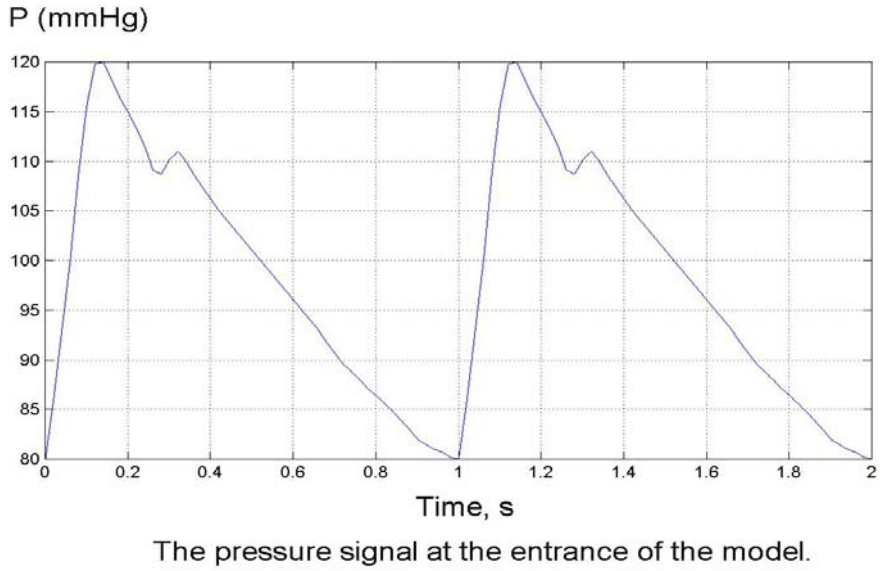

Figure 3.3 Input pressure waveform (Hillen et al., 1982)

The output pressure p_{out} was calculated by applying a lumped peripheral resistance in the unknown section shown in Figure 3.4. It is assumed that the resistance between output pressure and venous pressure is constant. Figure 3.4 gives a simplification of total arterial vasculature.

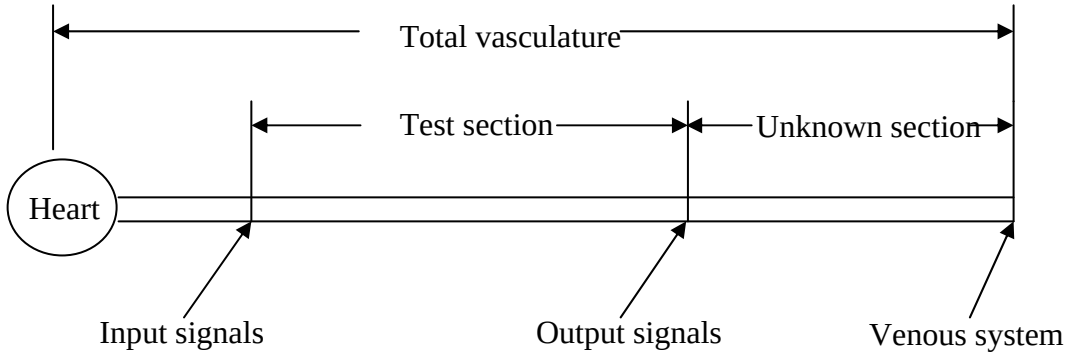

Figure 3.4 Diagram of simplified total arterial vasculature

According to the Poiseuille's equation:

$$Q_t = \frac{\pi R_0^4}{\mu} \frac{1}{8} \frac{P_I - P_O}{L} \tag{3.18}$$

where Q_t is the total mean flow rate, P_I the input mean pressure from input pulsatile pressure p_{in}, P_O the output mean pressure which is the only unknown in the above equation. The initial radius R_0 and length L of the vessel can be specified by the measurements. The viscosity coefficient μ is constant for the blood. Therefore we can obtain P_O and apply it in the following equation to calculate the peripheral resistance R_p:

$$Q_t = \frac{P_O - P_v}{R_p} \tag{3.19}$$

where P_v is the venous pressure. Here we take P_v 10 mmHg. Since R_p is known from equation 3.19, we change the P_O and Q_t into instantaneous values p_{out} *and* q_t, because the instantaneous value q_t is constant along the vessel at any specific time and can be calculated from the program, we can obtain the boundary condition of the pressure p_{out} at the distal end. At any time and any point, the pressure can be easily

transformed into cross-sectional area by the tube law. As aforementioned, there is no difference in starting the program by p *and* u or A *and* u.

The velocity boundary condition at the proximal end is evaluated by the following scheme:

$$u_0^{n+1} = u_0^n - \frac{\Delta t}{\Delta x}\left[\left(\frac{u^2}{2}+\frac{p}{\rho}\right)_1^n - \left(\frac{u^2}{2}+\frac{p}{\rho}\right)_0^n\right] - \Delta t F_0^n \tag{3.20}$$

which is an uncentered approximation of the momentum equation between 0 and 1 where 0 denotes the entry point and 1 is the point just Δx distant from the entry point. The other boundary condition of velocity can be obtained by applying the uncentered approximation between M and M-1. The scheme is as follows:

$$u_M^{n+1} = u_{M-1}^n - \frac{\Delta t}{\Delta x}\left[\left(\frac{u^2}{2}+\frac{p}{\rho}\right)_M^n - \left(\frac{u^2}{2}+\frac{p}{\rho}\right)_{M-1}^n\right] - \Delta t F_{M-1}^n \tag{3.21}.$$

3.2.4 Tube laws in one-dimensional model

Now we have two equations but three unknown parameters A, u and p. In order to close the system, we define an explicit algebraic relationship between the sectional pressure p and area A. Two relationships between pressure and cross-sectional area, which are usually named tube law, are compared in this study. One is linear and the other non-linear. The linear expression is as follows:

$$p = E_L\left(\frac{A}{A_0} - 1\right) \tag{3.22}$$

where $$E_L = \frac{E}{2}\frac{h}{R_0} \tag{3.23}$$

E denotes the Young's modulus of the vessel wall, and h the wall thickness. A_0 and R_0 represent, respectively, the cross-section area and the radius at zero transmural pressure.

The non-linear expression is expressed in logarithm between pressure and diameter as follows:

$$\ln(P/P_0) = \beta\left(D/D_0 - 1\right) \tag{3.24}$$

In the expression, β is stiffness parameter which defines the slope of pressure-diameter relation and expresses the indistensibility of tubular wall. Like the parameter E_L, it does not represent the inherent elastic properties of wall material since the stiffness parameter involves not only the elastic modulus of the material but also the wall dimensions such as wall diameter and thickness. Therefore the parameters E_L and β are thought as representing the apparent wall stiffness. It has been found that the value of β is higher in young people and intracranial arteries than in old people and extracranial arteries. Hayashi et al. (1980) shows the values of β in Figure 3.5.

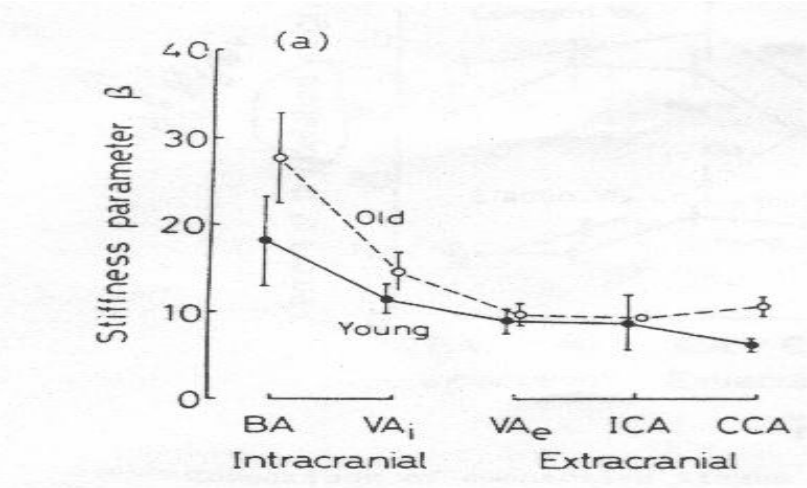

Figure 3.5 Averaged values of stiffness parameter

In order to investigate the difference of linear tube law and non-linear tube law and the influence of different parameters of stiffness, in our study, we choose two different values of 1.0×10^6 and $1.367\times10^6\,dyne.s/cm^5$ for E_L and two average values of 10 and 15 for β and compare the results of numerical calculation in a single vessel, respectively. We use the ICA as the model of single vessel. Two periods of waveforms of pressure, velocity and flow rate with linear and nonlinear tube laws are given in Figure 3.6. From Figure 3.6 we can see that there is no significant difference between different tube laws and the different stiffness parameters also do not result in significant difference.

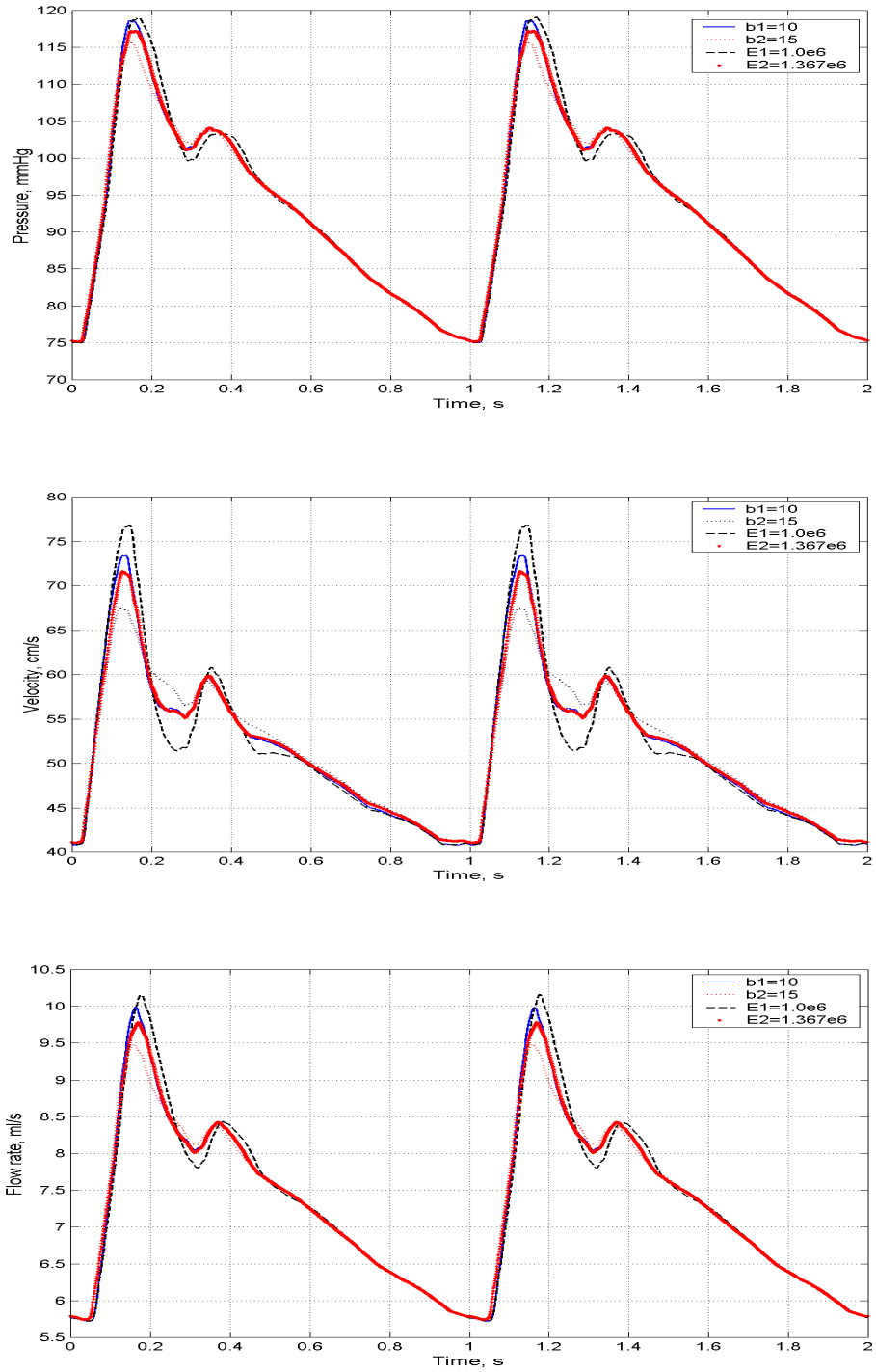

Figure 3.6 Comparison of waveforms of pressure, velocity and flow rate with different tube laws and stiffness parameters

3.2.5 Friction terms in one-dimensional model

In the equations, the parameter F is the friction term that accounts for viscous drag between the blood and the vessel wall. For the laminar flow, the friction term F is usually expressed in terms of true vessel cross-sectional area as

$$F = \frac{8\pi\mu}{\rho}\frac{u}{A} = 8\pi\upsilon\frac{u}{A} \tag{3.25}$$

which is the Poiseuille's friction term in a circular tube, μ being the viscosity coefficient which is 0.035 $dyne \cdot s \cdot cm^{-2}$ and υ the kinematic viscosity coefficient which is $0.035\, cm^2 \cdot s^{-1}$. Poiseuille's friction term is from steady flow, so it is a steady friction term. As aforementioned in Chapter 2, Zielke's friction term (1968) has been considered as an accurate method in describing unsteady viscosity. Following is its expression:

$$F = \frac{4\pi\mu}{\rho}\frac{1}{A}\left[2u(t) + \int_0^t \frac{\partial u}{\partial t}(\tau)W(t-\tau)d\tau\right] \tag{3.26}$$

This method is expressed in terms of convolution integral using past velocities and weight functions. A first-order difference approximation is used for the time interval of $2\Delta t$, increasing two units of time steps at a time to calculate the friction force. Rearranging this expression,

$$\begin{aligned} F &= F_1 + F_2 \\ &= 8\pi\upsilon\frac{u}{A} + \frac{4\pi\upsilon}{A}\int_0^t \frac{\partial u}{\partial t}(\tau)W(t-\tau)d\tau \end{aligned} \tag{3.27}$$

where,

$$F_2 = \frac{4\pi\upsilon}{A}\sum_{j=1,3,\ldots}^{k-1}\left(u_{i,j+1}-u_{i,j-1}\right)W\left((k-j)\Delta t\right)$$
$$= \frac{4\pi\upsilon}{A}\left[\begin{matrix}\left(u_{i,k}-u_{i,k-2}\right)W\left(\Delta t\right)+\left(u_{i,k-2}-u_{i,k-4}\right)W\left(3\Delta t\right)\\ +\cdots+\left(u_{i,2}-u_{i,0}\right)W\left((k-1)\Delta t\right)\end{matrix}\right] \tag{3.28}$$

in which W is a function of dimensionless time τ,

$$\tau = \frac{\upsilon}{R_0^2}t \tag{3.29}$$

and can be calculated by the first terms of a series for values of τ smaller than 0.02 and by a second series for values of τ greater than 0.02.

$$W(\tau) = 0.282095\tau^{-1/2} - 1.250000 + 1.057855\tau^{1/2}$$
$$+ 0.937500\tau + 0.396696\tau^{3/2} - 0.351563\tau^{2} \qquad for \quad \tau \le 0.02, \tag{3.30}$$

$$W(\tau) = e^{-26.3744\tau} + e^{-70.8493\tau} + e^{-135.0198\tau}$$
$$+ e^{-218.9126\tau} + e^{-322.5544\tau} \qquad for \quad \tau > 0.02 \tag{3.31}$$

The application of Zielke's friction term requires storage of all velocities computed at previous time steps at all computational points. Since the time step is very small, in order to satisfy the stability condition, the calculation and storage of past velocities in Zielke's friction term are time-consuming. Therefore it is necessary to do some improvements for Zielke's friction term. An improved Zielke's friction term given by Suzuki et al. (1991) is more efficient than Zielke's original method. For the purpose of

simplification and accuracy, in Suzuki's friction term the time step J is increased unit by unit, and a first-order difference approximation is also applied to the interval Δt. The friction force

$$F(K\Delta t)=\frac{8\pi\mu}{\rho}\frac{1}{A}u(K\Delta t)+\frac{4\pi\mu}{\rho}\frac{1}{A}\sum_{J=1}^{K}\left[u\left((K-J+1)\Delta t\right)-u\left((K-J)\Delta t\right)\right]W\left[(J-1/2)\Delta t\right]$$
$$=\frac{8\pi\mu}{\rho}\frac{1}{A}u(K\Delta t)+F_1(K\Delta t)+F_2(K\Delta t) \qquad (3.32)$$

The total time $t=K\Delta t$, so the K denotes the number of the time steps. In the weight functions of Zielke's friction term, when dimensionless time $\tau>0.02$, the values of W are less than 1 and become less and less with the increase of τ. It means that the past velocities after a specific time are insignificant to the friction force. Suzuki et al. (1991) defines an integer JT as a boundary of two methods of calculation as follows:

$$\frac{\upsilon\Delta t}{R^2}\left(JT-\frac{1}{2}\right)\le 0.02<\frac{\upsilon\Delta t}{R^2}\left(JT-\frac{1}{2}+1\right) \qquad (3.33)$$

When $J\le JT$, the previous velocities also need to be stored, but when $J>JT$, a recursive method is derived and the previous velocities are not to be stored. In our program, if the Δt is taken 0.001 and three periods are inputted, $K=3000$ and JT is about 30. In Zielke's method, at each point the total calculating times are $\sum_{K=1}^{3000}\sum_{J=1}^{K}J=4.5\times10^9$. However, in Suzuki's method, the total calculation times are less than $(1+\sum_{J=1}^{JT}J)\times3000=1.4\times10^6$. Therefore, in Suzuki's method the calculating time

and storage requirement are significantly reduced. The calculation of three friction terms is given in table 3.2.

Table 3.2 Comparison of calculation time of three friction terms

Friction Terms	Poiseuille	Suzuki	Zielke
Calculation Time (sec.)	42	885	165608

An important condition for the validity of the above three friction terms is that the flow is laminar. For pulsatile flow the standard Reynolds number Re is not a reliable index for the transition to turbulence. A new criterion for the transition range from laminar to turbulence in pulsatile flow is given by $\kappa = \mathrm{Re}/\alpha = 250 - 1000$ (Reuderink, 1989). In our study, the value of this parameter is 220.

In the single vessel, we compare the waveforms of pressure, velocity and flow rate of numerical model with three friction terms. The results are shown in Figure 3.7 and the Womersley number α is equal to 3. We can see the difference of waveforms of pressure, velocity and flow rate from three friction terms is very small (less than 2%).

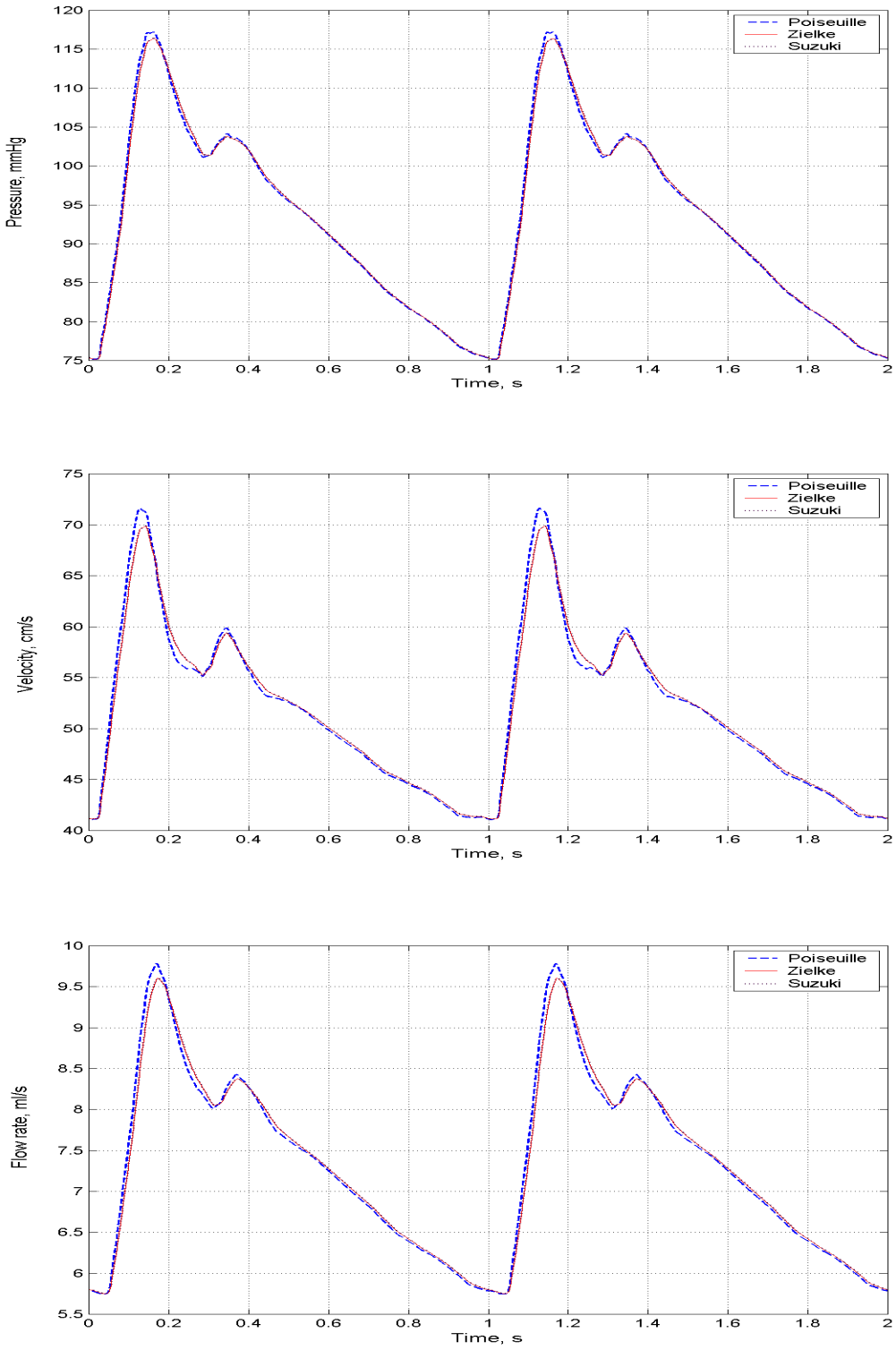

Figure 3.7 Comparison of waveforms of pressure, velocity and flow rate obtained from numerical model with three friction terms when Womersley number is equal to 3

Because the results between Zielke's model and Suzuki's model are exactly the same and Suzuki's model costs less time for calculation, we choose Suzuki's model to compare with Poiseuille's model when Womersley number α increases to 6. The results are shown in Figure 3.8 from which we can see that for pressure waveform, the difference between two friction terms is very small. For velocity, the difference increases but if we consider average value of velocity, the difference is still very small (less than 3%).

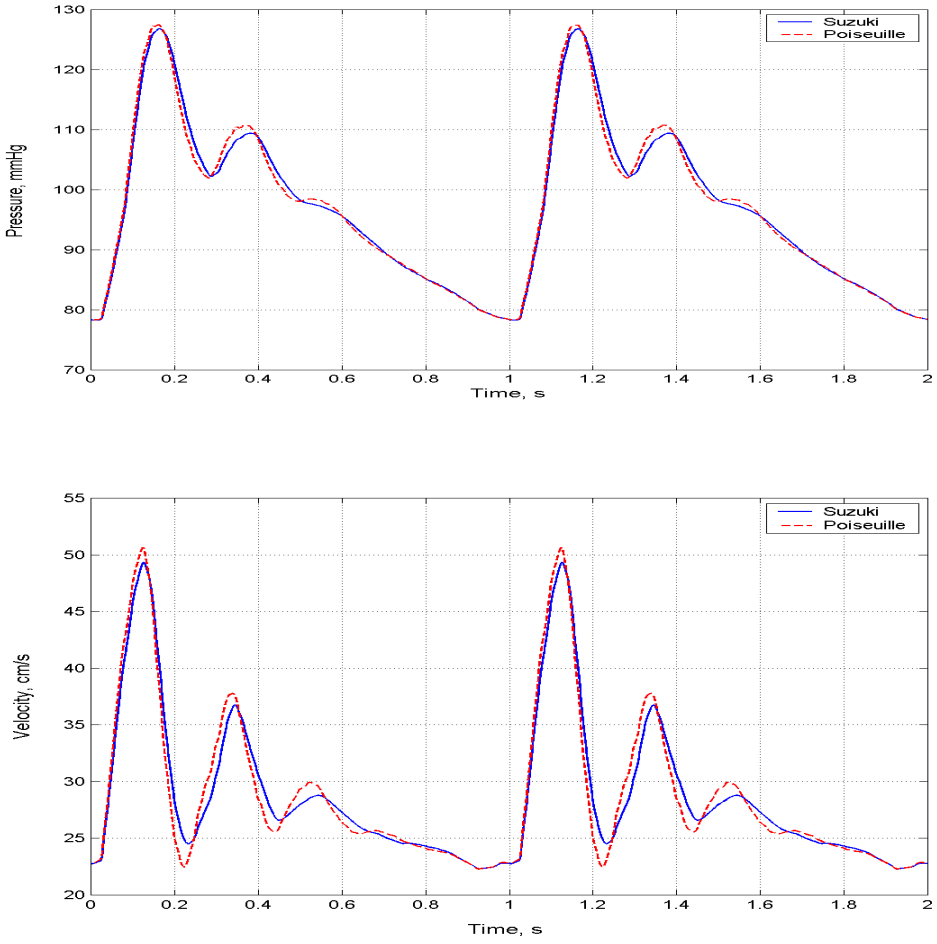

Figure 3.8 Comparison of waveforms of pressure, velocity obtained from numerical model with two friction terms when Womersley number is equal to 6

Since blood flow in vascular system is unsteady and pulsatile, the pulsatile effect of blood viscosity has engendered the interest of researchers. Hillen et al. (1988) indicated that the differences between frictional losses in steady and pulsatile flow are mainly determined by the radius of the tube, the viscosity and density of the fluid and the frequency of the pulsations. Reuderink et al. (1989) showed that the effect of unsteady viscosity was significant in the circulatory system simulation. In order to investigate the significance of unsteady effect of blood viscosity, Kitawaki et al. (2000) applied Poiseuille's friction term (quasi-steady) and frequency-dependent friction terms into a linear model. Then the numerical results were compared with the experimental measurements. In this study, Poiseuille's friction term and frequency-dependent friction terms are applied into a nonlinear model. The results show that the difference between Poiseuille's friction term and frequency-dependent friction terms is very small (less than 2%). Physically, since the wave velocity in vessels is around 5-10m/s (Nichols et al., 1997) and the vessel length is short (0.2m in this study), the "frequency effect" on blood viscosity can not be memorized. Therefore, the frequency-dependent friction losses can be negligible in the study of blood flow in the CoW. The numerical results presented in this study confirmed the above analysis.

3.2.6 Numerical algorithm

In Figure 3.9, the numerical marching procedure is given. The initial conditions of an immobile flow with estimated diastolic values are used to evaluate the right-hand sides of the equations in step I, from which one obtains the new values of A, u and p at the next half time step and half distance step. These new values are expressed by the intersections of the dash line in Figure 3.9, and they in turn are used to evaluate the

right-hand sides of the equations in step II, which then yields the values of A, u and p. These values are the intersections of the solid line in Figure 3.9. With the given and calculated boundary conditions, we can obtain the values of A, u and p in the whole time range.

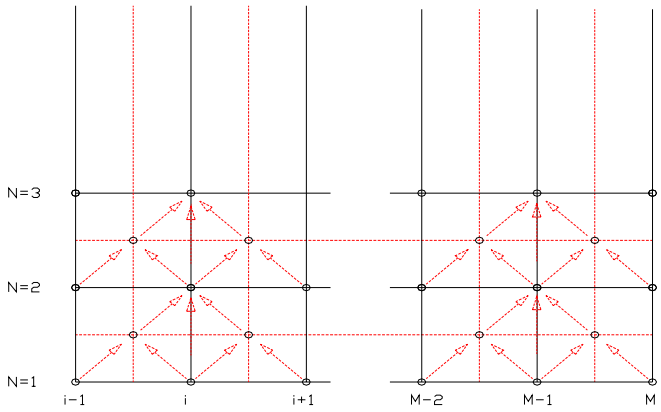

Figure 3.9 Marching procedure of the numerical method

In Table 3-2 we give the flow chart for the program in a single vessel that is helpful to understand the original program. In the numerical model of CoW, some programs calculating the values at bifurcations are written, but the flow chart is not much different with the one in single vessel.

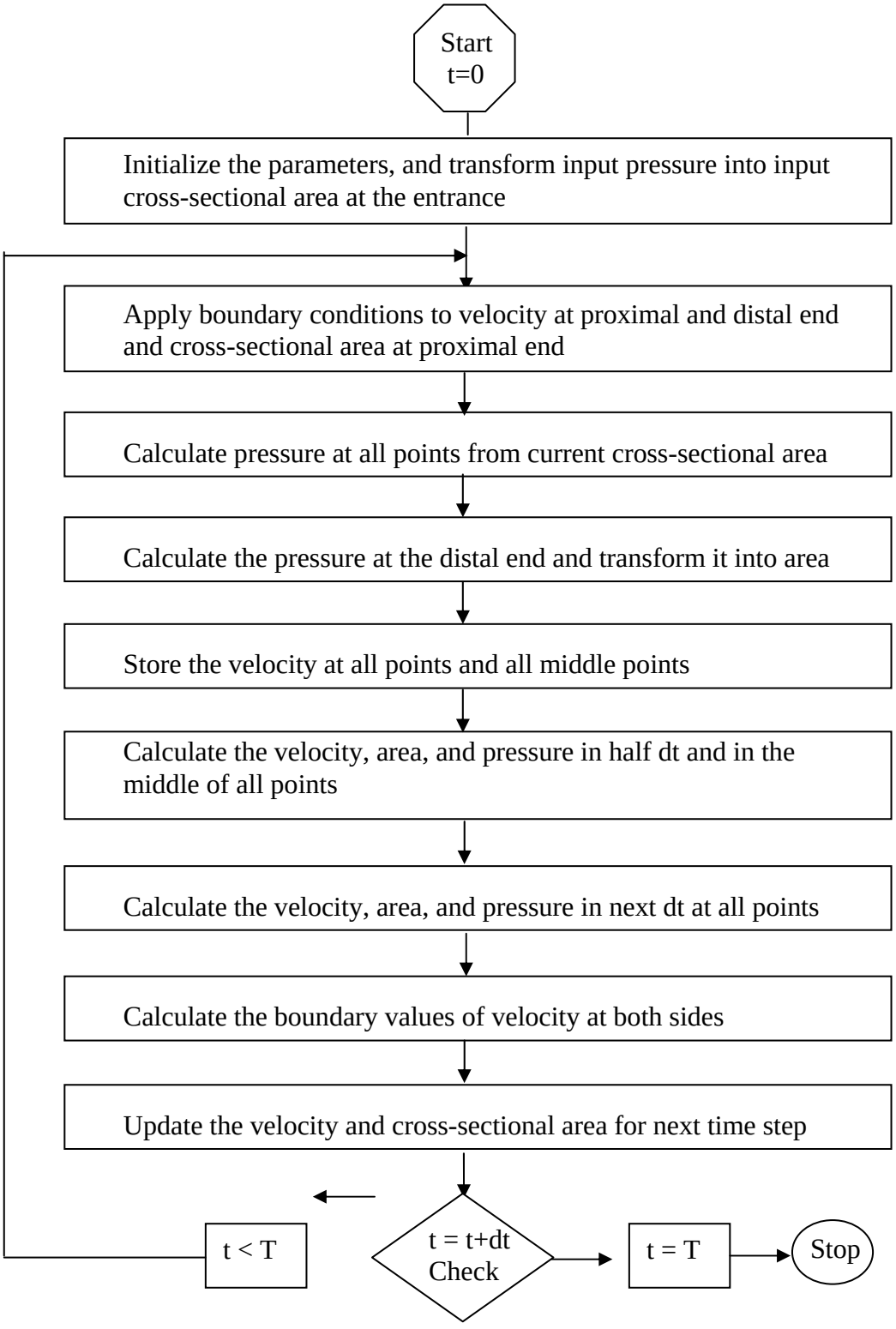

Figure 3.10 Flow chart of the computer program for a single vessel

3.3 Numerical model of the CoW

3.3.1 Geometrical data of the CoW

Figure 1.4 shows the geometrical structure of the CoW. The input pressure p_{in} enters synchronously the system from the four afferent vessels and each efferent vessel is terminated with a lumped peripheral resistance. To determine the peripheral resistances at the end of efferent arteries, we review the distribution of blood flow in the six efferent arteries in the literature in Table 3.3.

Table 3.3 Blood flow distribution of efferent arteries of the CoW in the literature

	ACAs, %	MCAs, %	PCAs, %
Zagzoule et al. (1986)	20.2	57.6	22.2
Hillen et al. (1986)	22.2	45.0	32.8
Hillen et al. (1988)	22.1	44.8	33.1
Lyden et al. (1997)	21.2	53.6	25.2
Macchi et al. (1994)	23.2	53.4	23.7
Viedma et al. (1997)	24.5	45.5	30.0
Average	22.64	48.46	28.96

The clinical measurements indicated that total cerebral blood flow in human brain was 12.5 cm^3/s (Nichols et al., 1990). According to the average value of blood distribution of efferent arteries in the literature shown in table 3.3, we determine the blood flow distribution in numerical model is 22% for ACA, 48% for MCA and 30% for PCA. Therefore, for each one of efferent arteries, blood flow is 1.375 ml/s in ACA, 3.0 ml/s in MCA and 1.875 ml/s in PCA. Using a regressive program we find the terminal resistances are $7.9\times10^4\, dyne\cdot\sec/cm^5$, $3.7\times10^4\, dyne\cdot\sec/cm^5$ and $5.8\times10^4\, dyne\cdot\sec/cm^5$ for each one of ACAs, MCAs and PCAs respectively.

Table 3.4 gives the data of the vessels used in this model, which is obtained from the literature. The geometrical data are obtained by processing anatomical data found in the study of Hillen et al. (1986). The Poiseuille's friction term and the linear tube law introduced above are used in this model. The elasticity coefficient E_L is taken from the study of Zagzoule and Marc-Vergnes (1986).

Table 3.4 Geometrical data and elasticity of the vessels of the CoW

Vessels	Length, mm	Diameter, mm	Elasticity, $10^5\, dyne/cm^2$
ICAs	250	4.00	13.67
VAs	200	3.00	13.67
BA	30	4.00	27.35
A1	20	2.50	27.35
ACA	50	2.50	30.08
ACoA	5	1.00	27.35
MCA	70	3.50	30.08
P1	20	3.00	27.35
PCA	70	3.00	30.08
PCoAs	20	1.00	27.35

At the bifurcations among the vessels, the following relations are used

$$(Au)_1 = (Au)_2 + (Au)_3 \tag{3.34}$$

$$p_1 = p_2 = p_3 \tag{3.35}$$

where subscripts1 denote the parent vessel and 2, 3 the daughter branches.

For the bifurcation formed with one parent vessel and two branches, there are nine unknowns (p, A, u for three vessels) and only six conditions. The three remaining

equations are obtained by approximating the continuity equation at the point $i-1$ of the parent vessel and point 0, 1 of the daughter vessels with the following schemes:

$$\left[\frac{A_i^{n+1}+A_{i-1}^{n+1}}{2}-\frac{A_i^n+A_{i-1}^n}{2}+\frac{\Delta t\left[(Au)_i^{n+1}-(Au)_{i-1}^{n+1}\right]}{\Delta x}\right]_1=0 \qquad (3.36)$$

$$\left[\frac{A_1^{n+1}+A_0^{n+1}}{2}-\frac{A_1^n+A_0^n}{2}+\frac{\Delta t\left[(Au)_1^{n+1}-(Au)_0^{n+1}\right]}{\Delta x}\right]_i=0 \qquad (3.37).$$

3.3.2 Numerical results of an idealized CoW

Table 3.5 shows the calculation results of the efferent arteries of the numerical model in an idealized CoW. The blood flow distribution in the efferent arteries is 22.1% for ACA, 47.8% for MCA and 30.1% for PCA. The calculated total CBF is 12.5 ml/s which is the same as that reported in the literature (Nichols et al., 1990).

Table 3.5 Numerical results of the efferent arteries of the CoW

	ACA	MCA	PCA
Pressure (mmHg)	92.33	93.44	92.54
Flow rate (ml/s)	1.3816	2.9848	1.8793
Resistance (dyne s/cm^5)	79000	37000	58000

Figure 3.11, 3.12 and 3.13 give the waveforms of pressure, flow rate and velocity in the middle point of the vessels obtained from numerical calculation. Because of symmetry, results of the vessels constituting the left side of the CoW are completely equal to that of the right-hand of the CoW, and there is no blood flow in the ACoA.

The blood flow rate and velocity in PCoAs are small, which means that in normal condition, ICA and BA can supply enough blood to the corresponding areas. The shapes of the curves of the pressure, velocity and flow rate are in good agreement with those depicted in the literature (Hillen et al., 1986).

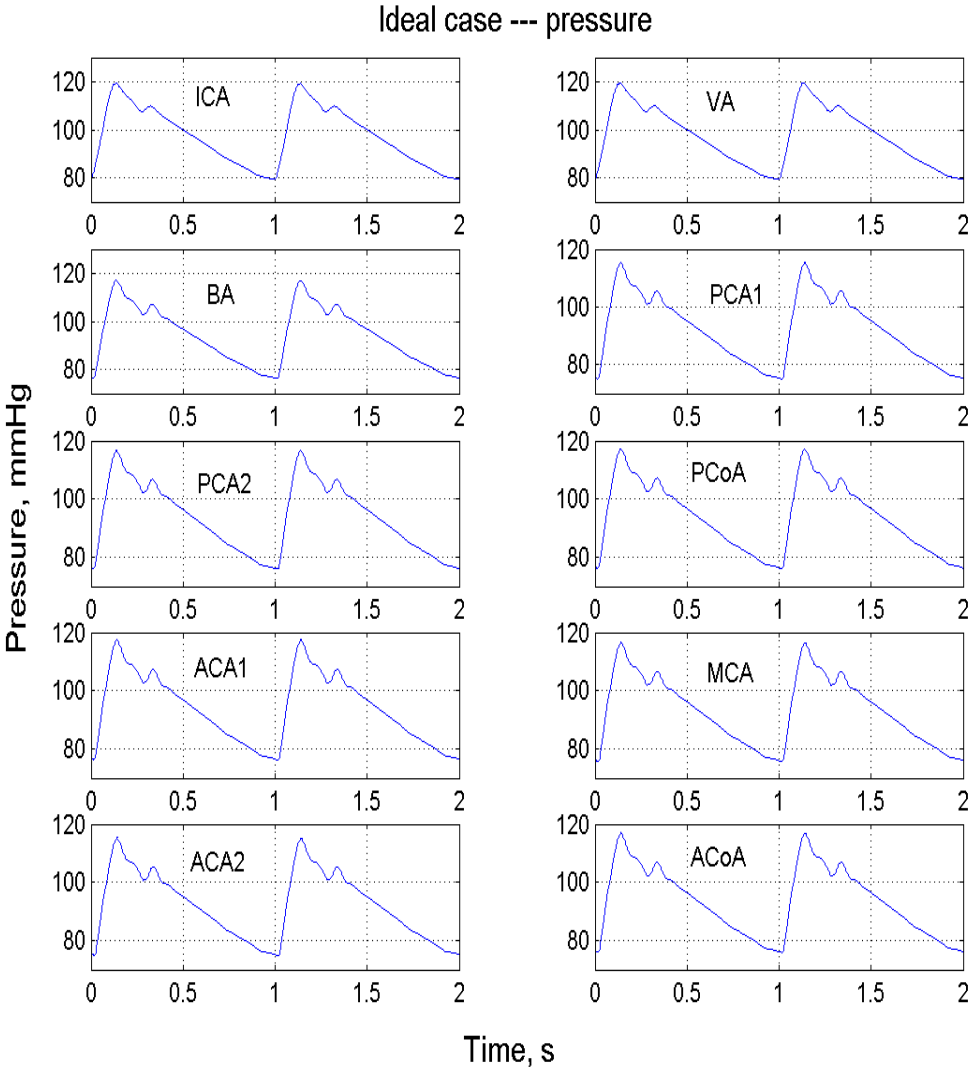

Figure 3.11 Pressure waveforms in the vessels of CoW obtained from numerical model

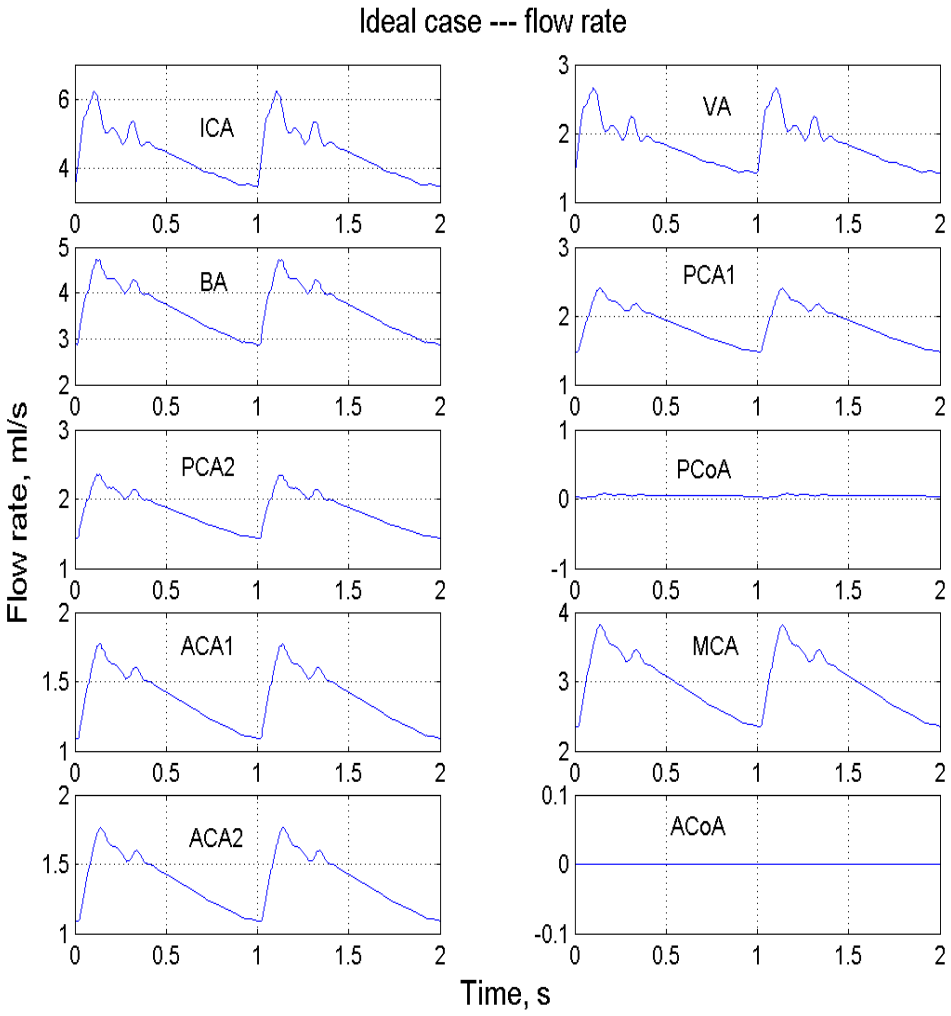

Figure 3.12 Flow rate waveforms in the vessels of CoW obtained from numerical model

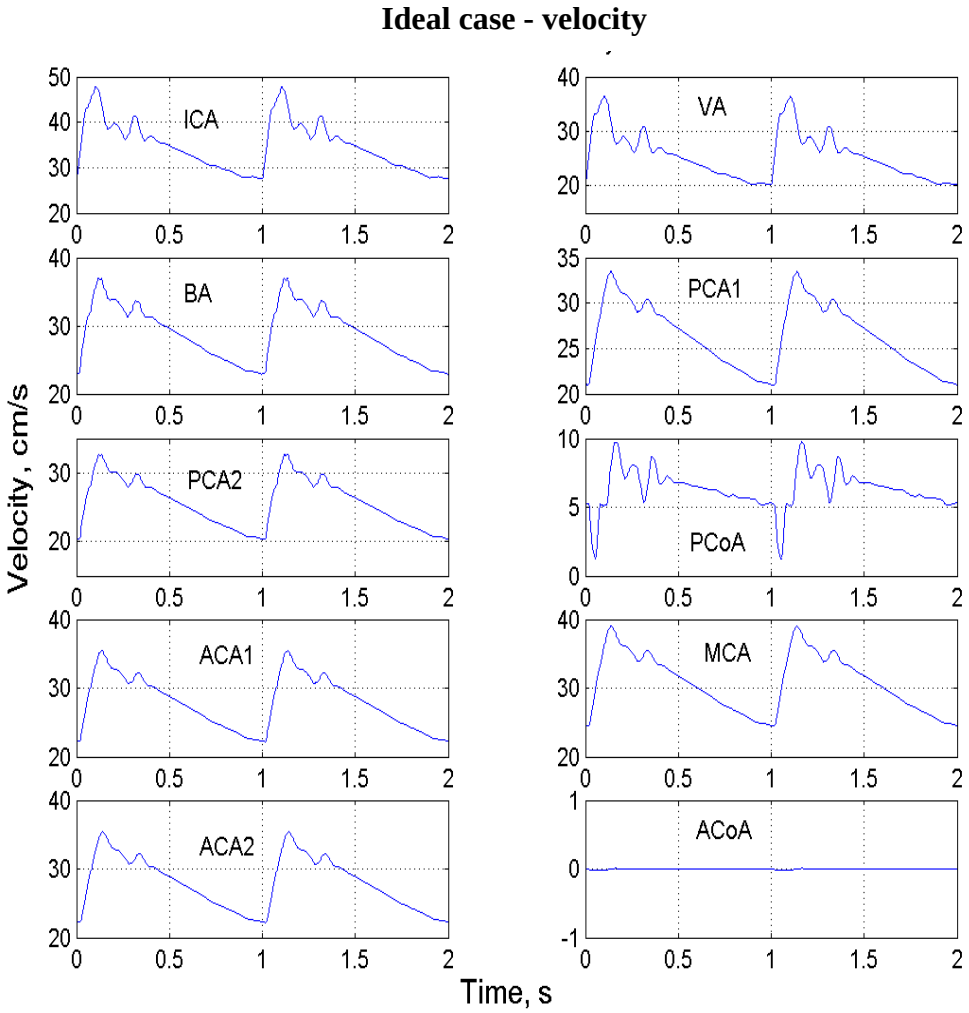

Figure 3.13 Velocity waveforms in the vessels of CoW obtained from numerical model

Chapter 4

Numerical studies on clinical cases

4.1 Introduction

In patients with severe stenosis or occlusion of ICA, cerebral blood supply potential (CBSP) may be insufficient and the patients may have risk for ischemic stroke. As aforementioned in section 2.1.4, CEA can reduce the risk for ischemic stroke by removal of the atheromatous plaque (Barnett et al., 1998; 2000). During the surgery, one of ICAs will be clamped, which will impair CBSP further. It is difficult to predict which patients will tolerate the clamping of ICA. If the patients can not tolerate the hemodynamic change resulting from the clamping of ICA, a shunt is needed. But the shunt itself may increase postoperative stroke. Therefore, prediction of the change of cerebral hemodynamics before and after the clamping of ICA is helpful for neurosurgeon to determine whether a shunt is necessary. Numerical model can predict the cerebral hemodynamic change and provide two advantages in reducing complications by helping clinicians to choose the optimal surgical technique and/or avoid unnecessary surgery (Kailasnath et al., 1998). This study is motivated by the possible clinical application of numerical model in the prediction of cerebral hemodynamics.

In the normal brain CBF remains relatively constant despite changes in the systemic blood pressure or CPP because of the function of cerebral autoregulation (CA). The

limits of CA are not fixed and influenced by both pharmacological agents and pathological conditions (Reilly and Bullock, 1997). CA can be evaluated by measuring relative blood flow changes in response to a steady-state change in the blood pressure (static method) or during the response to a rapid change in blood pressure (dynamic method). Static autoregulation models can be used to evaluate steady states of CA. In the literature static autoregulation models were developed to evaluate steady states of CA (Hudetz et al., 1982) and dynamic autoregulation models were developed to evaluate the transient dynamics of CA (Ferrandez et al. 2002; Moorhead et al. 2004a, 2004b). Tiecks et al. (1995) compared the static and dynamic CA measurements and found that in normal human subjects measurements of dynamic CA yielded similar results as static testing of intact and pharmacologically impaired CA.

In the numerical studies on hemodynamics of the CoW, most authors consider the distal peripheral resistance of the CoW as constant. Seldom includes the intrinsic function of CA which is an important hemodynamic adaptive factor for cerebral hypoperfusion. Ferrandez et al. (2002) built up a mathematical model of CA based on the clinical measurements of dynamic CA conducted by Newell et al. (1994) and applied the model into their numerical model of CoW. Moorhead et al. (2004a; 2004b) improved the model of Ferrandaz et al. (2002) and applied it into their 1D and 3D model of CoW. Based on local control of pressure and flow in the pial and intracerebral arteries, Hudetz et al. (1982) developed a simplified steady state CA model to describe regional CBF and tissue oxygenation during focal ischemia.

CBSP is influenced by various factors, such as carotid artery disease, collateral capacity of the CoW and the status of CA. Very recently, Reinhard et al. (2003a,

2003b) studied clinically the interrelation between different patterns of collateral blood flow and actual impairment of CA in patients with carotid artery disease. The aim of this study is to use numerical model with consideration of ICA stenosis, anomaly of CoW and static CA to predict CBSP before and after the clamping of ICA in the patients who undergo CEA.

4.2 Methods

The basic numerical model of CoW is given in Chapter 3. In this chapter, an autoregulative model developed by Gao et al. (1998) is added into the basic numerical model so that at the end of efferent arteries, the distal resistance is the function of perfusion pressure. The autoregulative model is an empirical formula of autoregulation modeled on basic hemodynamic principles and experimental data. Based on the modified numerical model, the process of clamping of ICA during CEA is simulated in two pathological cases, bilateral 75% stenosis of ICA and bilateral 75% stenosis of ICA with LPCoA missing.

The geometrical data of the CoW is the same as that of the model in Chapter 3. The diameters of ACoA and PCoA are fixed at 1mm. We use reduction of diameter to simulate the stenosis of ICA which is located at the middle of ICA and has a length of 5 mm. We tested the influence of locations of stenosis in ICA and did not find significant difference. We use ICA occlusion to simulate the process of clamping during CEA. The results from the autoregulative model are given in Figure 4.1 in which the relationship between cerebrovascular resistance, CBF and effective diameter and pressure is shown. The figure is taken from the publication of Gao et al. (1998). Some experimental data is also given in the figure for comparison.

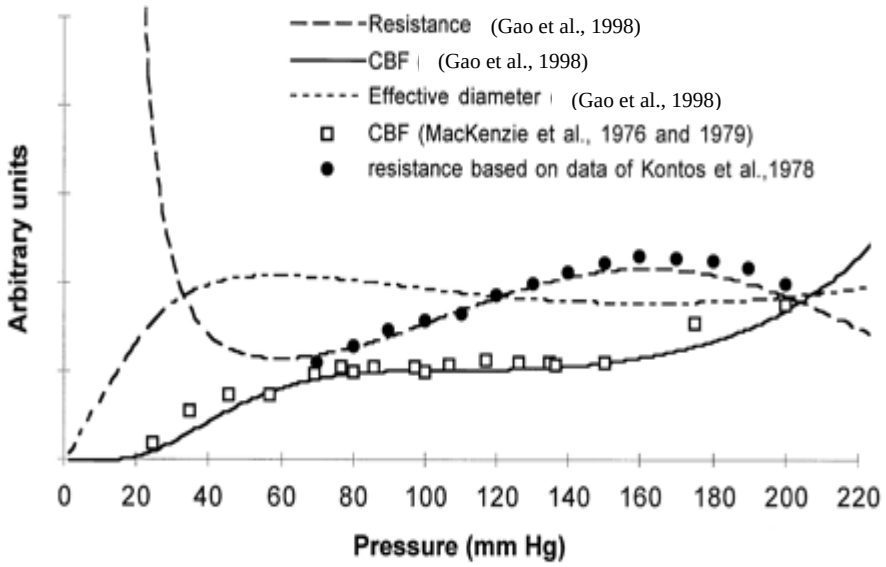

Figure 4.1 Results of cerebrovascular resistance, CBF, and effective diameter of an autoregulative model. Some experimental data are also plotted. Resistance is calculated directly from experimental data of Kontos et al. (1978). Experimental data of CBF are readings of 2 hand-fitted curves of data reported by MacKenzie et al. (1976 and 1978).

The relationship between cerebrovascular resistance and pressure is calculated from Equation 4.1. In the equation, R represents cerebrovascular resistance and P perfusion pressure.

$$R = 47.4 - 6.54\times10^{-2}P + 2.2\times10^{7}P^{-4} + 18\sin\left(\frac{2\pi P}{252.6} + 3.68\right) \quad (0 < P < 200) \qquad (4.1)$$

Plotting this equation in the range of 20-200 mmHg of CPP, we obtain Figure 4.2 which does not show the exact cerebrovascular resistance in the ordinate but show the relationship between cerebrovascular resistance and pressure.

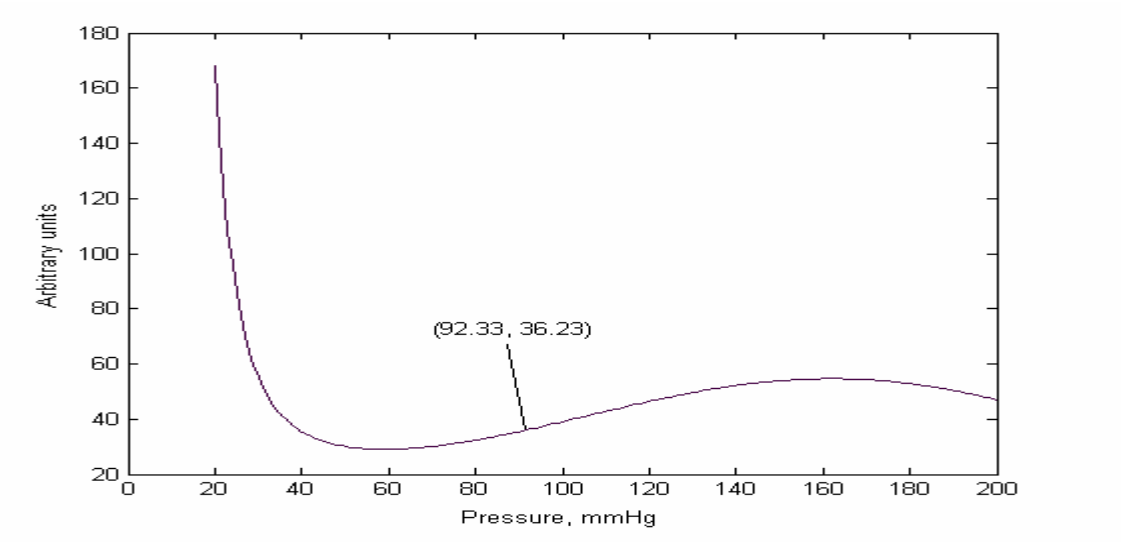

Figure 4.2 Relationship between cerebrovascular resistance and pressure calculated from Equation 4.1

Some research groups have reported that the cerebral vascular bed responded to changes in the perfusion pressure gradient in a similar fashion, whether they resulted from decreasing mean arterial pressure, increasing jugular venous pressure, or increasing ICP (Wagner et al., 1986). We assume that the autoregulative mechanism is the same in everywhere of the brain. We only show how to apply the autoregulative model at the end of ACA, because the procedures for applying autoregulative model at the end of MCA and PCA are the same. From Table 3.5 we obtain the average pressure and resistance in ACA are 92.33 mmHg and 79000 $dyne \cdot s / cm^5$. In Figure 4.2 we find that when P is equal to 92.33 mmHg, R is equal to 36.23. We multiply the curve in Figure 4.2 by a parameter 2180.5 (79000/36.23) and obtain a new curve shown in Figure 4.3. This new curve describes the relationship between cerebrovascular resistance and pressure at the distal end of ACA.

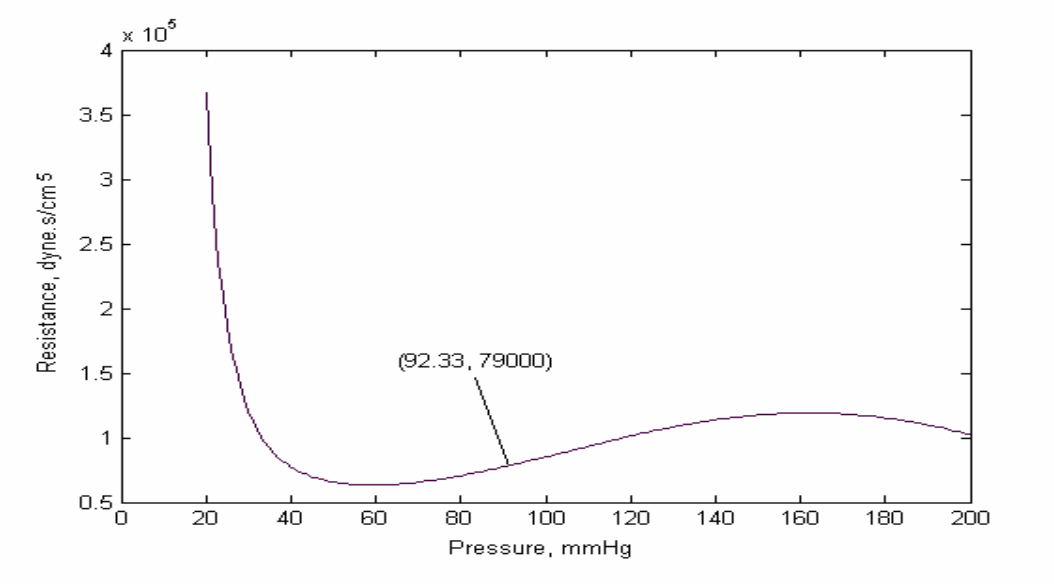

Figure 4.3 Autoregulative model used at the end of ACA

In Equation 4.1, let the derivative of R with respect to P be zero and we obtain Equation 4.2. By neglecting the units of y axis, plotting Equation 4.2 we obtain Figure 4.4 in which we find that the derivative in Equation 4.2 is positive between 59 and 162 mmHg. It means that in this range cerebrovascular resistance decreases with the decrease of pressure. Therefore the CBF could be maintained at relatively constant level.

$$\frac{dR}{dP} = -6.54\times10^{-2} - 8.8\times10^{7}P^{-5} + \frac{36\pi}{252.6}\cos\left(\frac{2\pi P}{252.6} + 3.68\right) = 0 \qquad (0 < P < 200) \qquad (4.2)$$

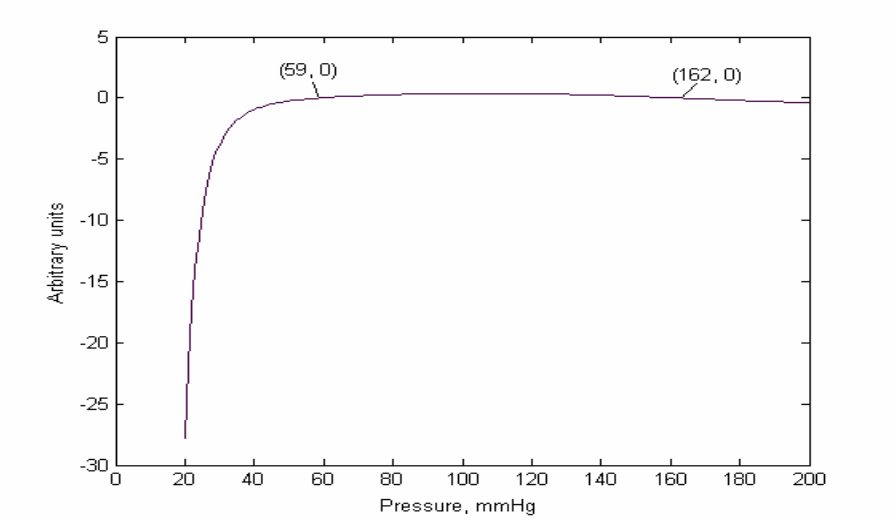

Figure 4.4 Derivative of cerebrovascular resistance with respect to pressure

According to Poiseuille's equation used in this numerical model $CBF = \frac{CPP - P_v}{R}$, we can obtain the relationship between CBF and pressure which is shown in Figure 4.5. In Figure 4.5 we can see when pressure is equal to 92.33 mmHg, CBF is equal to 1.38 ml/s which is excellent matched with the calculation results of the numerical model developed in Chapter 3. Figure 4.5 is also well matched with the autoregulative curve in Figure 17-4 in Guyton and Hall (2000) so that this model could be described as "clinical-static CA model".

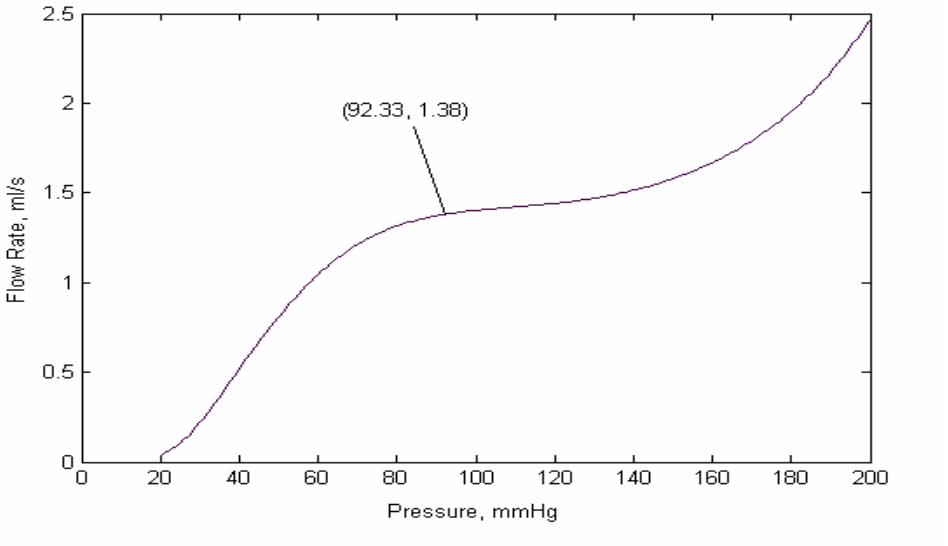

Figure 4.5 Relationship between CBF and CPP at the end of ACA

Plotting the derivative of CBF with respect to CPP we obtain Figure 4.6 from which we can see that in the range of 20-200 mmHg of CPP, the derivative of CBF with respect to CPP is positive, which means that CBF decreases with the decrease of CPP in the whole range of perfusion pressure, but the speed of decrease is not constant. In the range of 59-162 mmHg of CPP, the speed of decrease of CBF with respect to the decrease of CPP decreases, which is the effect of autoregulative mechanism.

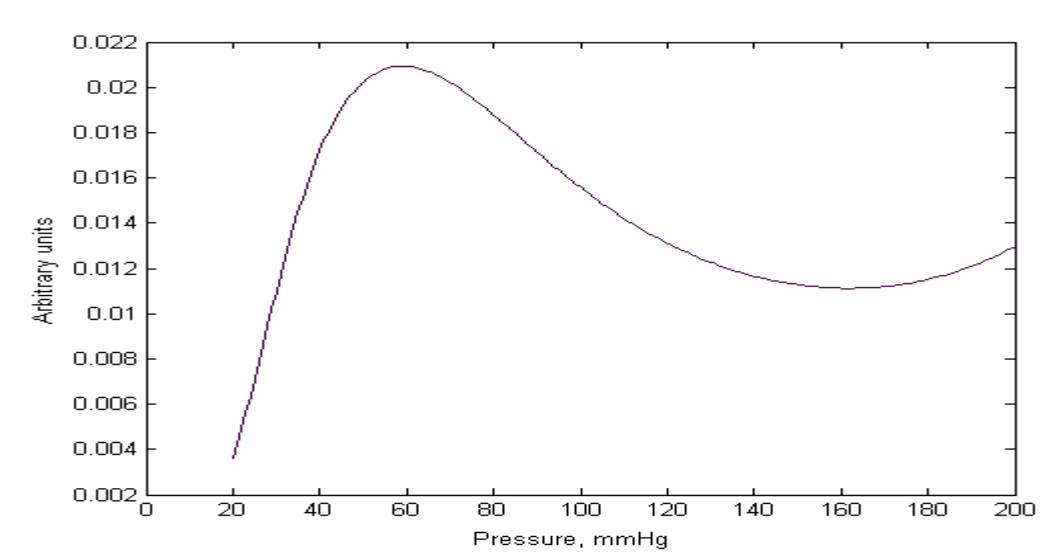

Figure 4.6 Derivative of CBF with respect to CPP

We analyze the formula 4.1 by plotting its figure and the figure of its derivative and found that this formula matches well with the physiological property of CA. Therefore, we developed a regressive sub-program in the numerical model and applied the curve shown in Figure 4.3 as the distal peripheral resistance of ACA. The sub-program is taken as the new distal boundary condition of ACA. At each cycle, the distal average pressure of ACA is calculated. The sub-program changes the distal resistance of ACA according to the calculated pressure value based on Figure 4.3. Therefore a new flow rate is calculated according to the new distal resistance. Based on the flowchart of the numerical model given in Figure 3.10, the flowchart of the sub-program is given in Figure 4.7.

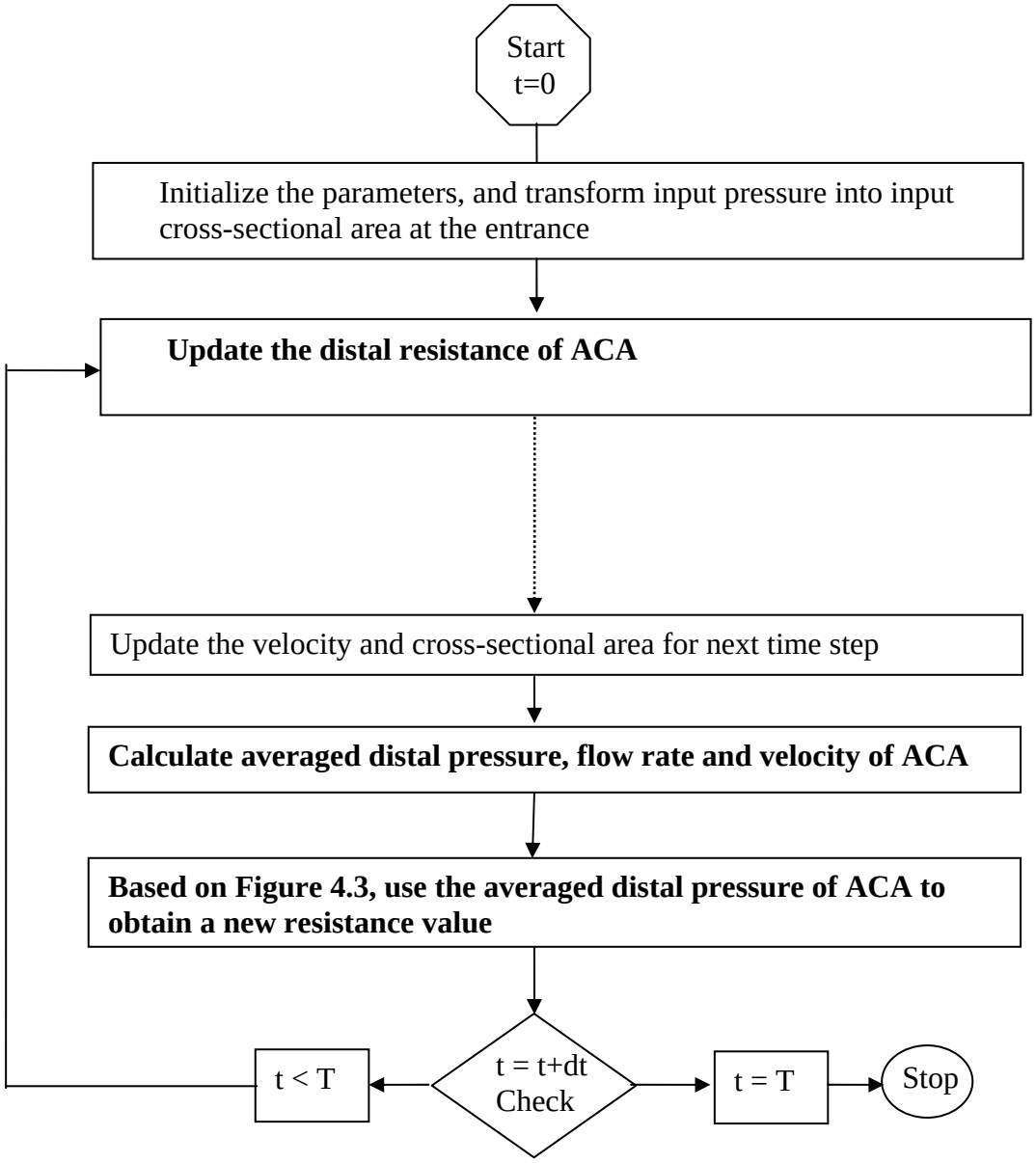

Figure 4.7 Flowchart of regressive sub-program based on flowchart of Figure 3.10

Finally, the autoregulative model is added into the numerical model of CoW. The distal peripheral resistance of ACA is no longer constant but changes with the distal perfusion pressure. We use the same procedures to add the autoregulative model in the distal end of MCA and PCA.

4.3 Results

4.3.1 Case 1- Normal circle of Willis

Figure 4.8 shows the averaged value of pressure, flow rate and velocity of all vessels of the normal CoW. In this study, all averaged values are calculated in the middle point of the vessels in one period. Because of symmetry, there is no blood flow in the ACoA. Hence, we only show the data of the vessels of half CoW. The blood flow in PCoA is very small and the direction is from ICA to PCA. The total blood inflow through ICAs and VAs is 12.5 ml/s and the total outflow is also 12.5 ml/s. The calculation error is very small and can be neglected. The transient waveforms of pressure, flow rate and velocity in the vessels of CoW can be found in the Figure 3.11, 3.12 and 3.13.

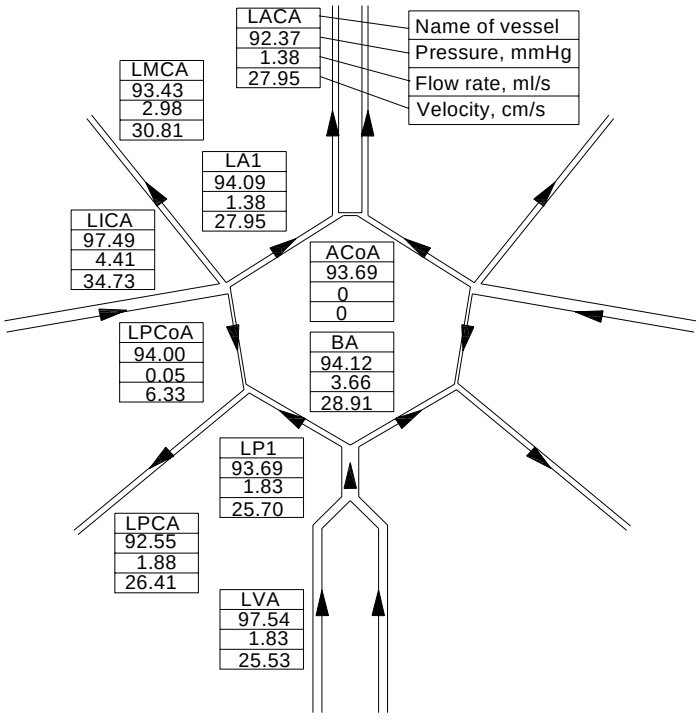

Figure 4.8 Averaged pressure, flow rate and velocity in the middle point of vessels in the normal CoW

4.3.2 Case 2-Bilateral 75% stenosis of ICA

The autoregulative feedback system is applied in all the pathological cases in this chapter. Figure 4.9 shows the averaged value of pressure, flow rate and velocity in some vessels of CoW with bilateral 75% stenosis of ICA. Due to symmetry, the results of both sides of the CoW are the same and there is no blood flow in ACoA. Because there is no stenosis added into BA system, flow rates in PCAs hardly change compared with the results of normal CoW. Compared to the results of the normal CoW, the largest flow rate loss in this case occurs at ACA which is 2.9%. Flow directions in PCoAs reverse but the collateral flow compensation is only 0.36 ml/s which is a small value.

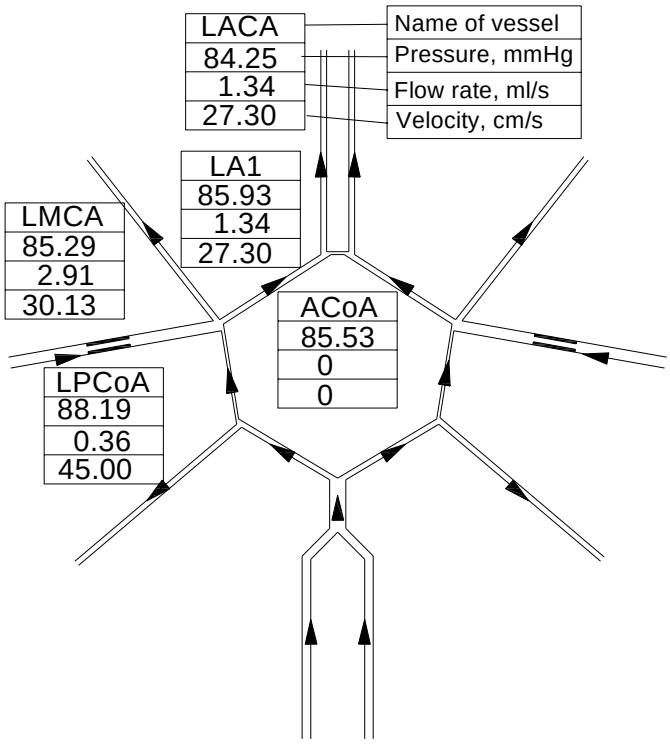

Figure 4.9 Averaged pressure, flow rate and velocity in the vessels of CoW with bilateral 75% stenosis of ICA

4.3.3 Case 3-Occlusion of LICA and 75% stenosis of RICA

In case 3, we simulate that the LICA is undergoing CEA and therefore, the LICA is occluded. Figure 4.10 shows the averaged value of pressure, flow rate and velocity in several vessels of the CoW in case 3. Compared to the results from normal case, the largest flow loss occurs at LMCA which is 15.4%. In this figure we can see that blood flow in four vessels reverses to compensate the deprived side. Compared with the results of case 2, collateral flow in ACoA increases from zero to 2.36 ml/s and in LPCoA increases from 0.36 to 1.34 ml/s. Compensative flow in ACoA (2.36 ml/s) is much larger than that in LPCoA (1.34 ml/s), which means that ACoA plays a more important role in the process of compensation.

Comparing the results in case 3 with that in case 2, we can see that after the clamping of LICA, blood flow in the CoW is redistributed. The reductions of flow rates in case 3 are 12.7% at LACA and 13.4% at LMCA compared with the flow rate in case 2. Blood flow in LA1 reverses and plays an important role in the compensation to LMCA through ACoA. Although blood direction in RA1 does not change, the flow rate in RA1 increases significantly from 1.34 to 3.64 ml/s. It means that RA1 also plays an important role in the process of compensation. Compared to the LPCoA in case 3 (1.34 ml/s), RPCoA (0.63 ml/s) plays a less important role in the process of compensation. There is no change in the blood flow in PCAs, but blood flow in BA increases to compensate the ICA system through PCoAs. The changes of hemodynamic factors between case 2 and case 3 after the clamping of LICA indicate that the collateral pathways play important roles in the prediction of cerebral hemodynamics during CEA.

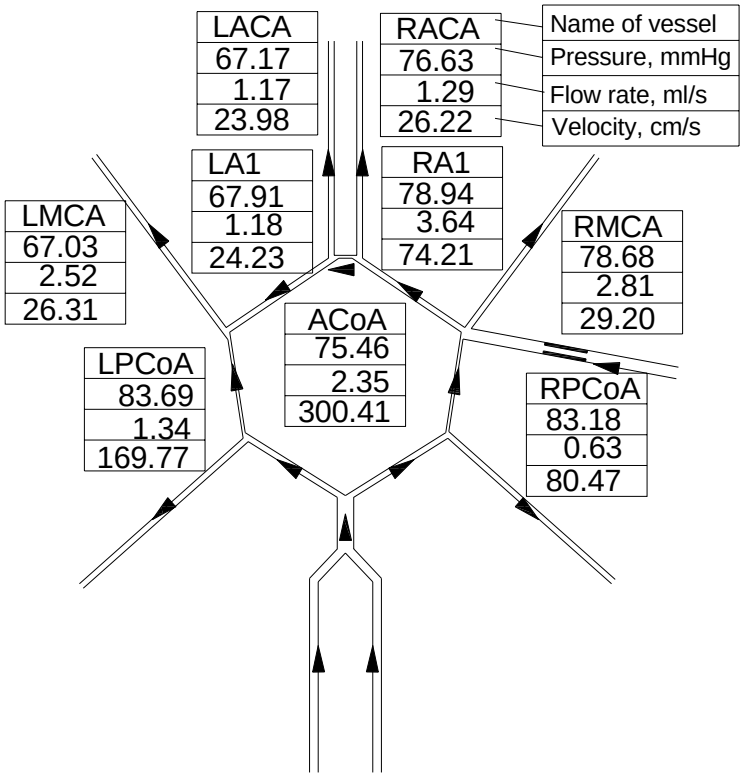

Figure 4.10 Averaged pressure, flow rate and velocity in the vessels of CoW with LICA occlusion and 75% stenosis of RICA

4.3.4 Case 4-Bilateral 75% stenosis of ICA with LPCoA missing

Complete CoW is only around 20-50% in the population. Therefore, simulation of an incomplete CoW is of clinical significance in the understanding of cerebral hemodynamics in incomplete CoW. Because there are various anatomical anomalies of CoW, it is difficult to simulate all the anomalies of CoW. Since the most common type of hypoplasia of CoW is the unilateral PCoA missing or hypoplasia, in this study we simulate LPCoA missing in the CoW with bilateral 75% stenosis of ICA. The average pressure, flow rate and velocity in the vessels of CoW in case 4 are shown in Figure 4.11. Compared with the case with bilateral 75% stenosis of ICA without LPCoA missing (Case 2), the results of these two cases are almost the same. It means

that in bilateral 75% stenosis of ICA, one PCoA missing has no influence on the global cerebral hemodynamics. Collateral blood flow in ACoA is very small (0.11 ml/s), which means collateral pathway of ACoA does not play an important role in this case. Compared with the results in case 2, the blood flow in RPCoA only has very small increase from 0.36 to 0.39 ml/s. It means that in the CoW with bilateral 75% stenosis of ICA and LPCoA missing, collateral blood supply is not significant.

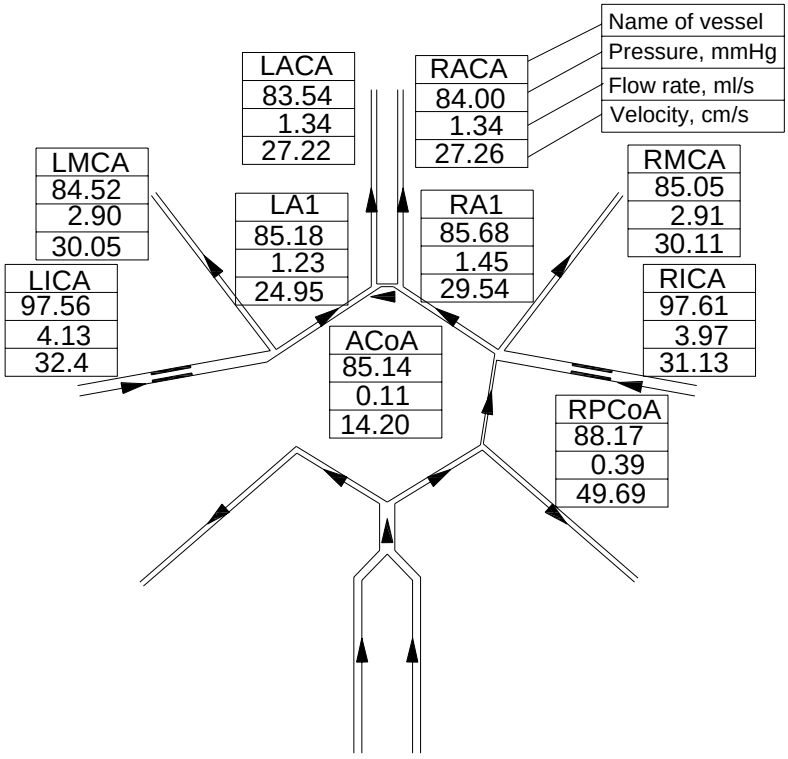

Figure 4.11 Averaged pressure, velocity and flow rate in the vessels of CoW with bilateral 75% stenosis of ICA and LPCoA missing

4.3.5 Case 5-75% stenosis of LICA and occlusion of RICA with LPCoA missing

Since LPCoA is missing, from clinical point of view, it is safer to conduct the CEA in the RICA. In case 5 we simulate the clamping of RICA based on case 4. Figure 4.12

shows the averaged value of pressure, flow rate and velocity in the vessels of CoW in case 5. Compared to the results in normal CoW, the largest flow loss occurs at RMCA which is 16.4%, and the largest pressure loss occurs also at RMCA which is 29.2%. Compared with the results of case 4, the largest difference between the outflows of efferent arteries of these two cases occurs at RMCA which is 14.4%. Significant increases of flow rates in ACoA (from 0.11 to 2.22 ml/s) and RPCoA (from 0.39 to 1.43 ml/s) are found, which means in case 5 collateral pathways play important roles. In case 5, we also find that collateral flow in ACoA (2.22 ml/s) is much larger than that in RPCoA (1.43 ml/s). It means that in this case collateral pathway of ACoA is more important than that of PCoA.

Since the CoW in case 2 is symmetrical, there is no difference between clamping of LICA and RICA. Therefore in case 3 if we clamp RICA, we can have the same results as that presented in Figure 4.9. Then we can compare the results of right side of case 5 with the results of left side of case 3. The largest difference occurs between the RA1 in case 5 and LA1 in case 3 which is a decrease of 10.1% in flow rate. But the flow rate in RPCoA in case 5 increases 6.7% compared with that in LPCoA in case 3. It means that in case 5 LPCoA missing increases slightly the importance of RPCoA. The difference in flow rate of ACoA between case 5 and case 3 is a decrease of 5.5%, which means that LPCoA missing decreases the importance of ACoA, but the decrease is not significant.

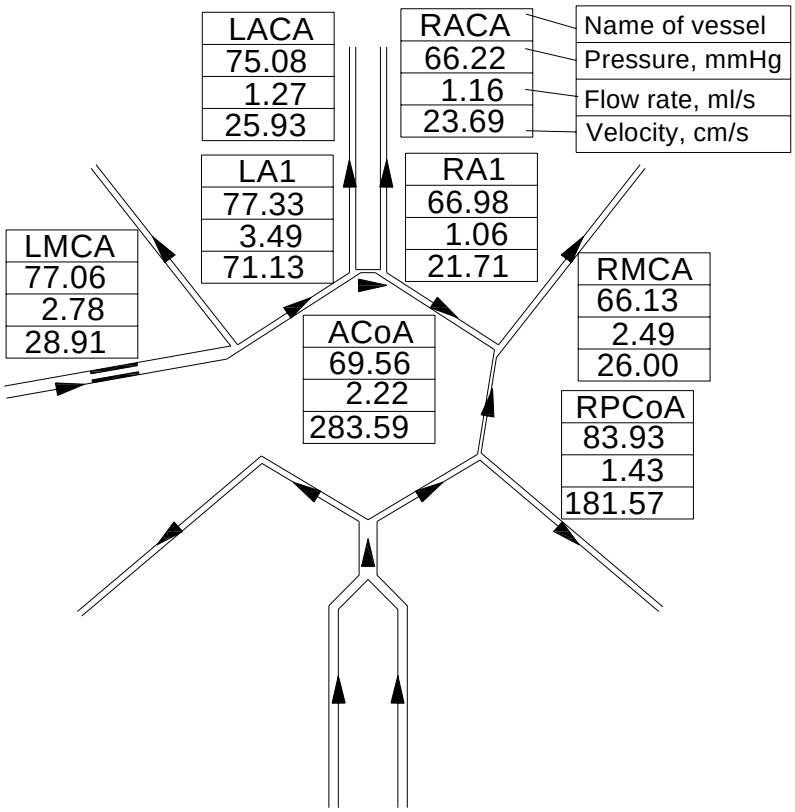

Figure 4.12 Averaged pressure, velocity and flow rate in the vessels of CoW with 75% stenosis of LICA and occlusion of RICA and LPCoA missing

4.3.6 Numerical results in case 5 without autoregulation

In order to compare the influence of the autoregulative model to the results of numerical model, we show the results of case 5 without autoregulative model in Figure 4.13. Compared to the results in case 5 with autoregulative model, we can see that pressures in all vessels increase and flow rates in all vessels decrease if neglecting autoregulation. The largest underestimate of flow rate occurs at RMCA which is 13.7%. Collateral flows in ACoA and RPCoA also decrease significantly, which means omission of CA influences the predication of collateral ability of ACoA and PCoA.

Comparing the pressure in Figure 4.13 with that in Figure 4.12, we can see that the pressure in the CoW without autoregulation is higher than that in the CoW with autoregulation. It means that perfusion pressure in the CoW without autoregulative model is overestimated. Therefore the pressure gradient between input pressure and perfusion pressure inside the CoW decreases and results in less blood supply.

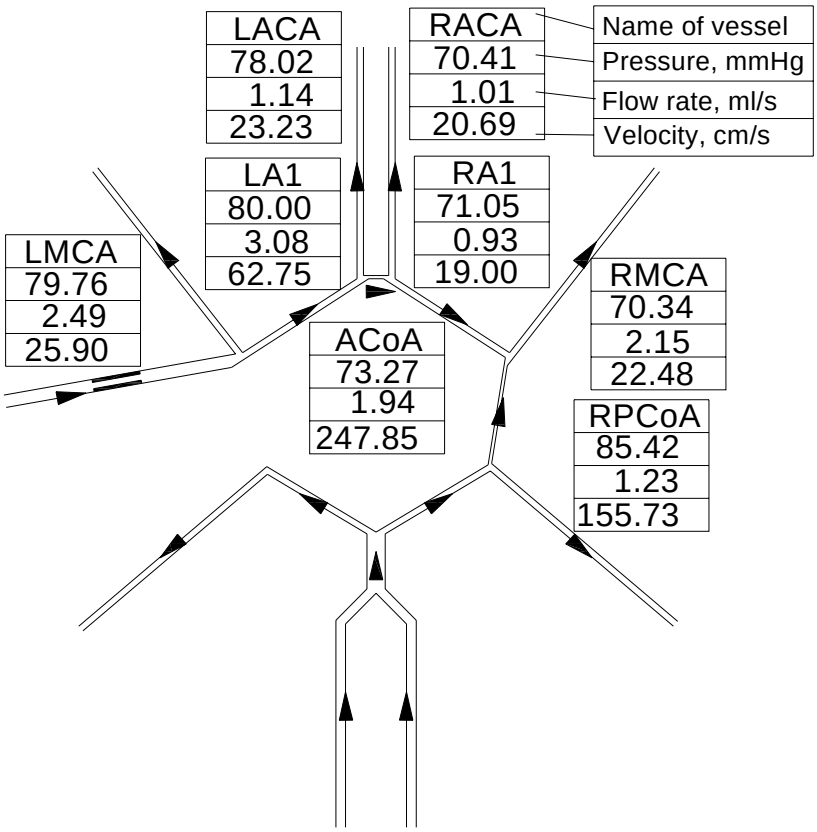

Figure 4.13 Averaged pressure, velocity and flow rate in the vessels of CoW with 75% stenosis of LICA and occlusion of RICA and LPCoA missing without autoregulation

4.4 Discussion

4.4.1 Comparison between distributed (unsteady and nonlinear) model and lumped (steady and linear) model

To investigate whether cerebral hemodynamics can be best considered linear or nonlinear, Giller et al. (2002) assessed the adequacy of linear modeling in four ways and found that there was strong evidence that blood pressure/velocity system was nonlinear. Some aspects of cerebral hemodynamics were poorly described by linear models.

Comparative studies between distributed (unsteady and nonlinear) model and lumped (steady and linear) model in the study of blood flow in the CoW have also been done by other authors (Hillen et al. 1986, 1988; Cassot et al, 1995, 2000). Motivated by clinical application of the numerical model, Hillen et al. (1988) built up a linear model which neglected the pulsatility and vessel wall elasticity. Compared with the results of nonlinear model (Hillen et al., 1986), the authors found that linear model can produce satisfactory results. By this analytical model, the authors concluded that the basic mechanism of blood flow in the CoW was similar to the principles of Wheatstone bridge, known from electrical circuit theory. However, Duros (1990) pointed out some limitations of the above linear model. Hillen et al. completely agree that the linear model is insufficient for investigations which typically require time dependent approach. Duros (1990) also suggested that both mean flows and mean pressures calculated with a nonlinear model would differ considerably with the results of a linear model.

Cassot et al. (1995) built up both nonlinear and linear models to study the effect of ACoA in the cerebral circulation. The authors found the linear model could provide

satisfactory results compared with the results of the nonlinear model. Furthermore, Cassot et al. (2000) built up a linear model to study the hemodynamic role of communicating arteries in the stenoses of ICAs. The results of the linear model were compared with that of nonlinear model and the authors found that there were no physiological significant differences between the linear and nonlinear model. Hence, the authors concluded that the linear model might be an essential tool for an accurate assessment of the cerebral hemodynamics in carotid diseases.

However, Piechnik et al. (2002) pointed out that linear methods were not applicable in general to the intracranial system. First, the linear model (Cassot et al., 2000) did not consider the function of autoregulation which is an intrinsic ability of cerebral vascular bed. Therefore, the downstream of the CoW in the linear model was passive and could not maintain relatively constant CBF. Piechnik et al. (2002) demonstrated that application of such passive-linear model resulted in significant miscalculation of pressure losses and overestimation of stenoses levels needed to produce clinical symptoms. Therefore, Piechnik et al. (2002) suggested that a nonlinear combination of passive and active model of downstream circulation and nonlinear proximal vessels was needed to obtain realistic maps of pressure changes in the cerebral circulation. Second, Piechnik et al. (2002) suggested that the nonlinear pressure-flow characteristic in large vessels should be considered.

Although some authors concluded that linear model could produce similar results compared with the nonlinear model, linear model had its limitations and engendered many arguments for the clinical application. Therefore, in this study, a nonlinear model has been developed and an autoregulation model obtained from the literature

has been applied into the nonlinear model. By this way, the limitations of the linear model (Cassot et al., 2000) indicated by Piechnik et al. (2002) have been overcome.

4.4.2 Clinical relevance of the numerical model

In this study hemodynamic change in the cerebral circulation between before and after clamping of ICA during CEA is simulated based on a nonlinear numerical model developed using MATLAB. Two pathological cases, bilateral 75% stenosis of ICA and bilateral 75% stenosis of ICA with LPCoA missing, are used to conduct the numerical tests. In patients with severe ICA stenosis or occlusion, cerebral hemodynamics is significantly impaired. Surgical treatment such as CEA can improve the cerebral hemodynamics of patients, but clamping of ICA increases the risk of ischemic stroke. Although various intraoperative monitoring methods can detect the risk for intraoperative ischemic stroke, numerical simulation can provide detailed preoperative information about the cerebral hemodyanmics of the patients. This kind of information could help clinicians to predict the cerebral hemodynamics of patients before the surgery and might help neurosurgeons to decide whether the shunt is necessary.

Previous numerical studies focus on the hemodynamics in the complete CoW. Seldom authors study the hemodynamics in the incomplete CoW, although incomplete CoW is frequently found in the literature. In this chapter two published models are combined into the study of hemodynamics in complete and incomplete CoW. The basic numerical model about CoW is widely used by many authors. The autoregulative model is obtained from experimental data and compared with experimental measurements. The results provide insight on cerebral hemodynamic change before and after clamping of ICA during CEA. We analyze the formula of autoregulative

model and find that the property of the model matches well with the physiology of autoregulation.

For patients with hypoperfusion resulting from carotid artery disease, dynamic CA is impaired and the relationship between perfusion pressure and CBF (static CA) is of more importance. Omission of CA in numerical model underestimates the calculated CBF. In this study we applied a developed mathematical model of static CA in the basic numerical model. The comparison in case 5 between CoW with and without autoregulative model shows that the largest underestimate in flow rate is 13.7% at RMCA. Cerebral hemodynamics in CoW in case 5 is severely impaired because the LICA has 75% stenosis, the RICA is occluded and LPCoA is missing. It means that in CoW with severely compromised hemodynamics underestimate of flow rate is high if CA is omitted in the numerical model.

Clinical measurements found that stenosed ICA still supplied enough blood to brain. In this study we find that in patients with bilateral 75% stenosis of ICA, either with or without one PCoA missing, collateral flows in ACoA and PCoA are small. Whether such small flow rates can be detected by clinical monitoring equipments is not clear. It means that collateral pathways only play insignificant roles in the CoW with bilateral 75% stenosis of ICA, which is well matched with the clinical findings (Hartkamp et al., 1999). Another important finding in this study is that LPCoA only plays an insignificant role in the collateral circulation either before clamping of ICA or after clamping of ICA. This could explain why unilateral PCoA missing is the most common type of hypoplasia of CoW in the clinical studies.

After clamping of ICA, collateral flows in communicating arteries increase significantly and the increase of collateral flow in ACoA is much larger than that in PCoA, which means that ACoA is a more important collateral pathway than PCoA. Many clinical studies highlighted the importance of collateral flow through ACoA (Hartkamp et al., 1999; Kluytmans et al., 1999; Miralles et al., 1995; Bisschops et al. 2003). Other numerical results also support that ACoA flow plays important role in the case with ICA occlusion or clamping (Moorhead et al, 2004a; 2004b). Some authors concluded that whether the patients with severe carotid artery stenosis can benefit from CEA is related to the patency of ACoA (Kluytmans et al., 1998). The significant increases of collateral flow after clamping of ICA in ACoA both in case 3 (from 0 to 2.35 ml/s) and in case 5 (from 0.11 to 2.22 ml/s) strongly support the aforementioned clinical findings.

Since we fix the diameter of ACoA and PCoA at 1.0 mm, we can not compare the collateral ability of ACoA and PCoA with different diameters. Clinically the diameters of ACoA and PCoA have large ranges in size (Hartkamp et al., 1999; Hoksbergen et al., 2000a) so that their collateral abilities change significantly with their diameters. Although the lengths of communicating arteries play less important roles than the diameters, when the diameters of communicating arteries are close, their lengths may have influence on the collateral ability. In our study we did not investigate the influence of length of vessels on the cerebral hemodynamics.

In the CoW with severe compromised hemodynamics, secondary collateral pathways may play roles in compensating blood flow to the deprived areas. However, OphA collateral was found a marginal effect on the compensation of cerebral perfusion

(Tatemichi et al., 1990) and leptomeningeal collateral is recruited only in the chronic ICA artery disease (Brozici et al., 2003). Therefore, these connections do not contribute significant cerebral collateral blood flow under circumstances of acute occlusion of the ICA, as occurs during CEA when ICA is clamped. Hence, in this study, the effect of secondary collateral blood supply is not considered.

Medical doctors highlighted the significance of computer model in helping clinicians to choose optimal surgical technique and/or avoid unnecessary surgery (Kailasnath et al., 1998). Very recently a patient-specific computer model was used to identify patients who can tolerate the balloon occlusion test (Charbel et al., 2004). The results showed that such kind of computer model could be used in the future clinical test. Due to its inexpensive time cost in calculation, one-dimensional numerical model presents high possibility in the future clinical application. The main limitation of this study is lack of experimental validation quantitatively. But the numerical result is well matched qualitatively with the clinical findings. The calculation time of our model for one case is less than 6 minutes, which makes it possible for future clinical application. In addition, our model considers the function of CA, which increases the accuracy of the numerical results.

4.5 Conclusions

For patients who have bilateral 75% stenoses of ICA and small diameters of communicating arteries (1 mm), stenosed ICA still can provide enough blood supply and collateral blood flow are not significant. When one ICA is clamped during CEA, blood flow in the CoW redistributes and collateral pathways play important roles. Collateral flow in ACoA is much larger than that in PCoA, which shows ACoA is the

preferential route for collateral blood flow. In the patient with bilateral 75% stenosis of ICA and LPCoA missing, the missing of LPCoA has very small effect on the global cerebral hemodynamics before and after clamping of RICA, but the collateral flow in RPCoA increases.

Chapter 5

Numerical studies on the interactive role of communicating arteries

5.1 Introduction

ACoA and PCoAs are component vessels of the CoW that have been considered as the primary collateral pathways (Liebeskind et al., 2003). In patients with severe stenosis or occlusion of the ICA, hypoperfusion or low flow areas may occur at the corresponding section of brain tissue and therefore results in high risk for ischemic stroke (Hedera et al., 1995). Primary collateral pathways redistribute blood to the deprived side and play important roles in maintaining adequate blood flow to the deprived side. The collateral capacity of primary collateral pathways is governed by morphological factors, mainly by diameters of the communicating arteries (Hartkamp et al., 1999). Therefore, the size of primary collateral pathways may be risk factors for cerebral infarction in patients with severe stenosis or occlusion of carotid arteries (Schomer et al., 1994). Many studies on hemodynamic role of the communicating arteries in the CoW have been conducted in a complete circle using one-dimensional model (Chao et al., 1971; Kufahl et al., 1985; Hillen et al., 1982, 1986, 1988; Zagzoule and Marc-Vergnes, 1986; Cassot et al., 1994, 2000; Viedma et al., 1997; Gao et al., 1997). Complete CoW, however, only accounted for a small percentage in some clinical studies, for example, 20% in Osborne et al. (1980), 22% (1999) and 29% (2000b) in Hoksbergen et al. Among the incomplete CoW, the most common type of

hypoplasia of CoW is unilateral hypofunctional PCoA, which accounts for 72% (1999) and 22% (2000b) in Hoksbergen et al. and 27% in Hartkamp et al. (1999). Hoksbergen et al. (2000b) summarized many clinical studies and found that on average 30% of the studied subjects had hypofunctional PCoAs. Although many authors concluded that ACoA played a more important role than PCoAs in patients with severe ICA stenosis or occlusion (Hartkamp et al., 1999; Hoksbergen et al., 2003a), others found that a small (<1mm in diameter) or absent ipsilateral PCoA was the only risk factor for ischemic cerebral symptom (Schomer et al., 1994; Hendrikse et al., 2001). The present study is motivated by the conflicting clinical findings about the role of ACoA and PCoAs in patients with obstructive disease of ICA.

Previous theoretical studies seldom considered the interactive role of ACoA and PCoA simultaneously in patients with ICA occlusion, and seldom authors studied the collateral capacity in the incomplete CoW. Viedma et al. (1997) concluded that it was necessary to consider simultaneously the role of both ACoA and PCoA to the affected hemisphere. Otherwise it was possible that all analyses with consideration of only one parameter could lead to an incorrect assessment of the CoW capacity. Although they calculated the reduced CBF subject to ICA occlusion with consideration of several combinations of the communicating artery sizes, in their study the largest diameters of ACoA and PCoA were 0.8 mm, which did not cover the whole range of diameters of ACoA and PCoA in clinical findings. In present study, we consider the diameter range of ACoA from 0.2 to 2.0 mm and the diameter range of PCoA from 0.2 to 2.5 mm. The aim of this study is to study the interactive role of ACoA and PCoA in an incomplete CoW in which LICA has different degree of stenosis, RICA is occluded and LPCoA is missing.

5.2 Methods

The basic numerical model is given in Chapter 3. The geometrical data and elasticity of the vessels of the CoW are given in table 3.3. The clinical-static autoregulative model developed in Chapter 4 is applied in this study. From clinical point of view, since patients with an ACoA and a PCoA that supply the hemisphere distal to a severe ICA stenosis have a risk of transient ischemic stroke (Henderson et al., 2000), we select a typical CoW with LPCoA missing and RICA occlusion to conduct this study. By this way the variables can be reduced and it becomes possible to study the interactive role of the other variables. In this study there are three variables which are the degree of stenosis of LICA, the diameters of RPCoA and ACoA.

From anatomical point of view, although the lengths of communicating arteries are also important morphological factor, we fix the lengths of communicating arteries in order to investigate the interactive role of their diameters. In the study of Zbornikova et al. (1985), the patients were classified in groups representing slight (<50% diameter reduction), moderate (50% to 75%), or severe (>75%) ICA stenosis. Based on their study, we classify the degree of stenosis of LICA in four groups: 0% stenosis, 50% stenosis, 75% stenosis and 95% stenosis.

5.3 Results

Since low cerebral blood flow is the direct risk factor for ischemic stroke and current technologies such as MRA can monitor blood flow in the major arteries of CoW, in our results, we only show blood flow in major arteries of the CoW. In the normal case of our model, total calculated blood flow rate is 12.5 ml/s, and the percentages of calculated flow rate for major efferent arteries are 22.1%, 47.8% and 30.1% for ACA,

MCA and PCA respectively. In normal case, the diameters of ACoA and PCoAs are fixed at 1 mm. In Figure 5.1, we show the simplified incomplete CoW in which blood supply to RACA and RMCA is dependent only on the collateral capacity of ACoA and RPCoA. The arrows give flow directions and negative values in numerical results represent reverse flow compared with the flow directions shown in Figure 5.1.

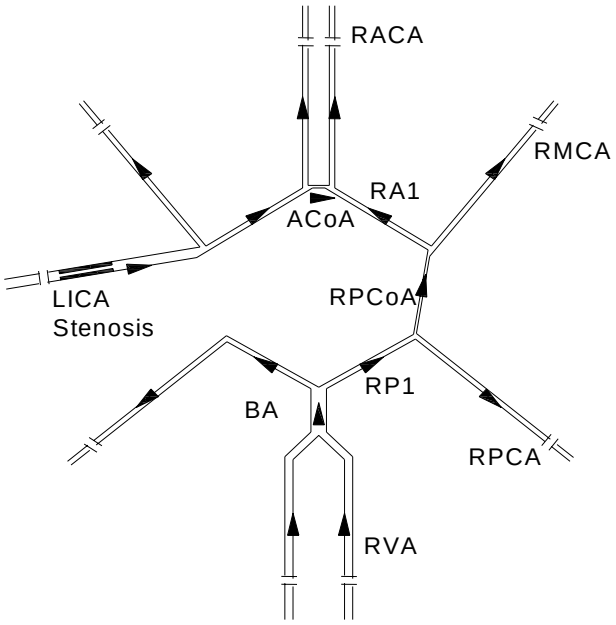

Figure 5.1 Simplified incomplete CoW with LICA stenosis, RICA occlusion and LPCoA missing

Because blood flow in both RACA and RMCA is only dependent on collateral supply from ACoA and RPCoA in the incomplete CoW, diameters of ACoA and RPCoA play important roles in providing collateral blood flow to the corresponding area. In this study, we change diameter of ACoA from 0.2 mm to 2.0 mm and diameter of RPCoA from 0.2 mm to 2.5 mm. These ranges almost cover the diameters of ACoA and PCoAs in clinical findings. We study the changes of flow rates in five vessels which are RACA, RMCA, ACoA, RPCoA and RA1 in order to investigate how blood flows

in these arteries change with the degree of stenosis of LICA and diameters of ACoA and RPCoA.

5.3.1 Relative flow in RMCA and RACA

Relative flow is defined as following formulation:

Relative flow = flow rate in the incomplete CoW/flow rate in normal case.

Relative flow in RMCA with different degree of stenosis of LICA and different diameters of ACoA and RPCoA is shown in Figure 5.2. Relative flow in RACA is very similar to that in RMCA whatever diameters of RPCoA and ACoA and degree of stenosis of LICA. Therefore, we only show the relative flow in RMCA. When degree of stenosis of LICA is not larger than 50%, changes of relative flow in RMCA with diameters of PCoA and ACoA are almost the same. When degree of stenosis of LICA increases to 75% and diameter of ACoA is larger than 1mm, relative flow in RMCA is independent on diameter of ACoA but dependent on diameter of PCoA. When degree of LICA stenosis increases to 95%, relative flow in RMCA is highly dependent on the diameter of RPCoA but is independent on the diameter of ACoA. For cases with less than 75% stenosis of LICA, when diameter of ACoA is larger than 1mm and diameter of RPCoA is larger than 1.4mm, relative flow in RMCA is almost independent on the diameters of ACoA and RPCoA. Below these ranges, relative flow in RMCA increases with the increase of diameters of RPCoA and ACoA.

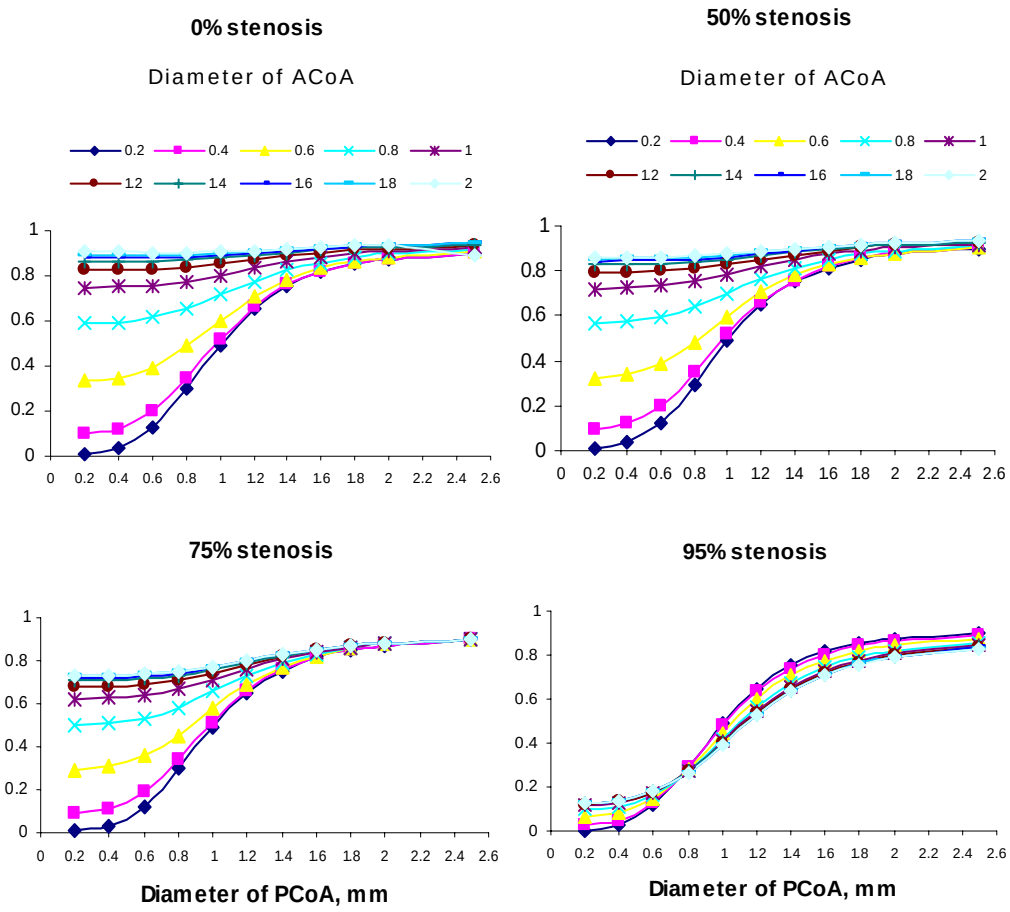

Figure 5.2 Relative flow in RMCA with different degree of stenosis of LICA and different diameters of ACoA and RPCoA

5.3.2 Relative contribution of ACoA

Relative contribution is defined as following formulation:

Relative contribution of ACoA = flow rate in ACoA in the incomplete CoW / (flow rate in RACA in normal case + flow rate in RMCA in normal case).

In our model of incomplete CoW, the blood flow of RACA and RMCA is supplied by the collateral pathways of ACoA and RPCoA. From the definition we can see that relative contribution of ACoA represents the relative compensation of blood flow to

RACA and RMCA only through ACoA. Since the purpose of this study is to investigate the interactive role of ACoA and PCoA in the process of compensation, relative contribution of ACoA can show the compensative ability of ACoA.

Figure 5.3 shows the relative contribution of ACoA changes with the diameters of ACoA and RPCoA and the degree of stenosis of LICA. From Figure 5.3 we can see that relative contribution of ACoA decreases with the increase of degree of stenosis of LICA. When degree of stenosis of LICA is not larger than 50%, the decrease of relative contribution of ACoA with respect to the degree of stenosis of LICA is very small, but for cases with not less than 75% stenosis of LICA, the decrease is significant, especially for cases with large diameters in ACoA and RPCoA. When the degree of stenosis of LICA increases to 95%, the circle is almost bilateral occlusion in ICAs, and for cases with diameter of RPCoA larger than 0.74 mm, blood flow in ACoA is reserved. It means that there is no relative contribution to RACA and RMCA through ACoA. Therefore, in the case with 95% stenosis of LICA, collateral blood supply is provided only by the RPCoA as long as its diameter is larger than 0.74 mm. For all cases, when diameter of ACoA is larger than 1mm, relative contribution of ACoA is almost independent on diameter of ACoA. When diameter of ACoA is less than 1mm, relative contribution of ACoA increases with both the increase of diameter of ACoA and the decrease of diameter of RPCoA.

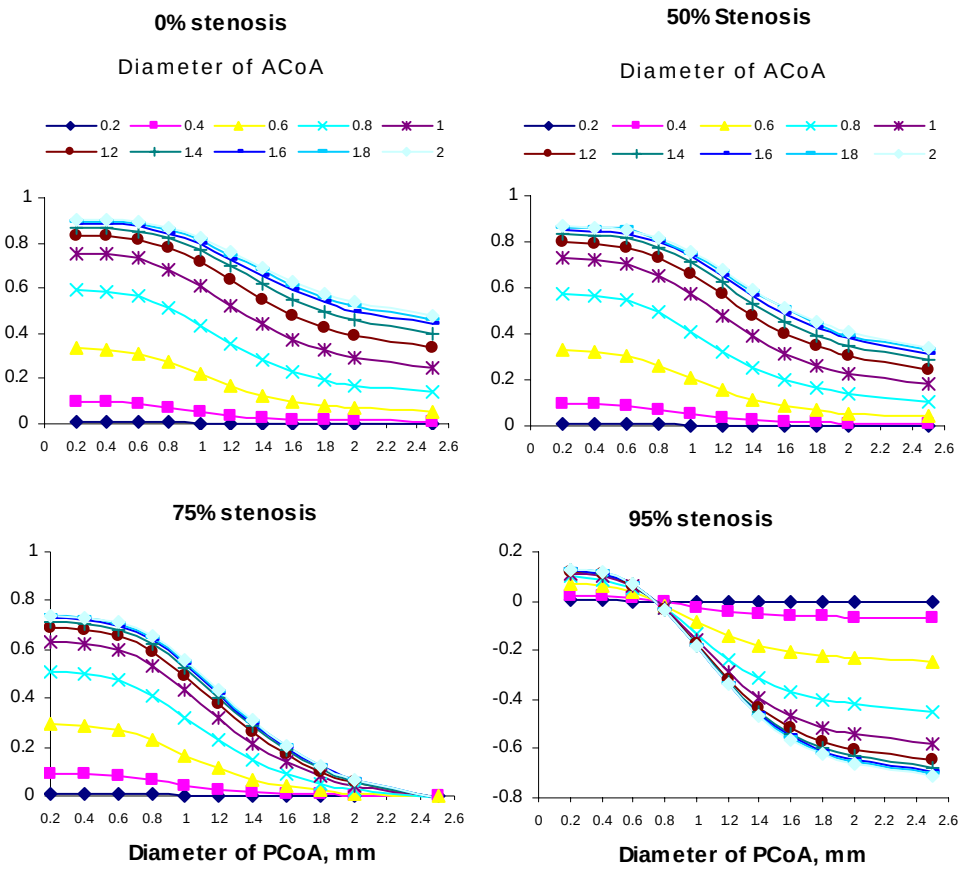

Figure 5.3 Relative contribution of ACoA with different degree of stenosis of LICA and different diameters of ACoA and RPCoA

5.3.3 Relative contribution of RPCoA

Relative contribution of RPCoA has the same definition as that for ACoA. The changes of relative contribution of RPCoA with the diameters of ACoA and RPCoA and the degree of stenosis of LICA are shown in Figure 5.4. We can see from Figure 5.4 that the relative contribution of RPCoA is highly dependent on the diameter of RPCoA and increases with the increase of diameter of RPCoA. Relative contribution of RPCoA increases with the increase of degree of stenosis of LICA, but when degree of stenosis of LICA is not larger than 50%, the influence of stenosis of LICA is very small. In the cases with not larger than 75% stenosis of LICA and not less than 0.8 mm

diameter of RPCoA, relative contribution of RPCoA decreases significantly with the increase of diameter of ACoA. In the case with 95% stenosis of LICA, when diameter of RPCoA is less than 1mm, the influence of diameter of ACoA to the relative contribution of RPCoA is almost equal to zero. When diameter of RPCoA is larger than 1mm, the relative contribution of RPCoA increases with the increase of diameter of RPCoA and ACoA. It means that 95% stenosis of LICA significantly reduces the perfusion pressure in left side of the CoW. Although RICA is occluded, the perfusion pressure of right side of CoW is higher than left side of CoW due to the LPCoA missing and the severe stenosis of LICA. In this case, the diameter of ACoA is important to the compensation of left side of the CoW.

When the relative contribution of RPCoA is close to or larger than 1, it means that only RPCoA can supply collateral blood flow to the right side of CoW. From Figure 5.3 and 5.4 we can see that the diameter of ACoA and RPCoA play important roles in supplying collateral blood flow to the corresponding deprived area. The stenosis of LICA mainly influences the collateral ability of ACoA.

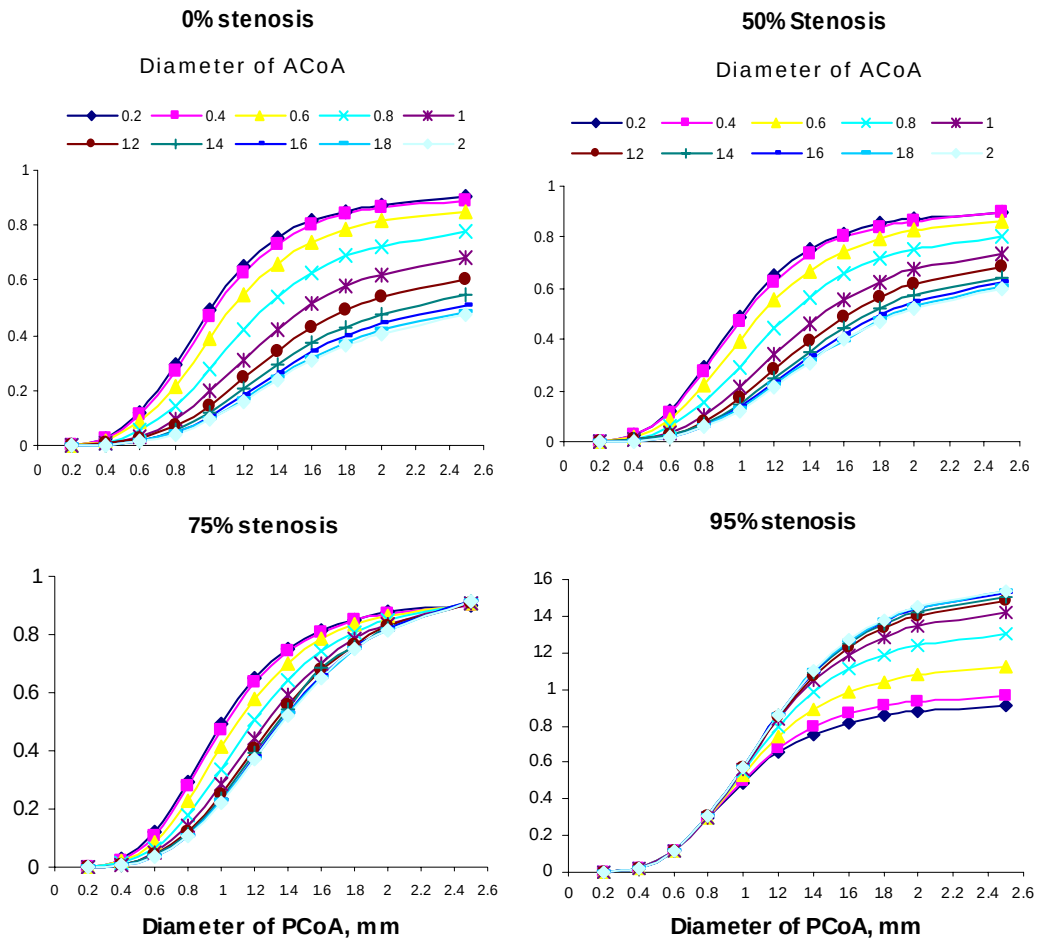

Figure 5.4 Relative contribution of RPCoA with different degree of stenosis of LICA and different diameters of ACoA and RPCoA

5.3.4 Relative flow rate in RA1

In our study, we fix the diameter of RA1 at 2 mm. Since RA1 is an important component in the CoW and connects the RACA and RMCA, we define the relative flow in RA1 to show the effect of RA1 on the compensation to RACA and RMCA. The definition is as follows:

Relative flow in RA1 = flow rate in RA1 in the incomplete CoW/flow rate in RA1 in the normal case.

The relative flow in RA1 shown in Figure 5.5 is influenced by degree of stenosis of LICA, diameter of ACoA and diameter of RPCoA. The contribution to relative flow of RMCA and RACA for different diameters of RA1 was not discussed in this study. From Figure 5.5 we found that for constant diameter of RA1, the contribution for connecting anterior and middle part is significant.

In normal case the flow rate in RA1 is 1.38 ml/s from RICA to RACA (see Figure 4.7). In the incomplete CoW studied in this chapter, the RA1 play an important role in balancing the collateral ability of ACoA and RPCoA. It means that through RA1 the compensation of collateral blood flow from ACoA and RPCoA is interactive. From Figure 5.5 we can see that in the case with not larger than 75% stenosis of LICA, relative flow in RA1 is not larger than 1. It means that the flow in RA1 is less than that in the normal case. The negative relative flow represents reverse of blood flow in the RA1 compared with the normal case. Overall, relative flow in RA1 increases with the increase of diameter of RPCoA and the increase of degree of stenosis of LICA, and decreases with the increase of diameter of ACoA.

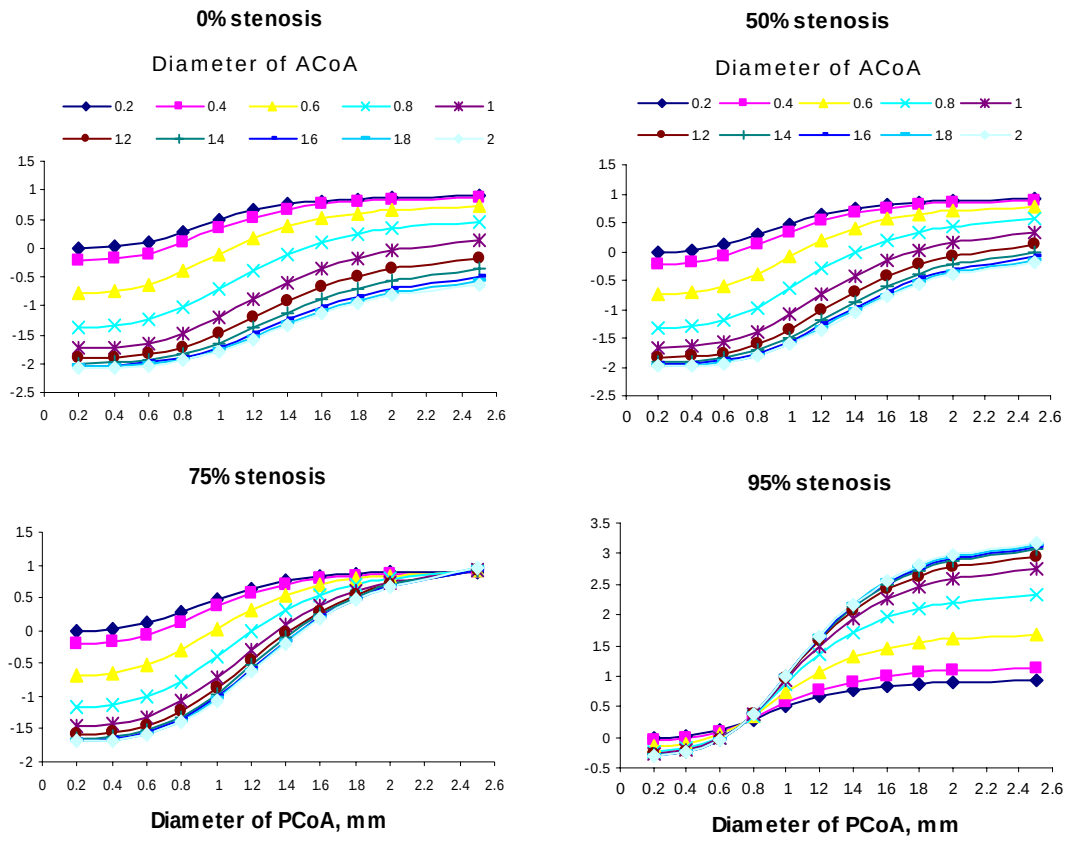

Figure 5.5 Relative flow in RA1 with different degree of stenosis of LICA and different diameters of ACoA and RPCoA

5.4 Discussion

In this chapter the interactive role of ACoA and PCoA in the collateral circulation of CoW with different degree of ICA stenosis is studied based on a simplified one-dimensional numerical model of CoW with autoregulation. Despite three dimensional simulation of vascular network has gained a great deal of interest over the last decade, one-dimensional numerical model is still playing an important role on studying hemodynamics in human vascular system, particularly if only the average values are of interest (Formaggia et al., 2003; Sherwin et al., 2003). In this study we select a typical incomplete CoW in which LPCoA is missing, RICA is occluded and LICA has

different degree of stenosis. Unilateral PCoA missing is the most common type of hypoplasia of the CoW (Hartkamp, et al., 1999; Hoksbergen et al., 1999). Unilateral ICA occlusion is also frequently found in the clinical studies. The integration of ICA occlusion and anomaly of CoW makes the patients sensitive to the hemodynamic change in the CoW.

5.4.1 Comparison with others' study

Our results have some agreements with the previous clinical findings and published numerical results. Hartkamp et al. (1999) observed that the prevalence of collateral ACoA flow was higher in group of unilateral occlusion of ICA than it was in group of ipsilateral ICA stenosis and contralateral ICA occlusion, which means stenosis of ipsilateral ICA reduced the collateral contribution of ACoA. This is in agreement with our results in which relative contribution of ACoA in case with 75% stenosis of LICA is smaller than that in case with 0% stenosis of LICA.

Hoksbergen et al. (2000) studied 12 acute stroke patients and compared with their postmortem and concluded that the threshold diameter allowing for cross-flow through the primary collateral arteries of the CoW is between 0.4 and 0.6 mm. Cassot et al. (1995) and Dickey et al. (1996) numerically concluded that the smallest luminal diameter allowing for cross-flow through the ACoA was 0.4 mm. Figure 5.6 shows the flow rates of ACoA with diameter of 0.2 and 0.4 mm in different degree of stenosis of LICA and different diameters of RPCoA. From Figure 5.6 we can see that for ACoA with diameter of 0.2 mm, flow rate in ACoA is almost equal to zero for all diameters of RPCoA. But for ACoA with diameter of 0.4 mm, when diameter of RPCoA decreases from 2.5 mm to 0.2 mm, flow rate in ACoA increases from 0.2 to 27.3

ml/min. Therefore, for small diameters of RPCoA, ACoA with diameter of 0.4 mm allows blood flow to go through it.

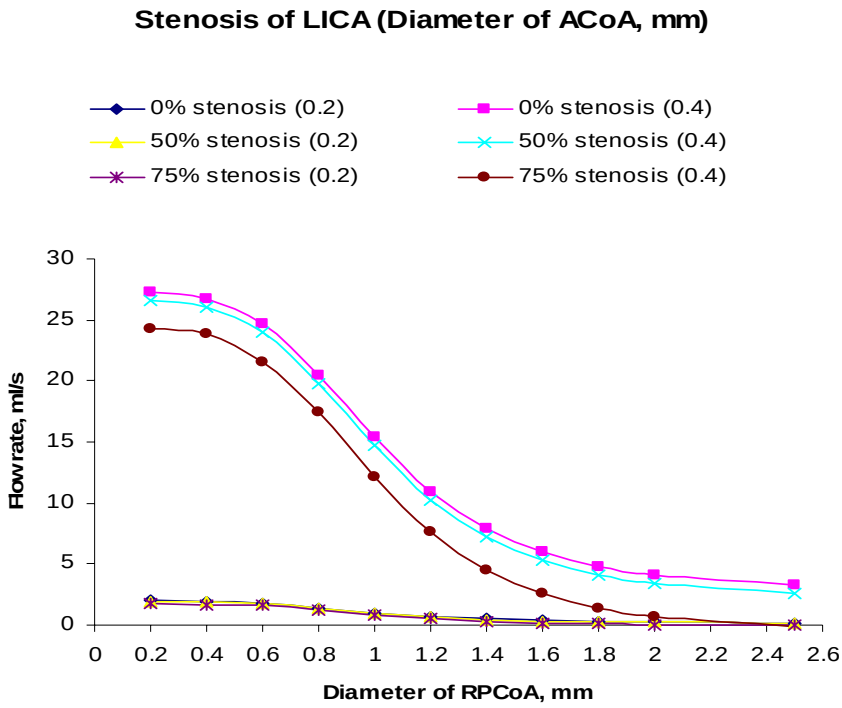

Figure 5.6 Flow rates in ACoA with different degree of stenosis of LICA and different diameters of ACoA and RPCoA

Moreover, Dickey et al. (1996) found that in patients with ICA occlusion and a well-functioning ACoA, the collateral supply from the PCoA to the deprived hemisphere fell to zero when its diameter was set at levels < 0.5 to 0.6 mm. Figure 5.7 shows the flow rates in RPCoA with diameter of 0.4 and 0.6 mm in different degree of stenosis of LICA and different diameters of ACoA. From Figure 5.7 we can see that when diameter of RPCoA is equal to 0.4 mm, for cases with different degree of stenosis of LICA, flow rate in RPCoA decreases to almost zero with the increase of diameter of ACoA. It shows that our results are matched with that of Dickey et al. (1996).

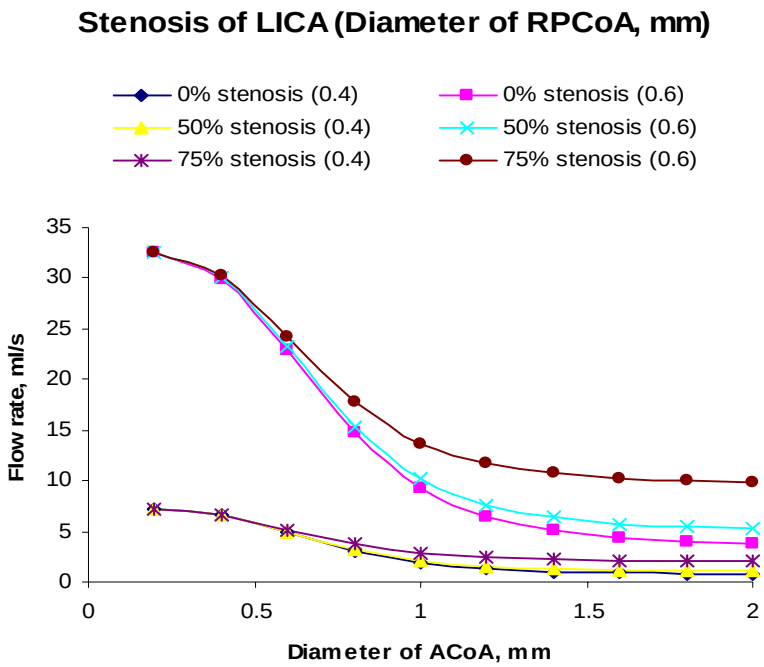

Figure 5.7 Flow rates in RPCoA with different degree of stenosis of LICA and different diameters of ACoA and RPCoA

Hoksbergen et al. (1999) hypothesize that collateral ability of PCoA (perhaps ACoA also) increase during the slow progression of carotid artery stenosis. Our results confirmed that collateral contribution of PCoA increase with the increase of carotid artery stenosis. But our study found that collateral ability of ACoA decreases when one ICA is occluded and the other ICA has progressing stenosis. The collateral ability of ACoA perhaps increase with the slow progression of carotid artery stenosis in such case that one ICA is stenosis-free and the other ICA has progressing stenosis.

5.4.2 Significant findings of this study

Our results show that relative flow in RACA and RMCA is dependent on the diameters of both ACoA and RPCoA and the degree of stenosis of LICA. Relative contribution of ACoA is influenced by the degree of stenosis of LICA. Relative

contribution of ACoA and PCoA are highly interactive, especially when diameters of ACoA and RPCoA are in small size. Although we fix the diameter of RA1 at 2mm, this vessel plays an important role in balancing the collateral blood flow from ACoA and RPCoA. Therefore, if the RA1 is well developed in the patients, it is necessary to simultaneously study the collateral ability of ACoA and RPCoA.

From this study it is found that cerebral hemodynamics in the incomplete CoW is not influenced by only one factor but many factors such as the degree of stenosis of ICA and the diameters of ACoA and RPCoA. Because the influence of these factors is interactive, we can not neglect any one factor when we study the influence of the other factors. Otherwise it may lead to incorrect assessment of the CoW capacity (Viedma et al., 1997).

5.4.3 Explanation for the conflicting clinical findings

Some authors found that in pathological cases the ACoA might be a key collateral pathway as a non-functioning ACoA was associated with an increased risk of developing low-flow infarcts (Hartkamp et al., 1999; Kluytmans et al., 1999; Miralles et al., 1995; Bisschops et al. 2003). Hartkamp et al. (1999) gave a possible explanation that the resistance to flow across the PCoA was greater than that across the ACoA, because the PCoA was usually a longer vessel, which implied that lengths of communicating arteries also played roles in collateral capacity of the CoW. Our results show that relative flow in RMCA and RACA is regulated not only by diameter of ACoA but also by diameter of RPCoA. The conclusion that ACoA plays key role in collateral capacity might be due to patient selection or different geometrical data of the CoW between the patients and our model, which makes the PCoA play an

insignificant role in the collateral capacity. Another possible reason is that A1 segment could be hypoplastic which results in the disconnection of ACoA and corresponding PCoA. In our study we find that RA1 plays an important role in balancing the collateral blood flow in ACoA and RPCoA. The hypoplasia of RA1 may severely damage the interactive compensative ability of ACoA and RPCoA, as stated by Ferrandez et al. (2002) that a missing or dysfunctional A1 seemed to be the worst case. Under this condition, the collateral abilities of ACoA and PCoA may be separated. Therefore, the conflicting findings about the role of ACoA and PCoA may be found in the clinical studies.

5.4.4 Asymmetry of diameters of PCoAs

In a complete CoW, diameters of two PCoAs are seldom the same. Since unilateral hypofunctional PCoA accounted for about 30% of studied subjects with stenosis or occlusion of ICA (Hartkamp et al., 1999), the pathological case discussed in this study is possible to be found in studied subjects. One PCoA missing in this study makes the asymmetry of diameters of PCoAs in the CoW. The effect of asymmetry was studied by some authors. Hillen et al. (1986) discussed the effect of asymmetry of PCoAs and found very small pressure difference between two sides of the CoW. Cassot et al. (2000) studied the interhemispheric pressure difference due to the asymmetrical PCoAs using an analytical model and found that whatever the PCoAs asymmetry, the interhemispheric pressure difference was relatively low if the ACoA diameter was equal to or greater than 1.0 mm and even negligible when ACoA was fully functional. Viedma et al. (1997) mentioned that a possible asymmetry of PCoAs was not significant because only one side PCoA was important to evaluate hemispheric flow.

5.4.5 Limitations of this study

There are some limitations in our study. First, we use one-dimensional model to study the practically 3D vascular network. The effect of tortuous route and taper of vessels, sudden reduction and expansion of cross-sectional area, branches and bifurcations is neglected. Some author concluded that these factors only played marginal roles in hemodynamics of vascular network (Hillen et al., 1988). Second, we only consider the primary collateral pathways in CoW. When severe hypoperfusion occurs in the CoW, secondary collateral pathways such as ophthalmic arteries and leptomeningeal collateral vessels may play roles in compensating cerebral vascular reserve. However, Anzola et al. (1995) concluded that the contribution of the ophthalmic pathway was probably of limited functional significance to the hemispheric blood supply. The last limitation is that the diameters of vessels in CoW are fixed except for that of ACoA and PCoA.

5.5 Conclusions

In the incomplete CoW studied in this chapter, the diameters of ACoA and RPCoA interactively play important roles in providing collateral blood flow. The cerebral hemodynamics of the CoW is influenced simultaneously by the degree of stenosis of LICA and the dimeters of ACoA and RPCoA. The results of this study can give insight to the interactive role of both ACoA and RPCoA on the collateral capacity of the incomplete CoW with ICA stenosis and/or occlusion. It is concluded that the collateral ability of ACoA and PCoA should be considered simultaneously in the future study on the collateral circulation in the CoW.

Chapter 6

In vitro experiment

6.1 Introduction

Since mathematical models have been widely used by many researchers in the study of blood flow in the CoW, experimental validation is highly expected. In vivo experimental validation faces difficulties in the invasive measurements of hemodynamic parameters in brain. It is mainly due to the encasement of the skull which makes invasive measurements of cerebral hemodynamic parameters unavailable. Although various monitoring equipments, such as MRA, MRI, TCCD and DSA, were developed recently to conduct non-invasive measurements in human brain, non-invasive measurements of hemodynamic parameters in the CoW were not enough for the clinical validation of mathematical modeling. In vitro experimental study on hemodynamics of the CoW is seldom found in the literature because it is difficult to simulate the complex physiological conditions of cerebral circulation. Therefore, in vitro experimental models were hardly used to validate the numerical models about blood flow in the CoW. The aim of this project is to build up an in vitro experiment to study blood flow in the CoW and validate the results of the numerical model.

To the best of our knowledge, in vitro experimental investigation of hemodynamics in the CoW can only be found in the study of Bossuet et al. (1999). But in their publication, details of the experimental setup and results were not found. Therefore,

our study about in vitro experimental investigation on blood flow in the CoW is conducted from the concept.

Due to the complex geometrical structure of CoW and its physiological condition, it is impossible to reproduce an anatomic CoW in an in vitro experiment. Previous studies in the flow phenomenon at arterial bifurcation used rigid tube to simulate the artery. Since artery is elastic, rigid tube can not simulate the property of wave propagation in arteries. Recently silicon tube is used to substitute for vessels in the study of blood flow. In this project, we use coupled rigid and silicon tubes to complete the cerebral circulatory system. To in vitro simulate blood flow in the CoW, we need to consider the factors involved in experiments such as vessels, blood, heart, CoW, terminal resistances at the end of vessels and measuring transducers.

Another problem in the experiment is to determine what kind of measurement needs to be conducted. Because of the physical structure of CoW in the experiment, non-invasive measurements are difficult to implement. Furthermore, invasive measurements will influence the local flow phenomenon since the velocities in the tubes are small. Because there are 18 tubes in the CoW, it is difficult to conduct the measurements in all the tubes. However, since we only need to measure the averaged value in the experiment, a convenient method can be used to conduct the non-invasive measurements by weighting the outflows in fixed time.

Blood flow propagation in the CoW can be described as pulse wave propagating in the network of elastic vessels. Since the wavelength of the pulse wave is much larger than the total vessel length, the vascular system only can memorize a small part of the wavelength. Therefore, the details of wave propagation are not the focus of this study.

CHAPTER 6 IN VITRO EXPERIMENT

The purpose of building up the physiological pressure waveform in the experiment is to create a similar condition to that in the numerical model. The emphasis of this study is to investigate the blood flow distribution in the CoW under conditions of different stenoses in the afferent tubes. To ensure the similitude between numerical and experimental simulation, the geometrical and dynamical similarity should be maintained. In this experiment, the geometry of the CoW is the same as that used in the numerical model. Therefore, the geometrical similarity has been ensured. To keep the dynamical similarity in the study of blood flow, Fung (1997) suggested that the Reynolds number ($\mathrm{Re} = \frac{VD}{\nu}$) and Womersley number ($\alpha = D\sqrt{\frac{\omega}{\nu}}$) should be the same, where V is velocity, D diameter, ν kinematic viscosity, ω frequency. In this experiment, the above parameters are kept the same as that in the numerical model. Therefore, the dynamical similarity has also been ensured.

6.2 Experimental setup

Figure 6.1 shows the schematic illustration of the experimental setup. The components inside dashed line are given at side view and the others are given at planform.

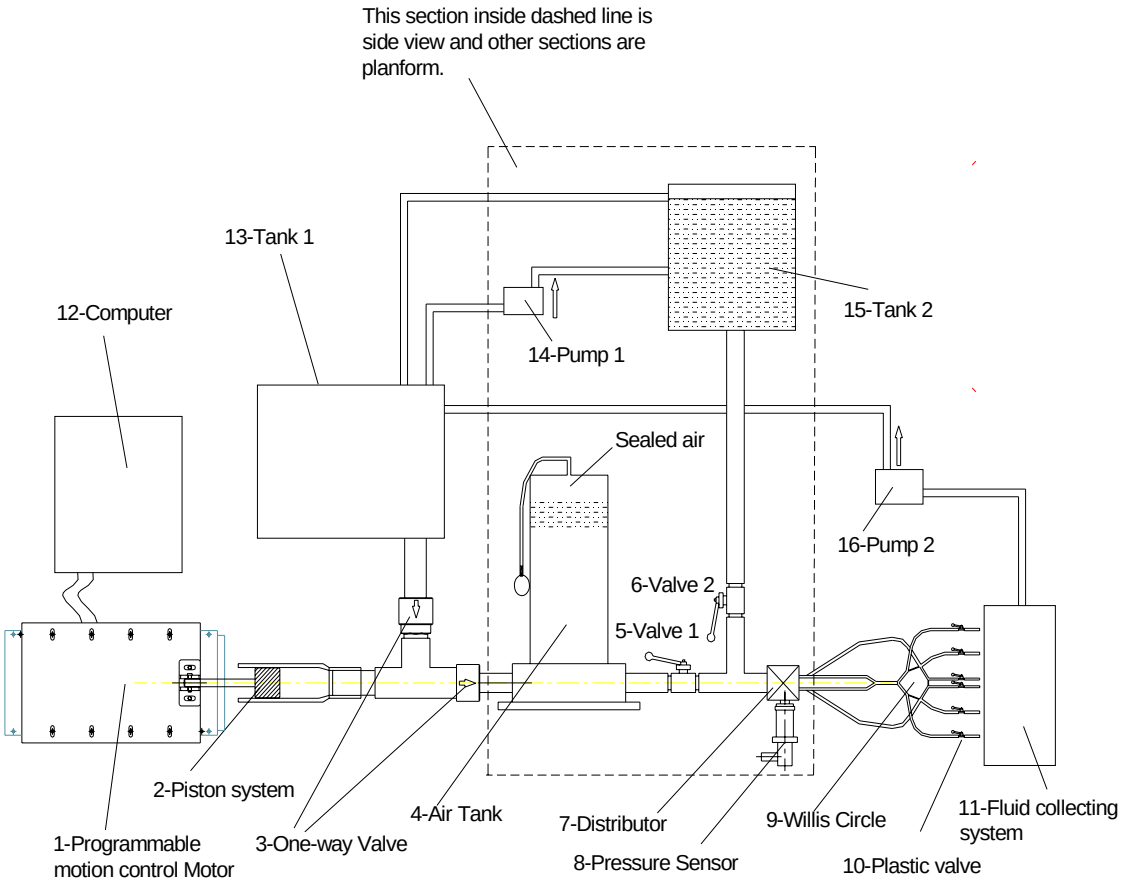

Figure 6.1 Schematic illustration of experimental setup

The apparatus used in the experiment are listed as follows:

1. Programmable motion control motor
2. Piston pump system
3. Two one-way valves
4. Air chamber with dischargeable valve
5. Valve used to control pulsatile flow
6. Valve used to control steady flow
7. Fluid distributor
8. Pressure transducer
9. Circle of Willis coupled with solid and silicon tubes
10. Plastic valves
11. Fluid collecting system
12. Computer with motion control card and A/D convert card
13. Tank for storing and supplying fluid
14. Pump used to supply fluid for steady water head
15. Water tank with constant water head
16. Pump used to circulate fluid in the system
17. Electronic weighting machine (EB-4000HU) with 0.01g readability

Figure 6.2 shows all the apparatus used in the experiment.

Figure 6.2 Photo of the apparatus used in the experiment

The drive in the experiment is given by a programmable linear motion control motor 1 (LMS 50_C4_L555_5, PBA Systems Pte Ltd, Singapore) with high speed (maximum velocity 5m/s) and high resolution ($5\mu m$), which is shown in Figure 6.3. The continuous force and peak force of the motor are 252 N and 918 N, respectively. Maximum acceleration is 100 m/s^2 and moving carriage weight is 2.54 kg. The movement of the motor is controlled by software (Automate v1.0.12, PBA Systems Pte Ltd, Singapore). The speed, acceleration and displacement of the motor are programmable controlled. Accompanied with the motor, a motion control card (MC4000) was installed in a PC. In order to avoid accident, a stop sensor was installed on the motor and a control panel was put on computer table.

Figure 6.3 Programmable motion control motor

Figure 6.4 shows the piston system and the two one-way valves used in the experiment. The piston system 2 is composed of a piston with diameter of 3.8cm and a cylinder with inner diameter of 4cm and length of 15cm. The piston is made of plastic and the cylinder is made of Perspex. Between the piston and cylinder, there are two elastic o-rings which are carefully selected according to the diameters of piston and cylinder. Too small o-ring results in leaking and too large o-ring increases the friction between piston and cylinder and subsequently results in vibration of the motion control motor when it is operating. An air discharging hole is drilled on the top of cylinder to release the air in the system. Two one-way valves 3 are installed at the end of cylinder to ensure that there is no backflow when piston operates.

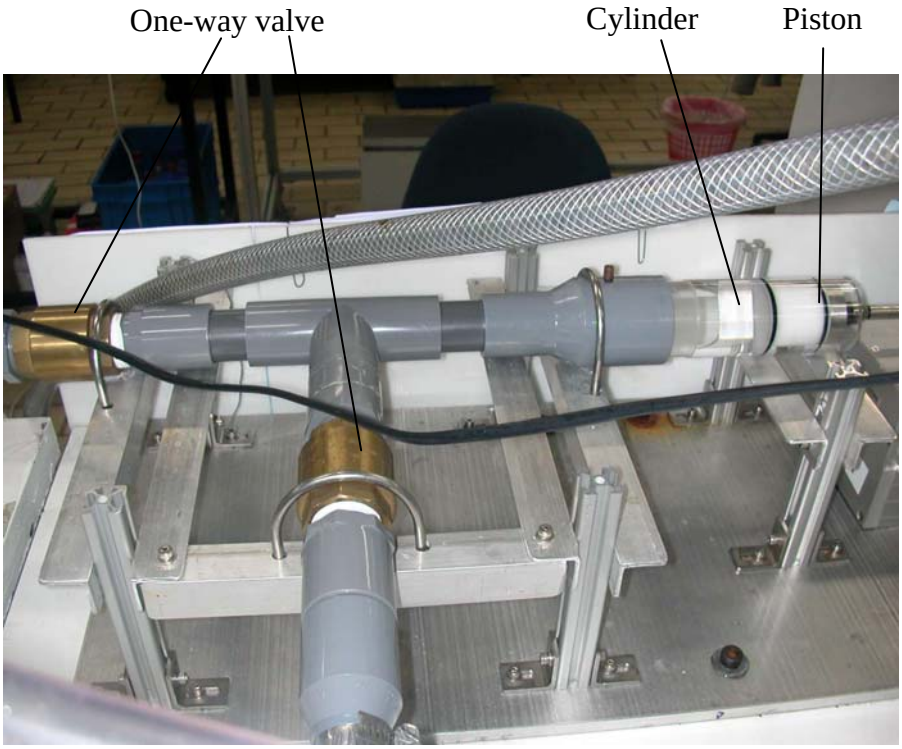

Figure 6.4 Piston system and two one-way valves

An air chamber 4 with dischargeable valve is installed into the system. A certain quantity of air can be sealed inside the tank and the quantity of air is adjustable. When fluid pressure increases, air inside the tank will be compressed. This function can simulate the compliance of the vessel. Valve 5 and valve 6 are used to change pressure from unsteady to steady input.

Figure 6.5 shows the circle of Willis, fluid distributor and pressure transducer. The circle of Willis is fabricated by coupled rigid and elastic tubes. The size of tubes has the same magnitude as the real size of cerebral vessels. All the tubes in the circle can be easily changed and therefore it is convenient to study the collateral capacity of communicating arteries with different sizes. Distributor 7 is designed to distribute

fluid to the circle of Willis 9 simultaneously. A pressure sensor 8 (ATM231.0310.0147.00, accuracy 0.5%) is installed in the distributor and therefore transient input pressure signals can be collected. The signals measured by pressure sensor are voltage signals. The voltages signals are transferred to an A/D card which is installed in the computer. Then the A/D card transforms the voltage signals into pressure signals.

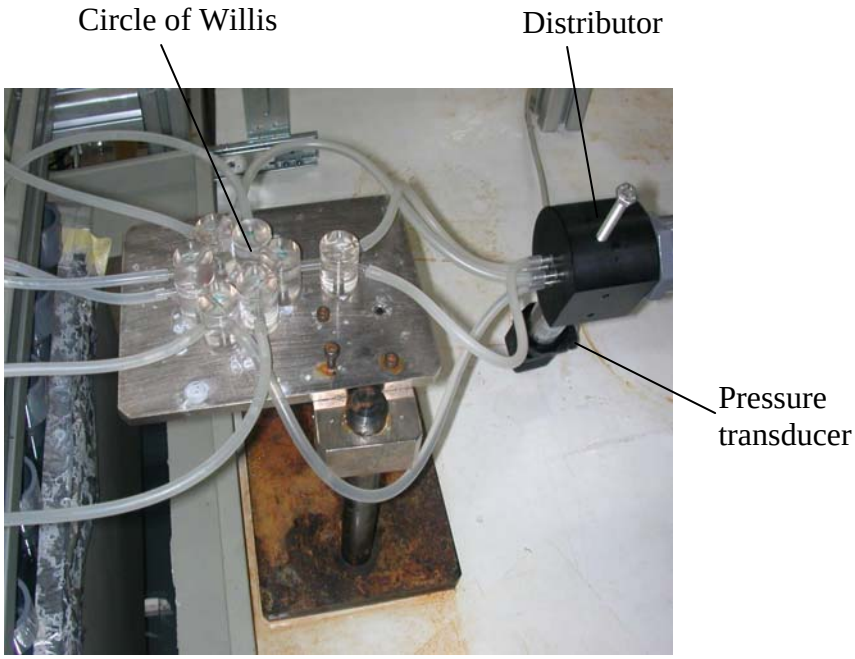

Figure 6.5 Circle of Willis, fluid distributor and pressure transducer

Figure 6.6 shows the fluid collecting system. The fluid collecting system simultaneously collects outflows from the CoW and distributes the fluid into six beakers.

Figure 6.6 Fluid collecting system

6.3 Procedures of experimental measurement

The fluid used in the experiment is mixture of 70% water and 30% glycerin. The viscosity of the mixture is around 3.8cp. The first procedure for experimental measurements is to program in the software to control the pump. In the program, the forward and backward movement profiles of piston are controlled by its speed, acceleration and displacement. The dwell time between forward and backward movement can be adjusted according to the requirement of period of waveform. Adjusting the speed, acceleration and dwell time, we can control the period of movement to be one second.

The quantity of air in the air chamber is used to simulate the arterial elasticity. More air in the chamber represents smaller stiffness parameter of arterial vessel. The quantity of air determines the amplitude of pressure waveform. By adjusting the air

quantity, the minimum and maximum values of the pressure waveform can be controlled.

Finally by adjusting the parameters in the program and the quantity of air in the air chamber, we obtain the suitable pressure waveform in the experiment which is shown in Figure 6.7. The mean pressure in one period in experiment is 99 mmHg and in numerical model is 98 mmHg. Comparing the two pressure waveforms, we can find that they are similar in the profile. Since the pressure waveform used in numerical model and shown in Figure 6.7 was smoothed by Hillen et al. (1982), we do not need to produce the exact same profile in experiment as that in numerical model. Therefore, the input pressure waveform in the experiment shown in Figure 6.7 can be used in the in vitro experimental study.

In the experiment, we use rigid tubes and silicon tubes to connect the whole system. The four afferent tubes and six efferent tubes in the CoW are silicon tubes, but the circle itself is made of rigid tubes. Since the length and diameter of the components of the CoW are small, the elasticity of the components of the CoW is high and could play insignificant role in the wave propagation. How much influence of the application of rigid tubes in the CoW to the experimental measurements is not clear. In the experiment, we avoid sharp edge in the way of forward fluid. In the distributor and the circle of Willis, slope is built up in everywhere to reduce the flow loss due to sudden change of cross section area.

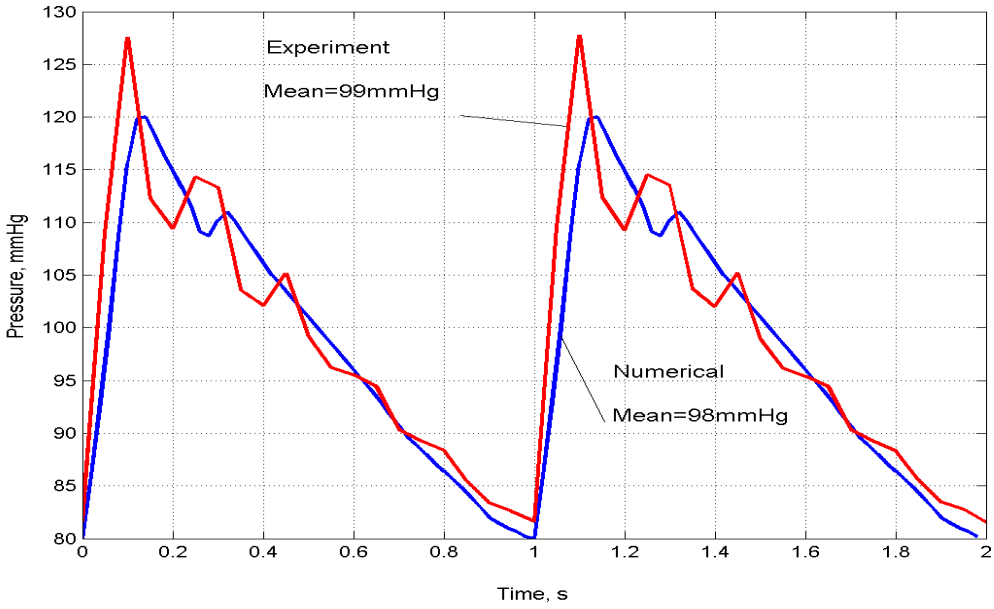

Figure 6.7 Input pressure waveform in experiment and numerical model

The pressure signals are measured at the entry of the CoW and transferred to an A/D card in the computer. Then the A/D card produces an excel file through which we can check the pressure waveform at any time.

Keep running the system for half an hour. Since the fluid system automatically circulates, we just check whether somewhere is leaking or there are bubbles in the system. When the system becomes stable and there is no leaking or bubbles, we start to collect the outflows from the CoW in a fixed time (5 minutes). We use a stop watch to record the time. Before collecting fluid, the six beakers are weighted and their net weights are recorded. After the collection of fluid, we balance the gross weight of six beakers then we can get the weight of fluid collected in five minutes. Since the density of fluid is known, we can calculate the mean flow rates of the efferent tubes.

For the pulsatile pressure inputs, the measurement for each case is repeated three times and the average is taken as the final result. For the steady pressure inputs, we only take one measurement to compare with the results of unsteady pressure inputs. We clamp the afferent elastic tube to simulate the ICA occlusion. The 75% stenosis of ICA is simulated by an elastic tube with diameter of 2mm and length of 5mm in the middle of ICA. The simulation of stenosis in experiment is the same as that in numerical model.

6.4 Comparison between experimental measurements and numerical results

The terminal resistances of the CoW are controlled by small plastic valves. By adjusting the plastic valves, the distal resistances can be changed. Therefore, we can control the distribution of outflows and the total flow rate in the system. In this experiment, we study five cases in which we measure the flow rates in six efferent tubes. The experimental measurements are compared with numerical results. The words “steady” and “unsteady” used in the thesis are defined as follows.

- Steady = Non-pulsatile flow
- Unsteady = Pulsatile physiological flow

6.4.1 Case 1-Normal case

Table 6.1 shows the comparison of flow rates in efferent arteries between experimental measurements and numerical results in the normal case. In the unsteady flow measurement, the input pressure waveform is given in Figure 6.7. In the steady flow measurement, the input pressure is given by a constant pressure head. Numerical

results are calculated based on the numerical model developed in Chapter 3. The distal resistance used in the numerical model is calculated according to the measurements of this experiment. In normal case, the difference between unsteady measurements, steady measurements and numerical results is very small, which can be seen in the Table 6.1.

Table 6.1 Comparison between experimental measurements and numerical results in the normal CoW

Flow rate (ml/s)	LACA	RACA	LPCA	RPCA	LMCA	RMCA	Gross
Experiment (unsteady)	78.6	76.8	122.6	124.1	200.4	207.3	809.7
Experiment (steady)	78.8	77.2	123.4	124.2	202.1	203.5	809.3
Numerical results	79.0	79.0	129.9	129.9	205.4	205.4	828.6

6.4.2 Case 2-75% stenosis of RICA

In this experiment, we neglect the effect of autoregulation. Therefore, the terminal resistance of the CoW is kept as constant. Since the stenosis or occlusion of ICA results in the redistribution of fluid in the CoW, the input pressure waveform is also changed. Hence, for each new case, we need to adjust the pressure waveform. The mean pressure is adjusted to 99 ± 1mmHg and the waveform is similar to that used in the numerical model.

Table 6.2 shows the comparison between experimental measurements and numerical results in the case with 75% stenosis of RICA. The difference between steady measurements and unsteady measurements is very small. Although the stenosis occurs at RICA, the largest difference between experimental measurements and numerical results occurs at LACA which is 6.7%. It means that the 75% stenosis of RICA does

not result in significant difference between experimental measurements and numerical results.

Table 6.2 Comparison between experimental measurements and numerical results in the CoW with 75% stenosis of RICA

Flow rate (ml/s)	LACA	RACA	LPCA	RPCA	LMCA	RMCA	Gross
Experiment (unsteady)	83.8	76.9	125.2	127.5	207.6	196.2	813.6
Experiment (steady)	80.8	75.2	124.3	123.2	203.2	200.8	807.5
Numerical results	78.0	73.7	129.3	129.2	203.4	190.7	804.3

6.4.3 Case 3-Bilateral 75% stenosis of ICA

Table 6.3 shows the comparison between experimental measurements and numerical results in the case with bilateral 75% stenosis of ICA. The difference between steady measurements and unsteady measurements is very small. Due to the symmetry, the difference between both sides of the CoW in the experiment is also very small. The largest difference occurs between LPCA and RPCA in the experiment which is 2.6%. It means that this experiment can ensure the symmetry of the CoW. This result also can be found in the results of normal case in the experiment in which the largest difference between two sides of the CoW occurs between LMCA and RMCA which is 3.4%. In case 3, the largest difference between experimental measurements and numerical results occurs at RMCA which is 5.1%. The difference of gross flow rates between experimental measurements and numerical results is 3.3%. It means that bilateral 75% stenosis of ICA has little influence in the distribution of outflows and the total flow rate of the CoW.

Table 6.3 Comparison between experimental measurements and numerical results in the CoW with bilateral 75% stenosis of ICA

Flow rate (ml/s)	LACA	RACA	LPCA	RPCA	LMCA	RMCA	Gross
Experiment (unsteady)	75.9	73.7	127.7	131.1	195.1	196.7	800.3
Experiment (steady)	74.5	73.0	125.3	128.7	194.5	195.2	791.2
Numerical results	71.8	71.8	128.6	128.6	186.6	186.6	774.0

6.4.4 Case 4-RICA occlusion

In case 4 we introduce the occlusion of RICA by clamping the right afferent elastic tube. Table 6.4 shows the comparison between experimental measurements and numerical results of this case. There is no significant difference between unsteady and steady measurements. But significant difference is found between the experimental measurements and numerical results at RACA and RMCA which are 40.7% and 19.9%, respectively. The experimental measurements of PCAs in both side of the CoW are the same, which means that the RICA occlusion does not influence the flow rate of the PCA system. The total flow rate in experiment is 9.4% smaller than that in the numerical results.

Table 6.4 Comparison between experimental measurements and numerical results in the CoW with RICA occlusion

Flow rate (ml/s)	LACA	RACA	LPCA	RPCA	LMCA	RMCA	Gross
Experiment (unsteady)	75.7	36.2	121.7	121.7	197.8	125.1	678.1
Experiment (steady)	76.0	37.5	122.5	121.2	200.1	124.6	681.9
Numerical results	75.8	61.0	128.1	127.7	199.5	156.1	748.2

6.4.5 Case 5-LICA occlusion and 75% stenosis of RICA

Table 6.5 shows the comparison between experimental measurements and numerical results in the case with LICA occlusion and 75% stenosis of RICA. For the experimental measurements there is no large difference between unsteady and steady flow rates. For the right side of the CoW, the largest difference between experimental measurements and numerical results occurs at RACA which is 3.9%. Large difference is found at the left side of the CoW where there are 30.4% and 19.2% difference at the LACA and LMCA respectively. The difference of gross flow rates is 6.7 between experimental measurements and numerical results.

Table 6.5 Comparison between experimental measurements and numerical results in the CoW with LICA occlusion and 75% stenosis of RICA

Flow rate (ml/s)	LACA	RACA	LPCA	RPCA	LMCA	RMCA	Gross
Experiment (unsteady)	39.2	64.6	122.6	126.8	116.7	180.0	649.2
Experiment (steady)	40.5	65.3	123.4	124.2	116.3	178.9	648.6
Numerical results	56.3	67.2	126.5	126.8	144.4	176.4	697.6

6.4.6 Case 6-Bilateral ICA occlusion

In case 6 we clamp both the ICAs to simulate bilateral ICA occlusion. Table 6.6 shows the comparison between experimental measurements and numerical results in the case of bilateral ICA occlusion. The difference between unsteady and steady flow is small. Due to symmetry, the experimental measurements of both sides of the CoW are almost the same. In this case both sides of ACA and MCA are supplied by the two PCoAs which have small diameter of 1mm. Significant difference is found between experimental measurements and numerical results at ACAs and MCAs which are

57.8% and 36.6% respectively. There is a 25.3% difference in the gross flow rates between experimental and numerical results. The largest difference at PCAs between experimental and numerical results is 6.2%. It means bilateral occlusion of ICA results in little influence in the outflows of PCAs.

Table 6.6 Comparison between experimental measurements and numerical results in the CoW with bilateral ICA occlusion

Flow rate (ml/s)	LACA	RACA	LPCA	RPCA	LMCA	RMCA	Gross
Experiment (unsteady)	18.0	17.9	116.9	118.4	69.7	70.6	411.5
Experiment (steady)	18.4	18.6	115.5	116.7	70.4	70.8	410.4
Numerical results	42.4	42.4	123.1	123.1	110.0	110.0	551.0

6.5 Discussion and conclusions

In this experiment the diameters of communicating arteries are fixed at 1mm. The variables of the five pathological cases are the grades of stenoses of both ICAs. The input pressure waveform is kept similar and the terminal resistances are fixed. Stenosis or occlusion of ICA redistributes the blood flow in the CoW and therefore collateral pathways are recruited. Hence, we can compare the collateral ability of individual collateral pathway between experiment and numerical model.

In all the five cases, the difference between unsteady and steady measurements is very small. It means that steady flow can provide the same results as that obtained from pulsatile flow when only averaged values are considered. In case 1, 2, 3, numerical results show good agreement with experimental measurements. In these three cases there is no occlusion of ICA, but there is unilateral or bilateral 75% stenosis of ICA. It means that unilateral or bilateral 75% stenosis of ICA can still provide enough fluid

supply to its corresponding areas, which is in good agreement with numerical results and clinical findings.

Since there is no stenosis or occlusion in VA-BA system, the difference of flow rates in PCAs between experimental measurements and numerical results is small (max. 6.4%). In case 4, 5, 6, unilateral or bilateral occlusion is added into the ICA. The occlusion of ICA results in significant difference between experimental measurements and numerical results in the occluded side. The reason is that in the CoW with occluded ICA collateral pathways through ACoA and PCoA are recruited. The significant difference indicates that the resistance in ACoA and PCoAs in experiment could be higher than that in numerical mode when ICA is occluded. In the study of Moorhead et al. (2004), similar results were obtained by comparing 1D and 3D modeling results. In part, the structures of ACoA and PCoAs used in the experiment increase the energy loss due to the sudden change of cross sectional area at the bifurcations and the change of flow direction. In the other part, the energy loss through ACoA and PCoAs could be underestimated in the numerical model since the sudden change of cross sectional area and the change of flow direction are neglected. Nonlinear effect at the bifurcations could also play an important role for the significant difference.

Bossuet et al. (1999) built up an in vitro experimental model of the CoW using a plane network of 20 tubes. They compared the results between a linear numerical model and the in vitro model and found that numerical results derived from the linear model fitted accurately the in vitro measurements in the cases with only ICA stenosis. But in unilateral ICA obstructive lesions, the linear model failed to predict the experimental

results due to non-linear effects induced by bifurcations and sudden constriction at the level of the communicating arteries. Our results show agreement with their findings.

There are some limitations in the in vitro experimental study. First, we neglect the function of autoregulation. The constant terminal resistances overestimate the distal resistances of CoW and therefore, overestimate the impairment of cerebral hemodynamics resulting from the stenosis or occlusion of ICA. Since CA is an intrinsic complex function of brain, currently it is beyond the state of the art to simulate it experimentally. In addition, as this experiment is built up from the scratch, our focus is to validate the idealized numerical model. To simulate the function of CA would be the next step of this experiment. For the purpose of comparison, the function of CA in numerical model in this chapter is also neglected.

Second, except the four afferent and six efferent tubes, the components of the circle itself are built up by rigid tubes. How much of the influence of coupling of rigid tubes with elastic tubes to the experimental results is not clear. Third, we do not measure the flow rates in the afferent arteries and the components in the circle. Therefore, we can not obtain more information from this experimental study. However, we build up an in vitro experiment about blood flow in the CoW from the concept, which can be used to validate the various numerical studies in the literature.

Chapter 7

Conclusions and suggestions for future work

7.1 Conclusions of this study

In this project a nonlinear one-dimensional numerical model of the CoW is developed to study the hemodynamics in cerebral circulation. In the model of single vessel, three friction terms and two tube laws are compared. It is found that different friction terms have little influence in the averaged value of hemodynamic parameters. It is also found that the linear tube law and nonlinear tube law do not result in significant difference in the averaged value of hemodynamic parameters. Therefore, in this study Poiseuille equation is chosen as the friction term and a linear model developed by Hillen et al. (1982) is chosen as the tube law. A numerical model of normal CoW is built up as the benchmark of subsequent numerical studies. In the model, the distal resistances of six efferent arteries are calculated according to a summary of previous publications. Total flow rate of the CoW obtained from the numerical model is 12.5 ml/s, which is well matched with that of previous publication (Hillen et al., 1986). The profiles of pressure, flow rate and velocity obtained from the numerical results of normal CoW are also well matched with that of previous publication (Hillen et al., 1986). It is concluded that this numerical model can produce similar results as the numerical model in the literature and can be used in the further study.

Based on the developed numerical model of CoW, two numerical studies are conducted to investigate the hemodynamics in cerebral circulation. The first numerical

study is to investigate the hemodynamic change in the CoW between before and after clamping of ICA during CEA. In this study we consider a most common type of CoW anomaly in the numerical model, which is unilateral PCoA missing. In addition, we add a clinical-static CA model at the end of six efferent arteries to simulate the function of autoregulation. It is found that the CA model is well matched with physiological properties of CA.

In the first numerical study, the diameters of ACoA and RPCoA are fixed at 1mm. Numerical results show that bilateral 75% ICA stenosis does not change the blood supply pattern and LPCoA missing does not result in blood flow redistribution in the CoW. However, RICA clamping during CEA results in significant redistribution of blood flow in the CoW with or without LPCoA missing. During the process of clamping of RICA, collateral blood flow in ACoA and RPCoA increases significantly. The quantity of increase of collateral blood flow in ACoA is much larger than that in RPCoA. It means that with fixed diameter of 1 mm, ACoA plays a more important role than RPCoA in the collateral circulation of the CoW. It is found that neglecting autoregulation overestimates the perfusion pressure inside the CoW and underestimates the outflows of the CoW. The collateral ability of the CoW is also underestimated due to the omission of autoregulation.

The second numerical study is to investigate the interactive role of ACoA and PCoA in an incomplete CoW with carotid artery disease. In the incomplete CoW, the LPCoA is missing and the RICA is occluded. The CA model developed in the first numerical study is also applied in this study. It is found that cerebral hemodynamics is not influenced by single factor. The diameters of ACoA and RPCoA significantly

influence the collateral abilities of the ACoA and RPCoA. The collateral flow of ACoA decreases with the increase of the degree of stenosis of LICA and the decrease of its diameter and the increase of the diameter of RPCoA. The collateral flow of RPCoA decreases with the decrease of the degree of stenosis of LICA and the decrease of its diameter and the increase of the diameter of ACoA. RA1 plays an important role in connecting the ACoA and the RPCoA. It is concluded that the grades of stenosis of LICA and the diameters of ACoA and RPCoA interactively influence the collateral capacity of the CoW.

In vitro experiment is built up from the concept to final completion. The purpose of this experiment is not only to investigate the blood flow in the CoW in vitro experimentally but also to validate the numerical results. It is found that steady and unsteady pressure inputs do not result in significant difference in the averaged value of flow rate, which suggests that steady pressure inputs could be used in the future experimental study on blood flow in the CoW for the studies focusing on averaged values. Comparing the experimental measurements with numerical results, it is found that unilateral or bilateral 75% stenosis of ICA does not result in significant difference in the outflows of the CoW, which is in good agreement with the previous numerical and in vitro experimental results and clinical findings. But unilateral or bilateral occlusion of ICA results in significant difference between experimental measurements and numerical results. It is because that in CoW with unilateral or bilateral occlusion of ICA, collateral flows in ACoA and PCoA are recruited. In numerical study, energy loss in ACoA and PCoA is underestimated, but the in vitro experiment increases the energy loss in the ACoA and PCoA.

7.2 Suggestions for future work

Future work is suggested to focus on the validation of the one-dimensional numerical model further in different pathological conditions using either in vivo or in vitro experiment. Although extensive numerical work has been done by various authors, how significant of the numerical conclusions to clinical studies remains open. In numerical studies, multidimensional model is an interesting topic if its results can be compared with that of one-dimensional model or validated by in vivo and/or in vitro experimental measurements.

Patient-specific clinical application of one-dimensional model is also suggested in the future study. If numerical models can be validated by in vivo experiment, they could provide valuable hemodynamic information for clinicians. Hemodynamic parameters such as pressure, flow rate and velocity in all the locations of vascular network can be calculated in very short time by the numerical model. It is suggested to explore clinical application of the one-dimensional numerical model by applying patient-specific physiological parameters obtained by imaging systems in the clinical test.

In vitro experimental study on blood flow in the CoW is strongly suggested to validate the existing various numerical studies in the literature. Based on the in vitro experiment built up in this project, some improvements could be done in the physical structure of the CoW and the distal resistances of efferent tubes. These improvements could reduce the difference between experimental measurements and numerical results in the CoW with unilateral or bilateral occlusion of ICA. It would also be interesting if pressure or flow rate inside the CoW could be measured in the in vitro experiment.

The one-dimensional model can be improved and several points are suggested. First, it is suggested to improve the mathematical description of blood flow in the stenosis of ICA. Since for severe stenosis of ICA, the luminal diameter is very small, non-Newtonian effect of blood may play an important role. The length and the profile of the stenosis may also influence the local hemodynamics. Second, at the bifurcations, non-linear effect may result in significant energy loss. Neglecting the non-linear effect at the bifurcations could underestimate the local resistance, especially in the arteries with small diameters. It is suggested to consider the energy loss at the bifurcations of CoW in the future numerical studies.

References

1. AhChong AK, Law CB and Chiu KM. Carotid endarterectomy for non-hemispheric cerebrovascular symptoms: an unusual indication. Hong Kong Medical Journal 1999;5:391-393.
2. Alpers BJ and Berry RG. Circle of Willis in cerebral vascular disorders. Archives of Neurology 1963;8:398-402.
3. American Heart Association. Heart Disease and Stroke Statistics — 2004 Update. Dallas, Tex.: American Heart Association; 2003.
4. Anzola GP, Gasparotti R, Magoni M, Prandini F. Transcranial doppler sonography and magnetic resonance angiography in the assessment of collateral hemispheric flow in patients with carotid disease Stroke 1995;26:214-217.
5. Ausman JI. Meeting review: 54th annual meeting of the Japan neurological society. Surgical Neurology 1996;46:295-300.
6. Barnett HJM. 1988. Cerebrovascular diseases. In J. B. Wyngaarden and L. H. Smith, (eds.), Cecil Textbook of Medicine, 18th ed. Philadelphia: Saunders, pp.2159-2180.
7. Barnett HJM, Taylor DW, Eliasziw M, Fox AJ, Ferguson GG, Haynes RB, Rankin RN, Clagett BP, Hachinski VC, Sackett DL, et al. Benefit of carotid endarterectomy in patients with symptomatic moderate or severe stenosis: North American Symptomatic Carotid Endarterectomy Trial Collaborators. The New England Journal of Medicine 1998;339:1415-1425.
8. Barnett HJM, Gunton RW, Eliasziw M, Fleming L, Sharpe B, Gates P, Meldrum H. Causes and severity of ischemic stroke in patients with internal carotid artery

stenosis. JAMA : The Journal of the American Medical Association 2000;283:1429-1436.

9. Bassez S, Flaud P and Chauveau M. Modeling of the deformation of flexible tubes using a single law: Application to veins of the lower limb in man. Journal of Biomechanical Engineering 2001;123:58-65.

10. Battacharji SK, Hutchinson EC, McCall AJ. The circle of Willis: The incidence of developmental abnormalities in normal and infracted brains. Brain 1967;90:747-758.

11. Baumgartner RW, Baumgartner I, Schroth G. Diagnostic criteria for transcranial colour-coded duplex sonography evaluation of cross-flow through the circle of Willis in unilateral obstructive carotid artery disease. Journal of Neurology 1996;243:516-521.

12. Bisschops RH, Klijn CJ, Kappelle LJ, van Huffelen AC, van der Gound J. Collateral flow and ischemia brain lesions in patients with unilateral carotid occlusion Neurology 2003; 60:1435-1441.

13. Blaser T, Hofmann K, Buerger T, Effenberger O, Wallesch CW and Goertler M. Risk of stroke, transient ischemic attack, and vessel occlusion before endarterectomy in patients with symptomatic severe carotid stenosis. Stroke 2002;33:1057-1062.

14. Bossuet P, Fuseri J, Marc-Vergnes JP, Zagzoule M, Lajeunie R, Rieu R, Cassot F. In vitro validation of mathematical models of the cerebral macrocirculation in cases of carotid stenoses and/or occlusions. 6th European Stroke Conference, Amsterdam, May 1997.

15. Botnar R, Rappitsch G, Scheidegger MB, Liepsch D, Perktold K and Boesiger P. Hemodynamics in the carotid artery bifurcation: A comparison between

numerical simulations and in vitro MRI measurements. Journal of Biomechanics 2000;33:137-144.

16. Brozici M, van der Zwan A, Hillen B. Anatomy and functionality of leptomeningeal anastomoses. Stroke 2003;34:2750.
17. Caplan LR and Hennerici M. Impaired clearance of emboli (washout) is an important link between hypoperfusion, embolism, and ischemic stroke. Archives of neurology 1998;55:1475-1482.
18. Cassot F, Vergeur V, Bossuet P, Hillen B, Zagzoule M, Marc-Vergnes JP. Effect of anterior communicating artery diameter on cerebral hemodynamics in internal carotid artery disease. A model study. Circulation 1995;92:3322-3331.
19. Cassot F, Zagzoule M, Marc-Vergnes JP. Hemodynamic role of the circle of Willis in stenosis of internal carotid arteries. An analytical solution of a linear model. Journal of Biomechanics 2000;33:395-405.
20. Cebral J, Castro MA, Soto O, Lohner R and Alperin N. Blood flow models of the circle of Willis from magnetic resonance data. Journal of Engineering Mathematics 2003;47:369-386.
21. Charbel FT, Zhao M, Amin-Hanjani S, Hoffman W, Du X, Clark ME. A patient-specific computer model to predict outcomes of the balloon occlusion test. Journal of Neurosurgery 2004;101:977-988.
22. Chao JC, Hwang NHC. A dynamic model of the circle of Willis. Journal of Biomechanics 1971;4:141-147.
23. Charbel FT, Guppy KH, Zhao M, Clark ME. Computerized hemodynamic evaluation of the cerebral circulation for bypass. Neurosurgery Clinics of North America 2001;12:499-508.

24. Chaudhuri R, Padayachee TS, Lewis RR, Gosling RG, Cox TCS. Non-invasive assessment of the circle of Willis using transcranial pulsed Doppler unltrasound with angiographic correlation. Clinical radiology 1992;46:193-197.

25. Cikrit DF, Dalsing MC, Harting PS, Burt RW, Lalka SG, Sawchuk AP, Solooki B. Cerebral vascular reactivity assessed with acetazolamide single photon emission computer tomography scans before and after carotid endarterectomy. American Journal of Surgery 1997;174:193-197.

26. Coyle P, Panzenbeck MJ. Collateral development after carotid artery occlusion in Fischer 344 rats. Stroke 1990;21:316-321.

27. David T, Brown M and Ferrandez A. Auto-regulation and blood flow in the cerebral circulation. International Journal for Numerical Methods in Fluids 2003;43:701-713.

28. DePippo PS, Ascher E, Scheinman M, Yorkovich W, hingorani A. The value and limitations of magnetic resonance angiography of the circle of Willis in patients undergoing carotid endarterectomy. Cardiovascular Surgery 1999;7:27-32.

29. Deplano V and Siouffi M. Experimental and numerical study of pulsatile flows through stenosis: wall shear stress analysis. Journal of Biomechanics 1999;32:1081-1090.

30. Derdeyn CP, Yundt KD, Videen TO, Carpenter DA, Grubb RL, Powers WJ. Increased oxygen extraction fraction is associated with prior ischemic events in patients with carotid occlusion. Stroke 1998;29:754-758.

31. Derdeyn CP, Videen TO, Fritsch SM, Carpenter DA, Grubb RL, Powers WJ. Compensatory mechanisms for chronic cerebral hypoperfusion in patients with carotid occlusion. Stroke 1999a;30:1019-1024.

32. Derdeyn CP, Shaibani A, Moran CJ, Cross, DT, Grubb RL, Powers WJ. Lack of correlation between pattern of collateralization and misery perfusion in patients with carotid occlusion. Stroke 1999b;30:1025-1032.

33. Derdeyn CP, Videen TO, Yundt KD, Fritsch SM, Carpenter DA, Grubb RL, Powers WJ. Variability of cerebral blood volume and oxygen extraction: stages of cerebral hemodynamcis impairment revisited. Brain 2002;125:595-607.

34. Dickey PS, Kailasnath P, Bloomgarden G, Goodrich I, Chaloupka J. Computer modeling of cerebral blood flow following internal carotid artery occlusion. Neurological Research 1996;18:259-266.

35. Diehl RR. Cerebral autoregulation studies in clinical practice. European Journal of Ultrasound 2002;16:31-36.

36. Doerfler A, Eckstein HH, Eichbaum M, Heiland S, Benner T, Allenberg JR, Forsting M. Perfusion-weighted magnetic resonance imaging in patients with carotid artery disease before and after carotid endarterectomy. Journal of Vascular Surgery 2001; 34: 587–593.

37. Duros J. Comments on analysis of flow and vascular resistance in a model of the circle of Willis. Journal of Biomechanics 1990;23:507-508.

38. Evans WE, Hayes JP, Waltke EA and Vermillion BD. Optimal cerebral monitoring during carotid endarterectomy: neurologic response under local anesthesia. Journal of Vascular surgery 1985;2:775-777.

39. Felice CD, Capua BD, Tassi R, Mencattini G, Passali D. Non-functioning posterior communicating arteries of circle of Willis in idiopathic sudden hearing loss. The Lancet 2000;356:1237-1238.

40. Ferrandez A, David T, Bamford J, Scott J, Guthrie A. Computational models of blood flow in the circle of Willis. Computer Methods in Biomechanics and Biomedical Engineering 2000;4:1-26.

41. Ferrandez A, David T and Brown MD. Numerical models of auto-regulation and blood flow in the cerebral circulation. Computer Methods in Biomechanics and Biomedical Engineering 2002;5:7-20.

42. Fisher CM. The circle of Willis: anatomical variations. Vascular Diseases 1965;2:99–105.

43. Formaggia L, Nobile F, Quarteroni A, Veneziani A. Multiscale modeling of the circulatory system: a preliminary analysis. Computing and Visualization in Science 1999;2:75-83.

44. Formaggia L, Lamponi D, Quarteroni A. One-dimensional models for blood flow in arteries. Journal of Engineering Mathematics 2003;47:251-276.

45. Fung Y. C. (1997) Biomechanics Circulation, Second Edition. Springer, New York.

46. Gao E, Young WL, Ornstein E, Pile-Spellman J, Ma Q. A theoretical model of cerebral hemodynamics: Application to the study of arteriovenous Malformations. Journal of Cerebral Blood Flow and Metabolism 1997;17:905-918.

47. Gao E, Young WL, Ornstein E, Pile-Spellman J, Ornstein E, Ma Q. Mathematical considerations for modeling cerebral blood flow autoregulation to systemic arterial pressure. American Journal of Physiology. Heart and Circulatory Physiology 1998;274:H1023-H1031.

48. Giller CA and Mueller M. Linearity and non-linearity in cerebral hemodynamics. Medical Engineering and Physics 2003;25:633-646.

49. Gomes FB, Dujovny M, Umansky F, Berman SK, Diaz FG, Ausman JI, Mirchandani HG, Ray WJ. Microanatomy of the anterior cerebral artery. Surgical Neurology 1986;26:129-141.

50. Guyton AC and Hall JE (2000) Textbook of Medical Physiology 10th Edition, WB Saunders, USA.

51. Hartkamp MJ, van der Grond J, van Everdingen KJ, Hillen B, Mali WPTM. Circle of Willis collateral flow investigated by magnetic resonance angiography. Stroke 1999;30:2671-2678.

52. Hartl WH, Furst H. Application of transcranial Doppler sonography to evaluate cerebral hemodynamic variables. Stroke 1995;26:2293-2297.

53. Hayashi K, Nagasawa S, Naruo Y, Okumura A, Moritake K, Handa, H. Mechanical properties of human cerebral arteries. Third international congress of biorheology symposium on rheology of blood vessels. Biorheology 1980;17:211-218.

54. Hedera P, Bujdakova J, Traubner P. Effect of collateral flow patterns on outcome of carotid occlusion. European Neurology 1995;35:212-216.

55. Hegedüs K, Molnár L. Anatomical patterns of hypoplastic posterior communicating arteries and their implications for cerebrovascular disease. European Archives of Psychiatry and Nneurological Sciences 1987;236:241–246.

56. Henderson RD, Eliasziw M, Fox AJ, Rothwell PM, Barneet HJM. Angiographically defined collateral circulation and risk of stroke in patients with severe carotid artery stenosis. Stroke 2000;31:128-132.

57. Hendrikse J, Hartkamp MJ, Hillen B, Mali WPTM, van der Grond J. Collateral ability of the circle of Willis in patients with unilateral internal carotid artery

occlusion; Border zone infarcts and clinical symptoms. Stroke 2001;32:2768-2773.

58. Hendrikse J, Eikelboom BC, van der Grond J. Magnetic resonance angiography of collateral compensation in asymptomatic and symptomatic internal carotid artery stenosis. Journal of Vascular Surgery 2002;36:799-805.

59. Hendrikse J, Rutgers DR, Klijn CJM, Eikelboom BC, van der Grond J. Effect of carotid endarterectomy on primary collateral blood flow in patients with severe carotid artery lesions. Stroke 2003;34:1650-1654.

60. Hillen B, Gaasbeek T, Hoogstraten HW. A mathematical model of the flow in the posterior communicating arteries. Journal of Biomechanics 1982;15:441-448.

61. Hillen B, Hoogstraten HW, Post L. A mathematical model of the flow in the circle of Willis. Journal of Biomechanics 1986;19:187-194.

62. Hillen B, Drinkenburg BAH, Hoogstraten HW, Post L. Analysis of flow and vascular resistance in a model of the circle of Willis. Journal of Biomechanics 1988;21:807-814.

63. Hobson RW, Wright CB, Sublett JW et al. Carotid artery back pressure and endarterectomy under regional anesthesia. Archives of Surgery 1974;109:682-687.

64. Hoksbergen AWJ, Legemate DA, Ubbink DTh, de Vos HJ, Jacobs MJHM. Influence of the collateral function of the circle of Willis on hemispherical perfusion during carotid occlusion as assessed by transcranial colour-coded duplex ultrasonography. European Journal of Vascular and Endovascular Surgery 1999;17:486-492.

65. Hoksbergen AWJ, Fulesdi B, Legemate DA, Csiba L. Collateral configuration of the circle of Willis Transcranial color-coded duplex ultrasonography and comparison with postmortem anatomy. Stroke 2000a;31:1346-1351.

66. Hoksbergen AWJ, Legemate DA, Ubbink DT, Jacobs MJHM. Collateral variations in circle of Willis in atherosclerotic population assessed by means of transcranial color-coded duplex ultrasonography. Stroke 2000b;31:1656-1660.

67. Hoksbergen AWJ, Legemate DA, Csiba L, Csati G, Siro P, Fulesdi B. Absent collateral function of the circle of Willis as a risk factor for ischemia stroke. Cerebrovascular Diseases (Basel, Switzerland) 2003a;16:191-198.

68. Hoksbergen AWJ, Majoie CBL, Hulsmans FJH, Legemate DA. Assessment of the collateral function of the circle of Willis; Three-dimensional time-of-flight MR angiography compared with Transcranial Color-Coded Duplex Sonography. American Journal of Neuroradiology 2003b;24:456-462.

69. Hudetz, AG, Halsey JH, Jr, Horton, CH, Conger KA and Reneau DD. Mathematical simulation of cerebral blood flow in focal ischemia. Stroke 1982;13:693-700.

70. Kailasnath P, Dickey PS, Gahbauer H, Nunes J, Beckman C, Chaloupka JC. Intracarotid pressure measurements in the evaluation of a computer model of the cerebral circulation. Surgical Neurology 1998;50:257-263.

71. Kamouchi M, Kishikawa K, Okada Y, Inoue T, Ibayashi S and Iida M. Poststenotic flow and intracranial hemodynamics in patients with carotid stenosis: Transoral carotid Ultrasonography study. American Journal of Neuroradiology 2005;26:76-81.

72. Keunen RWM. Transcranial Doppler sonography of the cerebral circulation in occlusive cerebrovascular disease [Thesis]. Nijmegen, Netherlands: Benda BV;1990.

73. Khir AW, O'Brien A, Gibbs JSR and Parker KH. Determination of wave speed and wave separation in the arteries. Journal of Biomechanics 2001;34:1145-1155.

74. Khir AW and Parker KH. Measurements of Wave Speed and Reflected Waves in Elastic Tubes and Bifurcations. Journal of Biomechanics 2002;35:775-783.

75. Kirkham SK, Craine RE and Birch AA. A new mathematical model of dynamic cerebral autoregulation based on a flow dependent feedback mechanism. Physiological Measurement 2001;22:461-473.

76. Kim GE, Cho YP, Lim SM. The anatomy of the circle of Willis as a predictive factor for intra-operative cerebral ischemia (shunt need) during carotid endarterectomy. Neurological Research 2002;24:237–240.

77. Kitawaki, T., Shimizu, M., Liu, H. and Himeno, R. One-dimensional Numerical Analysis of Blood Flow with Consideration of Unsteady Viscous Influence. 10th international conference on biomedical engineering. Singapore, 2000, 395-396.

78. Klijn CJM, Kappelle LJ, Tulleken CAF, van Gijn J. Symptomatic carotid artery occlusion. A reappraisal of hemodynamic factors. Stroke 1997;28:2084-2093.

79. Kluytmans M, van der Grond J, Eikelboom BC, Viergever MA. Long-term hemodynamic effect of carotid endarterectomy. Stroke 1998;29:1567-1572.

80. Kluytmans M, van der Grond J, van Everdingen KJ, Klijn CJM, Kappelle LJ, Viergever MA. Cerebral hemodynamics in relation to patterns of collateral flow. Stroke 1999;30:1432-1439.

81. Kontos HA, Wei EP, Navari RM, Levasseur JE, Rosenblum WI and Patterson JL Jr. Responses of cerebral arteries and arterioles to acute hypotension and hypertension. American Journal of Physiology 1978;234:H371-H383.

82. Kufahl RH and Clark RH. A circle of Willis simulation using distensible vessels and pulsatile flow. Journal of Biomechanical Engineering 1985;107:112-122.

83. Liebeskind DS. Collateral Circulation. Stroke 2003;34:2279-2284.

84. Liepsch D, Seemann A, Siekmann J. Note on wave propagation in a thin elastic tube containing a viscous fluid. Journal of Biomechanics 1985;18:685-694.

85. Liu Y, Birch AA and Allen R. Dynamic cerebral autoregulation assessment using an ARX model: comparative study using step response and phase shift analysis. Medical Engineering and Physics 2003;25:647-653.

86. Lopez-Bresnahan MV, Kearse LA Jr, Yanez P, Young TI. Anterior communicating artery collateral flow protection against ischemic change during carotid endarterectomy. Journal of Neurosurgery 1993;79:379-382.

87. Lyden PD and Nelson TR. Visualization of the cerebral circulation using three-dimensional transcranial power Doppler ultrasound imaging. Journal of Neuroimaging 1997;7:35-39.

88. MacKenzie ET, Strandgaard S, Graham DI, Jones JV, Harper AM, and Farrar JK. Effects of acutely induced hypertension in cats on pial arteriolar caliber, local cerebral blood flow, and the blood-brain barrier. Circulation Research 1976;39:33-41.

89. MacKenzie ET, Farrar JK, Fitch W, Graham DI, Gregory PC, and Harper AM. Effects of hemorrhagic hypotension on the cerebral circulation. I. Cerebral blood flow and pial arteriolar caliber. Stroke 1979;10:711-718.

90. Macchi C and Catini C. The measurement of the calibers and blood flow velocity of the arteries of the circle of Willis: A statistical investigation of 120 living subjects using transcranial color-Doppler Ultrasonography. Italian Journal of Anatomy and Embriology 1994;99:9-16.

91. Markus H and Cullinane M. Severely impaired cerebrovascular reactivity predicts stroke and TIA risk in patients with carotid artery stenosis and occlusion. Brain 2001;124:457-467.

92. Miralles M, Dolz JL, Cotillas J, Aldoma J, Santiso MA, Gimenez A, Capdevila A, Cairols MA. The role of the circle of Willis in carotid occlusion: assessment with phase contrast MR angiography and transcranial duplex. European Journal of Vascular and Endovascular Surgery 1995;10:424-430.

93. Moorhead, KT, Moore, SM, Chase, JG, David, T and Fink, J (2004a). "1D and 3D Models of Autoregulated Cerebrovascular Flow", Proc 26th International Conf of IEEE engineering in Med and Biology Society (EMBS 2004), San Francisco, CA, Sept 1-5, pp.726-729, ISBN:0-7803-8440-7.

94. Moorhead KT, Doran CV, Chase, JG and David T. Lumped parameter and feedback control models of the auto-regulatory response in the circle of Willis. Computer Methods in Biomechanics and Biomedical Engineering 2004b;7:121-130.

95. Newell DW, Aaslid R, Lam A, Mayberg TS and Winn HR. Comparison of flow and velocity during dynamic autoregulation testing in humans. Stroke 1994;25:793-797.

96. Nielsen TG, Sillesen H and Schroeder TV. Seizures following carotid endarterectomy in patients with severely compromised cerebral circulation. European Journal of Vascular and Endovascular Surgery 1995;9:53-57.

97. Nichols WW and O'Rourke MF. McDonald's blood flow in arteries: Theoretic, experimental and clinical principles. Third edition. Lea & Febiger, 1990.

98. Nichols WW and O'Rouke MF. McDonald's Blood Flow in Arteries. Fourth Edition, Oxford University Press, 1997. P93.

99. Nicolaides AN. Asymptomatic carotid stenosis and risk of stroke: identification of a high risk group (ACSRS): a natural history study. International Angiology 1995;14:21-23.

100. Osborne AG. Introduction to cerebral angiography. Philadelphia: Harper & Row, 1980:146.

101. Pasterkamp G, Schoneveld AH, van Wolferen W, Hillen B, Clarijs RJG, Haudenschild CC and Borst C. The impact of atherosclerotic arterial remodeling on percentage of luminal stenosis varies widely within the arterial system. Arteriosclerosis, Thrombosis, and Vascular Biology 1997;17:3057-3063.

102. Pedley TJ. Mathematical modeling of arterial fluid dynamics. Journal of Engineering Mathematics 2003;47:419-444.

103. Piechnik SK, Czosnyka M, Cieslicki K, Ciesla D. Problems in application of pure linear models in cerebral circulation. Journal of Biomechanics 2002;35:553-554.

104. Quick CM, Young WL, Leonard EF, Joshi S, Gao E, and Hashimoto T. Model of structural and functional adaptation of small conductance vessels to arterial hypotension. American Journal of Physiology. Heart and Circulatory Physiology 2000;279:1645-1653

105. Reilly P and Bullock R. Head Injury. Chapman & Hall, London, 1997.

106. Reinhard M, Muller T, Guschlbauer B, Timmer J and Hetzel A. Dynamic cerebral autoregulation and collateral flow patterns in patients with severe

carotid stenosis or occlusion. Ultrasound in Medicine & Biology 2003a;29:1105-1113.

107. Reinhard M, Muller T, Roth M, Guschlbauer B, Timmer J and Hetzel A. Bilateral severe carotid artery stenosis or occlusion-cerebral autoregulation dynamics and collateral flow patterns. Acta Neurochirurgica 2003b;145:1053-1060.

108. Reuderink PJ, Hoogstraten HW, Sipkema P, Hillen B and Westerhof N. Linear and nonlinear one-dimensional models of pulse wave transmission at high womersley numbers. Journal of Biomechanics 1989;22:819-827.

109. Rutgers DR, Klijn CJ, Kappelle LJ, van Huffelen AC, van der Crond J. A longitudinal study of collateral flow patterns in the circle of Willis and the ophthalmic artery in patients with a symptomatic internal carotid artery occlusion. Stroke 2000a;31:1913-1920.

110. Rutgers DR, Blankensteijn JD, van der Grond J. Preoperative MRA flow quantification in CEA patients: flow differences between patients who develop cerebral ischemia and patients who do not develop cerebral ischemia during cross-clamping of the carotid artery. Stroke 2000b;31:3021-3028.

111. Rutgers DR, Klijn CJM, Kappelle LJ, Eikelboom BC, van Huffelen AC, van der Grond J. Sustained bilateral hemodynamics benefit of contralateral carotid endarterectomy in patients with symptomatic internal carotid artery occlusion. Stroke 2001;32:728-734.

112. Saeki N, Rhoton AL. Microsurgical anatomy of the upper basilar artery and the posterior circle of Willis. Journal of Neurosurgery 1977;46:563-578.

113. Schomer DF, Marks MP, Steinberg GK, Johnstone IM, Boothroyd DB, Ross MR, Pelc, NJ, Enzmann DR. The anatomy of the posterior communicating artery

as a risk factor for ischemic cerebral infarction. The New England Journal of Medicine 1994;330:1565-1570.

114. Sherwin SJ, Franke V, Peiro J and Parker K. One-dimensional modeling of a vascular network in space-time variables. Journal of Engineering Mathematics 2003;47:217-250.
115. Silvestrini M, Vernieri F, Pasqualetti P, Matteis M, Passarelli F, Troisi E, Caltagirone C. Impaired cerebral vasoreactivity and risk of stroke in patients with asymptomatic carotid artery stenosis. Journal of the American Medical Association 2000;283:2122-2127.
116. Simpson DM, Panerai RB, Evans DH and Naylor AR. A parametric approach to measuring cerebral blood flow autoregulation from spontaneous variations in blood pressure. Annals of Biomedical Engineering 2001;29:18-25.
117. Siouffi M, Deplano V and Pelissier R. Experimental analysis of unsteady flows through A stenosis. Journal of Biomechanics 1998;31:11-19.
118. Spencer MP. Transcranial Doppler monitoring and causes of stroke from carotid endarterectomy. Stroke 1997;28:685-691.
119. Suzuki K, Taketomi T and Sato S. Improving Zielke's method of simulating frequency-dependent friction in laminar liquid pipe flow. Journal of Fluids Engineering 1991;113**:**569-573.
120. Tatemichi TK, Chamorro A, Petty GW, Khandji A, Oropeza LA, Duterte DI, Mohr JP. Hemodynamic role of ophthalmic artery collateral in internal carotid artery occlusion. Neurology 1990;40:461-464.
121. Tiecks FP, Lam AP, Aaslid R, Newell DW. Comparison of static and dynamic cerebral autoregulatory measurements. Stroke 1995;26:1014–1019.

122. Tulleken CAF and Luiten MLFB. The basilar artery bifurcation: microscopical anatomy. Acta Neurochir 1987;85:50–55

123. Ursino M. Cerebrovascular modeling: a union of physiology, clinical medicine and biomedical engineering. Medical Engineering & Physics 2003;25:617-620.

124. Ustun C. Dr. Thomas Willis' famous eponym: the circle of Willis. Turkish Journal of Medical and Science 2004;34:271-274.

125. van Everdingen KJ, Visser GH, Klijn CJ, Kappelle LJ, van der Grond J. Role of collateral flow on cerebral hemodynamics in patients with unilateral internal carotid artery occlusion. Annals of Neurology 1998;44:167-176.

126. Vernieri F, Pasqualetti P, Dimedi M, Giacomini P, Rossini PM, Caltagirone C, Silvestrini M. Cerebral hemodynamics in patients with carotid artery occlusion and contralateral moderate or severe internal carotid artery stenosis. Journal of Neurosurgery 2001;94:559-564.

127. Viedma A, Jimenez-Ortiz C, Marco V. Extended Willis circle model to explain clinical observations in periorbital arterial flow. Journal of Biomechanics 1997;30:265-272.

128. Visser GH, van Huffelen AC, Wieneke GH, Eikelboom BC. Billateral increase in CO2 reactivity after unilateral carotid endarterectomy. Stroke 1997;28:899-905.

129. Vriens EM, Wieneke GH, Hillen B, Eikelboom BC, Van Huffelen AC, visser GH. Flow redistribution in the major cerebral arteries after carotid endarterectomy: A study with transcranial Doppler scan. Journal of Vascular Surgery 2001;33:139-147.

130. Wagner EM and Traystman RJ. Hydrostatic determinants of cerebral perfusion. Critical Care Medicine 1986;14:484-490.

131. White RP, Markus HS. Impaired dynamic cerebral autoregulation in carotid artery stenosis. Stroke 1997;28:1340-1344.

132. Yamauchi H, Kudoh T, Sugimoto K, Takahashi M, Kishibe Y and Okazawa H. Pattern of collaterals, type of infarcts, and haemodynamic impairment in carotid artery occlusion. Journal of Neurology Neurosurgery and Psychiatry 2004;75:1697-1701.

133. Yasargil MG. Microneurosurgery I. New York, NY: Thieme Stratton Inc; 1984.

134. Zachrisson H, Berthelsen B, Blomstrand C, Holm J, Volkmann R. Influence of poststenotic collateral pressure on blood flow velocities within high-grade carotid artery stenosis: Differences between morphologic and functional measurements. Journal of Vascular Surgery 2001;34:263-268.

135. Zachrisson H, Blomstrand C, Holm J, Mattsson E, Volkmann R. Changes in middle cerebral artery blood flow after carotid endarterectomy as monitored by transcranial Doppler. Journal of Vascular Surgery 2002;36:285-290.

136. Zagzoule M and Marc-Vergnes JP. A global mathematical model of the cerebral circulation in man. Journal of Biomechanics 1986;19:1015-1022.

137. Zbornikova V. Lassvik Claes, Johansson I. Prospective evaluation of the accuracy of duplex scanning with spectral analysis in carotid artery disease. Clinical Physiology 1985;5:257-269.

138. Zielke W. Frequency dependent friction in transient pipe flow. Journal of Basic Engineering 1968;90:109-115.